AD-A023 015

ADAPTIVE TRACKING FILTER DESIGN AND EVALUATION FOR GUN FIRE CONTROL SYSTEMS

Charles M. Brown, Jr., et al

Analytic Sciences Corporation

Prepared for:

Naval Ordnance Systems Command

23 January 1976

DISCLAIMER NOTICE

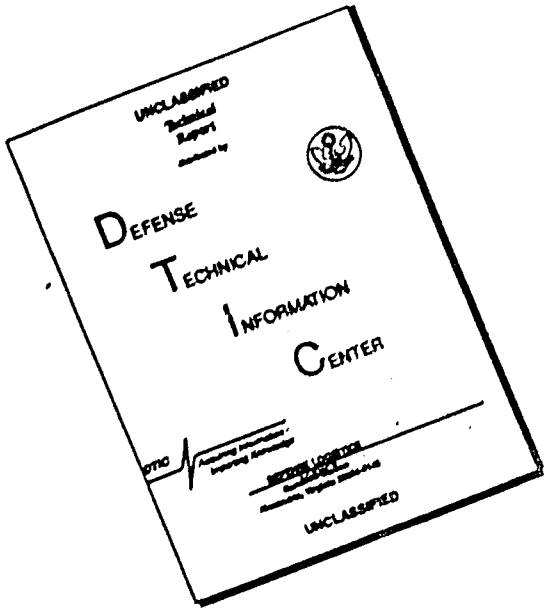

THIS DOCUMENT IS BEST QUALITY AVAILABLE. THE COPY FURNISHED TO DTIC CONTAINED A SIGNIFICANT NUMBER OF PAGES WHICH DO NOT REPRODUCE LEGIBLY.

TR-387-1

ADAPTIVE TRACKING FILTER DESIGN AND EVALUATION FOR GUN FIRE CONTROL SYSTEMS

23 January 1974

TASC

TR-387-1

ADAPTIVE TRACKING FILTER DESIGN AND EVALUATION FOR GUN FIRE CONTROL SYSTEMS

23 January 1974

Prepared Under:

Contract No. N00017-73-C-4323

for

NAVAL ORDNANCE SYSTEMS COMMAND
Arlington, Virginia

Prepared by:

Charles M. Brown, Jr.
Charles F. Price

Approved by:

Arthur A. Sutherland, Jr.
Arthur Gelb

THE ANALYTIC SCIENCES CORPORATION
6 Jacob Way
Reading, Massachusetts 01867

FOREWORD

This report documents work performed for the Naval Ordnance Systems Command under Contract No. N00017-73-C-4323. The authors wish to express appreciation for the consulting assistance provided by Professor John J. Deyst, Jr., of the Massachusetts Institute of Technology during the course of this study, and for several helpful technical discussions with Dr. Barry L. Clark of the Naval Weapons Laboratory.

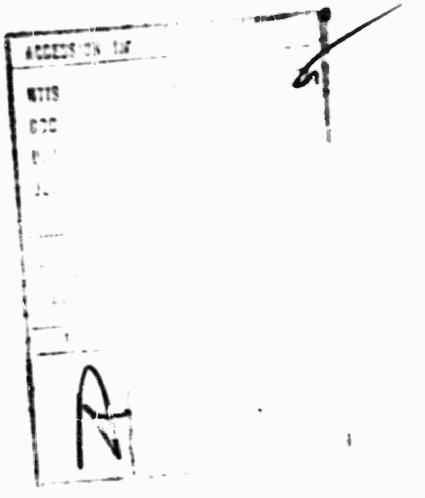

ABSTRACT

The purpose of this study is to investigate and evaluate adaptive tracking filters for shipboard gun fire control systems that must defend against evasive targets. Several design concepts are compared using both tracking error and predicted position error as performance measures. The effects of target evasion, sensor measurement noise level, modeling uncertainties, and length of the measurement interval are investigated, and the trade-offs between performance and algorithm complexity are discussed.

TABLE OF CONTENTS

TABLE OF CONTENTS (Cont.)

LIST OF FIGURES

LIST OF FIGURES (Cont.)

LIST OF FIGURES (Cont.)

1. INTRODUCTION

1.1 BACKGROUND: GUN FIRE CONTROL SYSTEMS

The need to develop shipboard gun fire control systems that are capable of destroying high-speed, maneuverable enemy missiles creates a requirement for pointing and tracking techniques that more accurately account for target motion than do conventional systems. In principle, this can be accomplished by hardware improvements, such as more accurate tracking sensors and higher bandwidth gun control loops, which allow the gun pointing line to respond more quickly to target maneuvers. However, an attractive alternative approach that does not depend upon advances in hardware technology is the use of modern estimation and control theory to develop sensor data processing techniques -- i.e., computer software -- which take maximum advantage of the known mathematical model of target motion. With respect to conventional weapon systems, this represents improved software, rather than hardware -- realized by improving the computational algorithms used to generate gun pointing commands.

The principal elements of a fire control system are illustrated in Fig. 1.1-1 for a single axis. Briefly, one or more tracking sensors provides target position measurements which are processed in a computer, together with measurements of ship's motion, to obtain estimates of target position, velocity, and acceleration in inertial coordinates. The latter are appropriately combined to determine the drive signal for bringing the actual pointing line into coincidence with the commanded pointing line.

A number of error sources illustrated in Fig. 1.1-1 can have an important effect on projectile accuracy; these include:

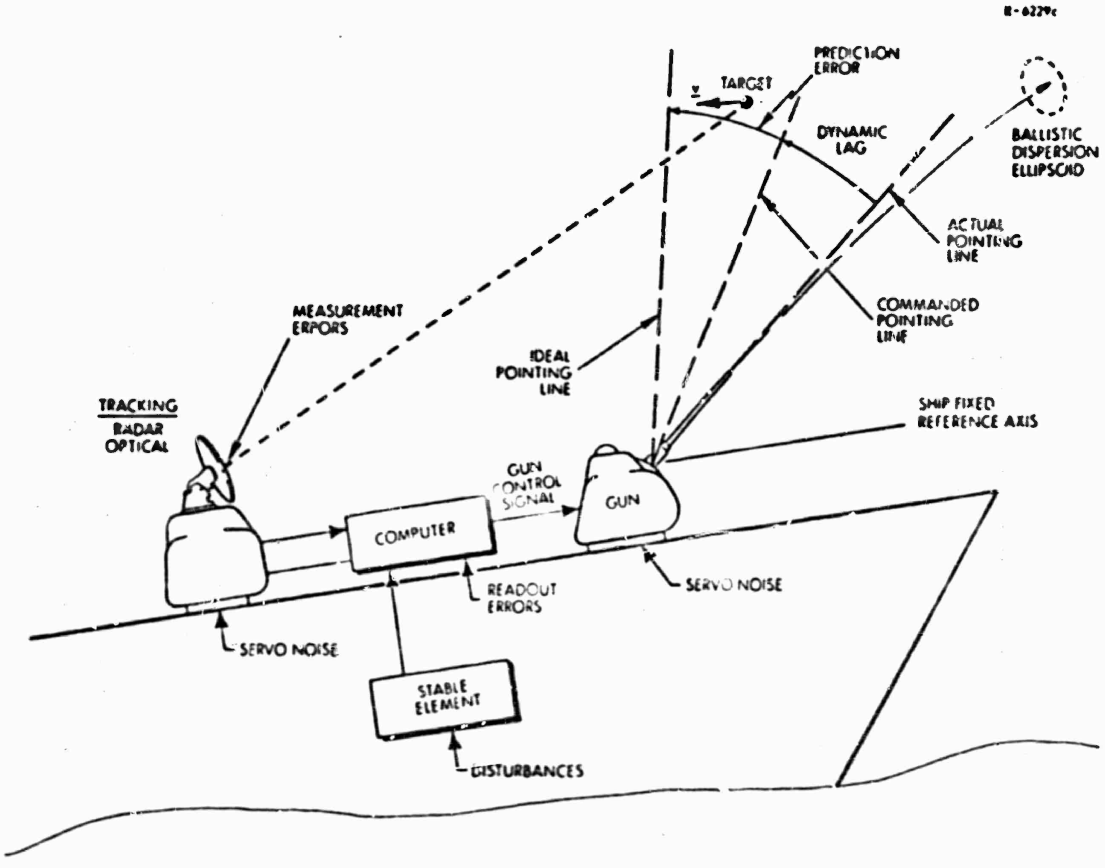

Figure 1.1-1 Principle Elements of a Shipboard Gun Fire Control System

- The dynamic lag attributed to the finite bandwidth of the gun servo which prevents achieving exact equality between the actual and commanded pointing lines against a moving target.

- The prediction error caused by the fact that the commanded pointing direction is not exactly in the direction required to hit the target because of target trajectory prediction errors. The latter are in turn caused by imperfect modeling of target motion and tracking sensor measurement noise.

- The projectile ballistic dispersion error produced by unknown aerodynamic effects along the projectile flight path, as well as non-uniformity in projectile characteristics and firing conditions.

To some extent the above errors will be reduced as specifications on component and instrument quality become progressively more stringent. However an important alternative (and potentially less costly) route to system improvement is to construct computer algorithms, using estimation theory, which extract the maximum amount of useful information from the tracking measurement data, thereby reducing the prediction error. This is especially important in the case of highly maneuverable targets where prediction error can easily be the most significant error source in the entire gun fire control system. The intent of this report is to investigate the potential for better prediction accuracy through software improvements.

The heart of the computer in Fig. 1.1-1 is the target tracking filter which combines the tracking measurements to estimate the target position, velocity, etc., with respect to a stabilized coordinate frame. The latter are required to ultimately calculate the projectile time of flight, the predicted target position at the impact point, and the gun pointing commands. Consequently, it is desirable that the tracking filter produce estimates whose errors are as small as possible, in some sense. Modern estimation theory provides a systematic procedure for accomplishing this goal. Basically, if the target's motion and the tracker measurement errors can be described by appropriate statistical mathematical models, then recursive digital algorithms such as the Kalman filter are available which will yield minimum variance estimates of the variables (called state variables) which describe the target's motion. Such an algorithm is called an optimal filter; its dependency upon the target's equations of motion and parameters and the noise statistics is emphasized in Fig. 1.1-2.

The concept of optimal filtering is currently under investigation by the Navy for both the MK 68 and MK 86 gun fire control systems. In future applications, a problem of particular concern is the degradation in tracking filter performance observed when a target performs significant unexpected maneuvers.

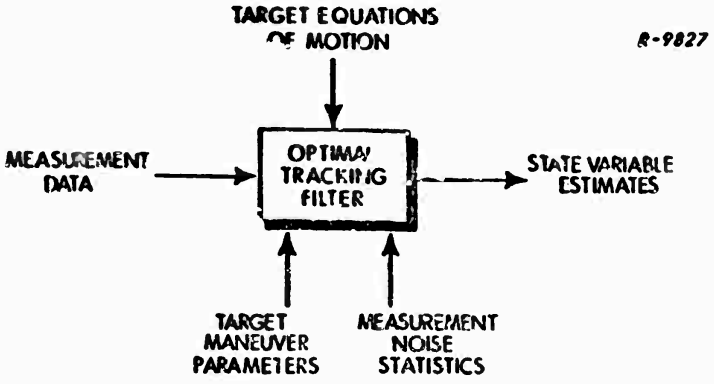

Figure 1.1-2 Illustration of Factors Entering into Tracking Filter Design

As stated above, the filter construction requires knowledge of the mathematical model of target motion; if the actual motion violates the model, then the filter is no longer optimal. Modeling errors can also arise with respect to the tracker measurement noise statistics. For example, the errors in radar measurements are to some extent dependent on the target reflection properties which are frequently not well known. Hence, the statistical parameters (rms noise levels) needed for designing the filter will be in error.

In practice, modeling errors are unavoidable because complete information about a maneuvering target and the tracking sensor measurement noise is not available. Thus optimal filter design is impossible and the problem is to design a suboptimal tracking filter which gives estimates that are close to optimum. One common approach to suboptimal design is to experimentally select the fixed filter which gives the best performance over the complete range of tracking situations that will be encountered, i.e. it is the best design "on the average". Another approach is to use an adaptive design of the type illustrated in Fig. 1.1-3, in which auxiliary real-time computations are performed to

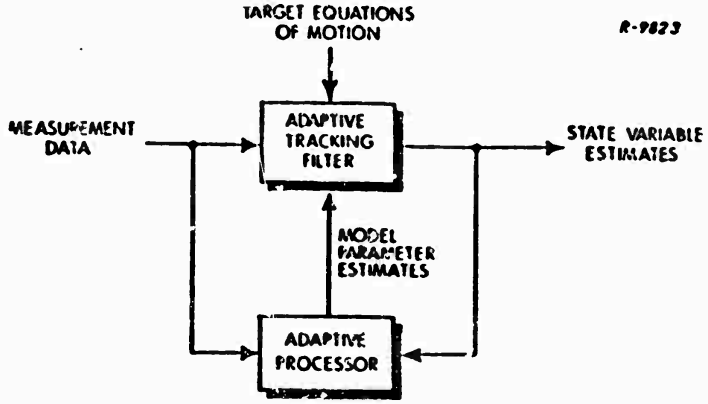

Figure 1.1-3 Structure of an Adaptive Tracking Filter

obtain better knowledge of the model parameters, and thereby improve the filter estimation accuracy on-line. The purpose of this study is to investigate adaptive filtering techniques that are designed to track highly manuverable missile-type targets, and to compare their performance with conventional fixed filters over a range of target engagement situations.

1.2 TECHNICAL APPROACH

In this report, a realistic but comparitively simple target tracking problem is defined. The optimum filter for this problem is discussed and several practical suboptimal designs are developed in detail. These include both adaptive and fixed filters which were selected after a careful review of the technical literature; they represent original work as well as applications of available techniques. A comparitive study of these designs is conducted using two related, but distinct, performance measures. First, they are evaluated on the basis of estimation error -- i.e., the error between the target's state variables (position, velocity, etc.) and their estimates. This indicates how well each filter can "track" the current behavior of the target. Since the ultimate

task of the tracking system is to predict the future position of the target so that a gun pointing line can be calculated, the various designs are also compared based upon their prediction error i.e., the error between the future target position and its predicted position. The sensitivity of each design to changes in target manuver behavior, range, and sensor noise are studied as well as the effects of noise correlation and measurement data rate. The results indicate the ultimate prediction accuracy possible with the various tracking filters for different target maneuver characteristics, and the tradeoff between algorithm complexity and tracking accuracy.

1.3 ORGANIZATION OF REPORT

In Chapter 2, the tracking problem is formulated and the assumptions and simplifications made for this work are discussed. Chapter 3 describes the design of tracking filters based upon optimal filtering theory, discusses practical suboptimal fixed configuration filters, and describes the use of adaptive techniques as a means of obtaining better tracking accuracy. Chapter 4 presents the simulation results obtained when each design is tested over a range of tracking conditions and its performance is measured in terms of estimation error and prediction error. A summary of the results and conclusions are presented in Chapter 5.

The appendices provide background material for the filtering techniques investigated. Appendix A summarizes optimal filtering and prediction theory and Appendix B discusses the details of designing adaptive filters.

2. TRACKING PROBLEM FORMULATION

2.1 TARGET TRACKING AND PREDICTION

In this chapter, the specific tracking problem to be studied is developed and discussed. This simplified, but realistic, formulation is the basis upon which tracking filters are designed in Chapter 3 and evaluated in Chapter 4.

The principal elements of a two-dimensional tracking problem are illustrated in Fig. 2.1-1. The radar (or other tracking sensor), for

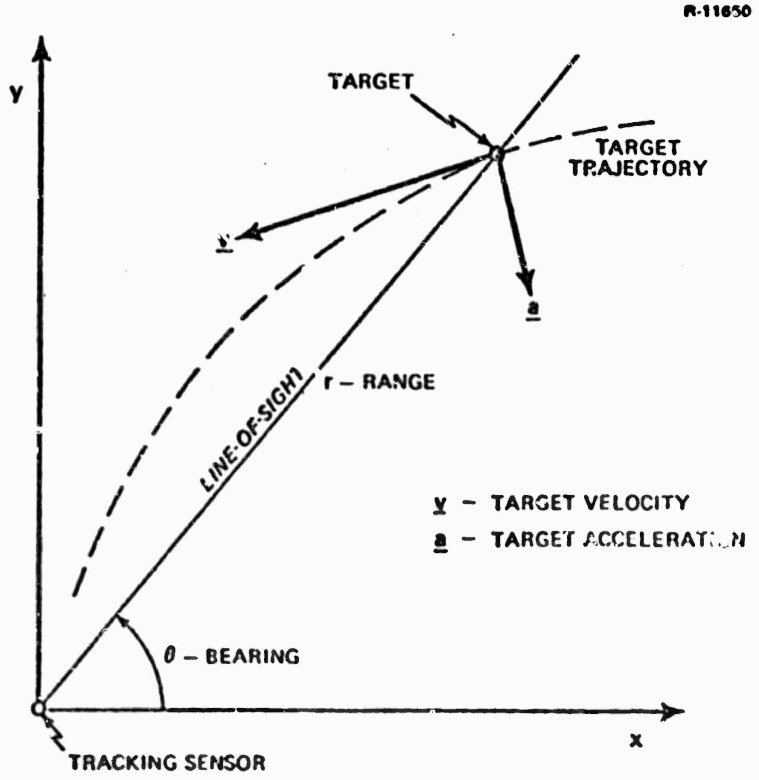

Figure 2.1-1 Tracking Sensor and Target Geometry

simplicity assumed to be fixed in inertial space,* takes noisy measurements of the target range (r) and bearing (θ) at regular intervals. The tracking filter processes these measurements and estimates the target's state variables -- i.e., those variables which describe the target's motion such as its position, velocity, acceleration, etc. Given these estimates the tracking filter is then used to predict the future position of the target by propagating the dynamic equations of the target forward in time from the current state estimates. The total error in predicted position depends upon the length of the prediction interval (the projectile flight time), unknown inputs to the target dynamics during this interval, errors in the target prediction model, and errors in the current estimates of the target's states. The ultimate objective is to minimize the prediction error. The length of the prediction interval is determined by the target's trajectory, firing delays, and projectile velocity. With the future inputs to the target dynamics unknown, the only way to reduce the prediction error is to model the target dynamics as accurately as possible and design a tracking filter which gives the best possible estimates of the target's current state.

Modern optimal estimation techniques, such as the Kalman filter, can be applied to the above tracking problem. However, they must be used with some care because the filter design requires complete knowledge of the target dynamic equations and the statistics of all random inputs. In this problem, the control policy or attacking strategy of the target is assumed to be partially or completely unknown. The target might be following a deterministic guidance law or it might be taking evasive action in a random manner. Another potentially unknown quantity is the level of measurement noise, which can depend upon atmospheric conditions and upon the size and shape of the target, its range, and its changing reflection properties as it maneuvers. With all of these

*Known sensor motion relative to inertial space can easily be subtracted out of the problem; hence no generality is lost with this assumption.

uncertain elements in the problem, it is impossible to design an optimum tracking filter. However modern estimation theory provides the basis upon which suboptimal filters can be designed to give fairly good performance over a wide range of possible conditions; the application of this technology to the fire control tracking problem is the goal of this report.

The remainder of this chapter formulates in detail the particular tracking problem to be studied and defines the conditions under which the tracking filters will be designed. The simplifying assumptions used in this work are also discussed.

2.2 CHOICE OF TRACKING COORDINATE SYSTEM

In this section the target's equations of motion and the tracking measurement equations are expressed in both rectangular and polar coordinates and a simplified target motion model based on polar coordinates is discussed.

Referring to Fig. 2.2-1, the equations of motion of the target defined in rectangular coordinates are

$$\begin{aligned} \ddot{x} &= a_x \\ \ddot{y} &= a_y \end{aligned} \tag{2.2-1}$$

Assuming that the radar or other tracking sensor takes noisy measurements, z_r and z_θ, of the target's range and bearing, the measurement equations are

$$\begin{aligned} z_r &= \sqrt{x^2 + y^2} + v_r \\ z_\theta &= \tan^{-1}(y/x) + v_\theta \end{aligned} \tag{2.2-2}$$

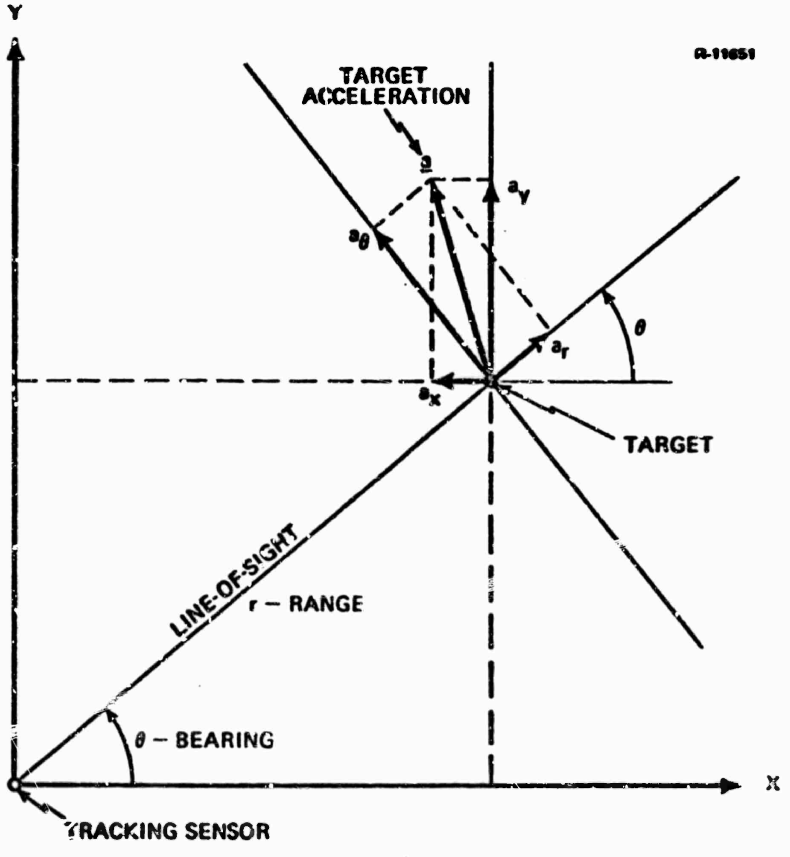

Figure 2.2-1 Target Acceleration Component Definitions

where v_r and v_θ are measurement errors. The range measurement, z_r, is the true range, r, plus the range measurement noise, v_r, and z_θ is similarly related to the true bearing, θ. Note that while the dynamic equations, Eq. (2.2-1), are linear in the rectangular (x, y) coordinates, the corresponding measurement equations, Eq. (2.2-2), are highly nonlinear.

To derive the equivalent set of equations in polar coordinates the following transformation is used:

$$x = r \cos \theta; \qquad y = r \sin \theta \tag{2.2-3}$$

Differentiating each of these equations twice with respect to time and solving the resulting pair of simultaneous equations for $\ddot{r}$ and $\ddot{\theta}$ gives

$$\ddot{r} = r\dot{\theta}^2 + \ddot{x}\cos\theta + \ddot{y}\sin\theta$$

$$\ddot{\theta} = \frac{-2\dot{r}\dot{\theta}}{r} + \frac{-\ddot{x}\sin\theta + \ddot{y}\cos\theta}{r} \qquad (2.2\text{-}4)$$

Note that the target's acceleration components along and perpendicular to the line-of-sight (see Fig. 2.2-1) are respectively given by

$$a_r = \ddot{x}\cos\theta + \ddot{y}\sin\theta$$

$$a_\theta = -\ddot{x}\sin\theta + \ddot{y}\cos\theta \qquad (2.2\text{-}5)$$

Substitution from Eq. (2.2-5) into Eq. (2.2-4) produces

$$\ddot{r} = r\dot{\theta}^2 + a_r \qquad (2.2\text{-}6)$$

$$\ddot{\theta} = \frac{-2\dot{r}\dot{\theta}}{r} + \frac{a_\theta}{r} \qquad (2.2\text{-}7)$$

The measurement equations are

$$z_r = r + v_r$$

$$z_\theta = \theta + v_\theta \qquad (2.2\text{-}8)$$

Thus, in polar (r,θ) coordinates the system has nonlinear dynamic equations but linear measurement equations.

For the purpose of evaluating different target tracking filters, a simplified tracking model, defined in terms of polar coordinates, is employed.

With respect to the target's angular motion, the term involving r in Eq. (2.2-7) is neglected, yielding

$$\ddot{\theta} = \frac{a_\theta}{r} \qquad (2.2\text{-}9)$$

This assumption is justified for evaluating design concepts because the primary error in tracking θ tends to be that caused by a_θ, the unknown target normal acceleration -- i.e., its acceleration perpendicular to the line-of-sight. Likewise in Eq. (2.2-6) the primary error in tracking range is caused by a_r, and this equation can be approximated by

$$\ddot{r} = a_r \qquad (2.2\text{-}10)$$

Since Eqs. (2.2-9) and (2.2-10) have the same form it is sufficient to test adaptive tracking schemes using Eq. (2.2-9) as the simplified model of the true system. Once a promising adaptive scheme has been found then it can be easily applied to tracking a target that actually obeys Eqs. (2.2-6) and (2.2-7).

In summary, the various filters in this report are tested against a target that obeys Eq. (2.2-9). These tests are made at a constant range, r, and sensitivity studies are performed to determine how the estimation errors vary with range.

2.3 MEASUREMENT NOISE AND TARGET REFERENCE MODEL

To test tracking filters using a computer simulation, a measurement noise and target reference model must be defined. In an actual tracking situation the measurement data comes from the sensor and only the filter is implemented in the tracking computer. In a computer simulation, the source

of the measurement data must be simulated as well. The measurement noise and target reference model performs this function. In this report the target reference model consists of the simplified tracking model Eq. (2.2-9), and a variety of profiles for the target's normal acceleration, a_θ. The measurement noise reference model consists of errors calculated using the computer random number generator. These errors are then added to the target's computed angular position, θ, to obtain noisy measurements, z_θ.

Figure 2.3-1 is a block diagram of the target and measurement reference model. For a particular test run the following must be defined:

- r - target range, (ft)
- $\dot{a}_\theta(t)$ - normal acceleration rate time history, (ft/sec^3)
- Δt - measurement interval, (sec)
- $v_\theta(t_n)$ - measurement noise sequence, (rad)
- $\theta(0)$ - initial angular position, (rad)
- $\dot{\theta}(0)$ - initial angular velocity, (rad/sec)
- $a_\theta(0)$ - initial normal acceleration, (ft/sec^2)

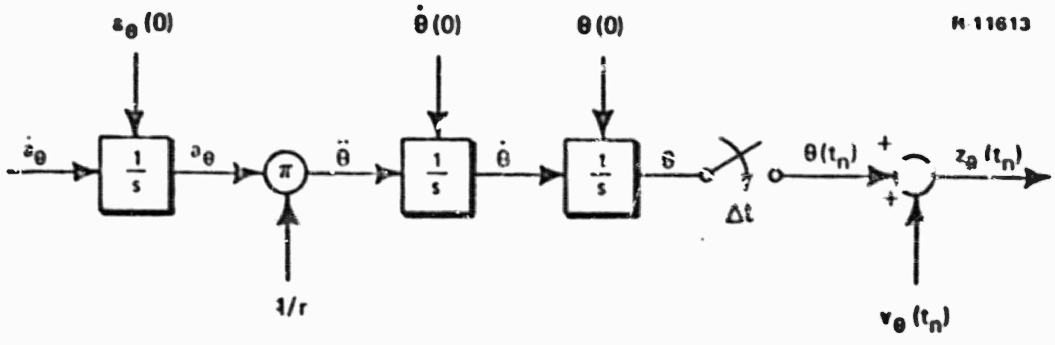

Figure 2.3-1 Target and Measurement Reference Model

The type of target trajectory produced by this model is determined by the choice of $\dot{a}_\theta(t)$. Figure 2.3-2 gives three examples of acceleration rate profiles that might be produced by a target with a large maneuver capability. Both $\dot{a}_\theta$ and the resulting a_θ are plotted for a ten-second trajectory. Part (a) of this figure, where the target has a constant normal acceleration, represents what will be called the nonevasive case. Part (b) is referred to as a "mildly" evasive target which changes its acceleration with the maximum absolute value of $\dot{a}_\theta$ being 50 ft/sec^3 and the rms value being 30 ft/sec^3 or about 1 g/sec. This is called the nominal case. Finally, part (c) of the figure is the highly evasive case which represents the worst evasive motion considered in this study and anticipates the possible capabilities of future antishipping missile threats. Here the maximum absolute value of $\dot{a}_\theta$ is 150 ft/sec^3 and the rms value is 90 ft/sec^3 or approximately 3 g/sec. The filters in this report are optimized for the nominal case, and then tested for all three cases to determine their performance over the complete range of target behavior.

Choosing the noise sequence, $v_\theta(t_n)$, defines the reference model for the measurement noise process. The set of times, t_n, are the sampling or measurement times. Two types of models are used in this report. The first is an uncorrelated, or white, gaussian sequence. Here the samples are chosen from a zero mean gaussian random number generator where the individual members of the sequence are independent of each other, and the rms value of the sequence is σ_v. That is,

$$E[v_\theta(t_n)] = 0 \qquad \text{for all } n$$

$$E[v_\theta(t_n)\, v_\theta(t_m)] = \begin{cases} 0 & n \neq m \\ \sigma_v^2 & n = m \end{cases}$$

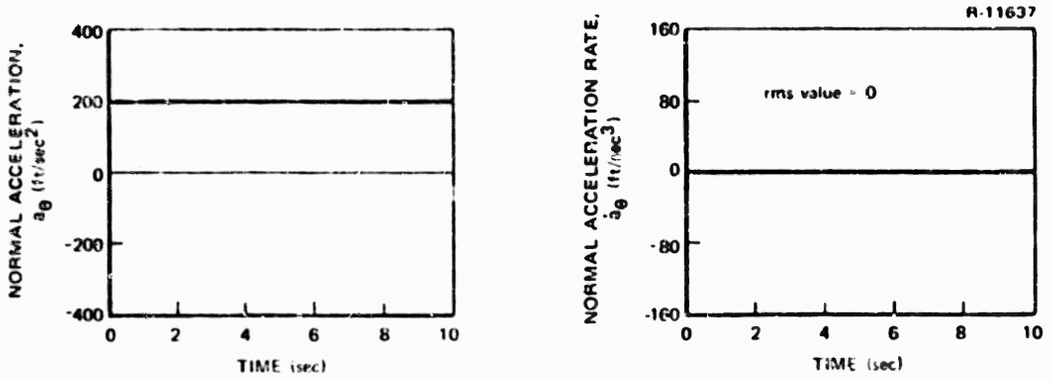

(a) Nonevasive Case, Constant Acceleration ($\dot{a}_\theta = 0$)

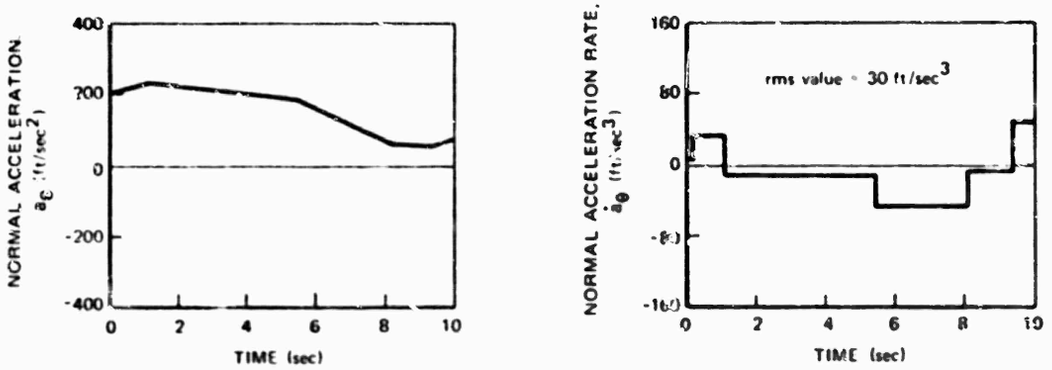

(b) Nominal Case, ($|\dot{a}_\theta| \leq 50$ ft/sec^3)

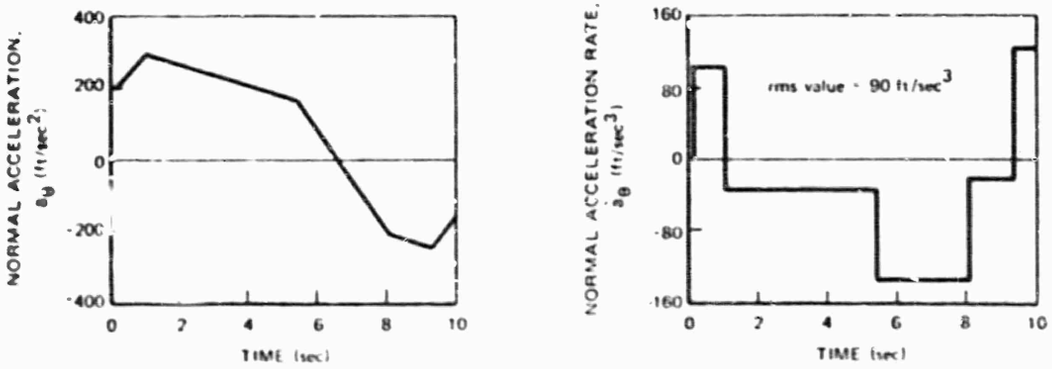

(c) Highly Evasive Case ($|\dot{a}_\theta| \leq 150$ ft/sec^3)

Figure 2.3-2 Target Normal Acceleration Profiles and Their Derivatives

The second noise model is a correlated or "colored" gaussian sequence, having correlated samples generated by passing a white sequence like that defined above through a low pass filter. Specifically, the measurement noise sequence is generated by driving the difference equation for a low-pass filter with the output of a gaussian random number generator. The equation is

$$v_\theta(t_n) = e^{-\Delta t/\tau} v_\theta(t_{n-1}) + w_{n-1} \qquad (2.3\text{-}1)$$

where w_n is a zero mean gaussian white noise sequence, τ is the correlation time, Δt is the measurement interval, and $v_\theta(t_n)$ is the measurement noise at time t_n. To keep the rms value of $v_\theta(t_n)$ equal to the nominal value, σ_v, the rms value of w_n, denoted σ, is given by

$$\sigma = \sqrt{1 - e^{-2\Delta t/\tau}}\ \sigma_v \qquad (2.3\text{-}2)$$

Thus $v_\theta(t_n)$ is a correlated, or "colored", gaussian noise sequence with an rms value equal to σ_v and a correlation time of τ seconds.

In the tracking problem, the sensor (e.g., radar) receiver noise is usually wide-band so that white gaussian noise is a good model. However the total measurement error can also contain low frequency, correlated noise components caused by a slowly varying target cross section, due to the target's own motion. These considerations motivate the two measurement noise models above.

3. TRACKING FILTER DESIGN

3.1 OPTIMAL FILTER DESIGN AND PERFORMANCE

The best tracking algorithm design possible in terms of achieving the minimum mean square estimation error is the Kalman filter outlined in Appendix A. This design requires that the tracking system dynamic and measurement equations be completely known and linear. In addition, the driving functions to the system differential equations must be white gaussian noise processes with known mean and spectral density and the measurement noise must be a gaussian sequence with known mean and covariance. If these conditions are met, the tracking filter design is completely determined.

In this study, the filter designs are based upon the simplified linear model

$$\ddot{\theta} = \frac{a_\theta}{r} \tag{3.1-1}$$

$$z_\theta(t_n) = \theta(t_n) + v_\theta(t_n) \tag{3.1-2}$$

where the range r is assumed known. Equations (3.1-1) and (3.1-2) have the same form as the reference model defined in Chapter 2; however the input to the reference model -- the target acceleration a_θ in Fig. 2.3-2 -- is not accurately represented as white noise and the statistical properties of the measurement noise sequence, $v_\theta(t_n)$, may not be known accurately. These facts prevent the design of an optimal tracking filter.

It is possible to artificially design an optimum filter for the reference model by assuming that the target acceleration rate is known and the measurement noise is gaussian white noise with known covariance. An analysis of this case gives a measure of filter performance under ideal conditions. Equations (3.1-1) and (3.1-2) are the system dynamic and measurement equations, where a_θ and r are given and the covariance (in this case the mean square value) of $v_\theta(t_n)$ is σ_v^2. The dynamic equation can be put into state variable form corresponding to Eq. (A.1-1) of Appendix A by defining

$$\underline{x}(t) = \begin{bmatrix} x_1(t) \\ x_2(t) \\ x_3(t) \end{bmatrix} = \begin{bmatrix} \theta(t) \\ \dot{\theta}(t) \\ a_\theta(t) \end{bmatrix}$$

$$F(t) = F = \begin{bmatrix} 0 & 1 & 0 \\ 0 & 0 & 1/r \\ 0 & 0 & 0 \end{bmatrix} \qquad G(t)u(t) = \begin{bmatrix} 0 \\ 0 \\ 0 \end{bmatrix}$$

and

$$\underline{b}(t) = \begin{bmatrix} 0 \\ 0 \\ \dot{a}_\theta(t) \end{bmatrix}$$

Then Eq. (3.1-1) becomes

$$\dot{\underline{x}}(t) = F\underline{x}(t) + \underline{b}(t) \qquad (3.1\text{-}3)$$

The measurement equation is put in the form of Eq. (A.1-8) by defining

$$z_n = z_\theta(t_n)$$

$$v_n = v_\theta(t_n)$$

$$H = H_n = [1\ 0\ 0]$$

Then

$$z_n = H\underline{x}(t_n) + v_n \tag{3.1-4}$$

Since measurements are taken only at discrete instants of time it is convenient to express Eq. (3.1-3) in discrete time also. It is assumed that the tracking filter is implemented on a digital computer so this formulation will be most natural and efficient.

Assuming a uniform measurement interval of length Δt and using the definitions of Appendix A, Eqs. (3.1-3) and (3.1-4) become

$$\begin{aligned} \underline{x}_n &= \Phi \underline{x}_{n-1} + \underline{b}_{n-1} \\ z_n &= H\underline{x}_n + v_n \end{aligned} \tag{3.1-5}$$

where

$$\Phi = e^{F\Delta t}$$

$$\underline{b}_{n-1} = \int_{t_n-\Delta t}^{t_n} e^{F(t_n-\tau)}\, \underline{b}\,(\tau)\, d\tau$$

To complete the definitions required for the filter equations note that the driving noise covariance matrix, Q_{n-1} is equal to zero (see Eq. A.1-7) and

$$R_n = E[v_n^2] = \sigma_v^2 \qquad (1 \times 1 \text{ matrix})$$

where σ_v is the rms measurement noise level of the reference model. By assuming values for the filter initial conditions, $\hat{\underline{x}}_0(-)$ and $P_0(-)$, the filter equations given in Fig. A.1-1 are completely defined. Again, it is emphasized that both $\dot{a}_\theta$ as a function of time and σ_v, the rms value of measurement noise used in the reference model, must be known to implement the optimum filter.

The filtering algorithm for the case defined above is

$$\hat{\underline{x}}_n = \Phi\hat{\underline{x}}_{n-1} + \underline{b}_{n-1} + \underline{k}_n[z_n - H(\Phi\hat{\underline{x}}_{n-1} + \underline{b}_{n-1})] \qquad (3.1\text{-}6)$$

where $\hat{\underline{x}}_n$ is the optimum state estimate of $\underline{x}_n$ immediately after the measurement z_n is taken and $\underline{k}_n$ is the Kalman gain vector defined by Eqs. (A.1-14), (A.1-15) and (A.1-16). The filter performance is shown in the figures that follow and is based upon the following parameter values:

$$\begin{aligned} \sigma_v &= 1.4 \text{ mrad} && \text{(rms measurement noise level)} \\ \Delta t &= 0.1 \text{ sec} && \text{(measurement sampling interval)} \\ r &= 10{,}000 \text{ ft} && \text{(target range)} \\ \hat{\underline{x}}_0 &= \underline{0} && \text{(initial state estimate)} \end{aligned} \qquad (3.1\text{-}7)$$

with

$$\underline{x}(0) = \begin{bmatrix} 2.0 \times 10^{-3} & \text{rad} \\ 4.0 \times 10^{-2} & \text{rad/sec} \\ 2.0 \times 10^{2} & \text{ft/sec}^2 \end{bmatrix}$$

(3.1-7) cont.

$$P_0(-) = \begin{bmatrix} 2.0 \times 10^{-6}\,\text{rad}^2 & 0 & 0 \\ 0 & 7.1 \times 10^{-4}\,(\text{rad/sec})^2 & 0 \\ 0 & 0 & 2.7 \times 10^{4}\,(\text{ft/sec}^2)^2 \end{bmatrix}$$

Figure 3.1-1 shows the target position, velocity, and acceleration estimation errors as functions of time for a ten-second simulation using the nominal case for $\dot{a}_\theta$ shown in Fig. 2.3-2(b). Part (a) of the figure shows the angular estimation error on the right vertical scale and the position estimation error (measured normal to the line-of-sight) on the left vertical scale. For a range of 10,000 ft. the small angle approximation $e_\theta \cong \sin(e_\theta)$ is valid since $e_\theta = \theta - \hat{\theta}$ is much less than 5 degrees. Thus

$$re_\theta \cong r \sin(e_\theta)$$

gives the position error in feet. Part (b) of the figure makes the same approximation to obtain the velocity error from the angular velocity error.

Since the target acceleration rate is assumed known, it is accounted for exactly by the term $\underline{b}_{n-1}$ in the filter equation, Eq. (3.1-6); therefore the errors shown in the figure are independent of the particular choice of $\dot{a}_\theta(t)$. This is a basic property of the optimal filter since the equtions which propagate and update the estimate of the error covariance matrix, P_n, (Eqs. (A.1-15) and (A.1-16)), are independent of the system input vector $\underline{b}(t)$, which contains $\dot{a}_\theta(t)$. Part (d) of Fig. 3.1-1 shows how the mean square estimation errors converge towards zero as calculated by the filter covariance equations. These

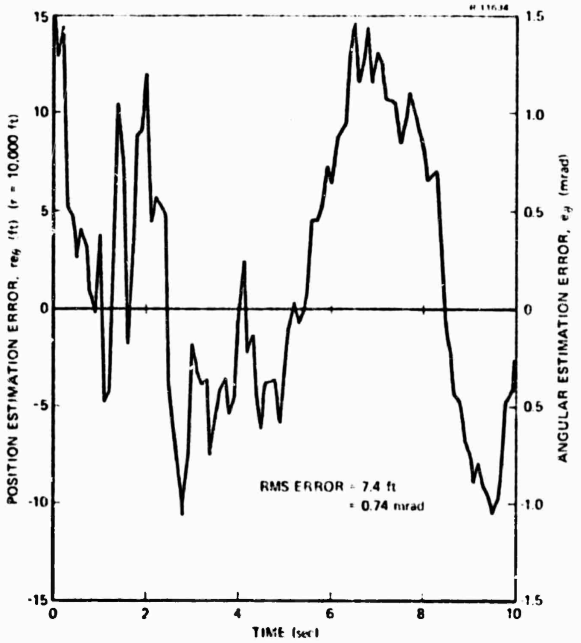

(a) Position Estimation Error

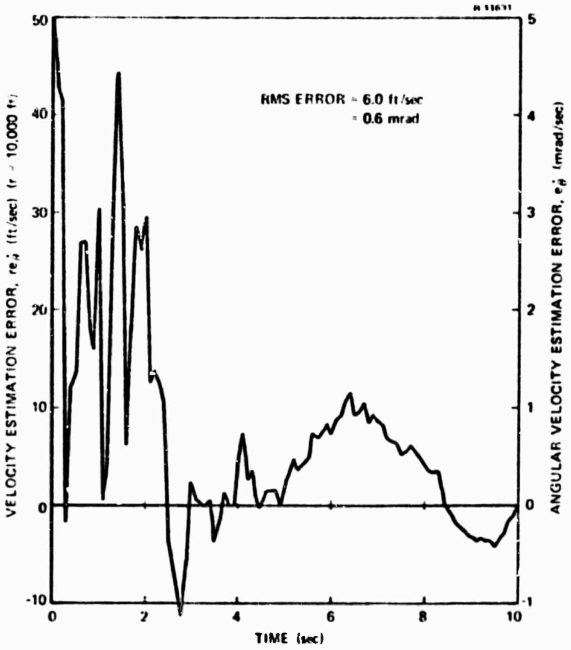

(b) Velocity Estimation Error

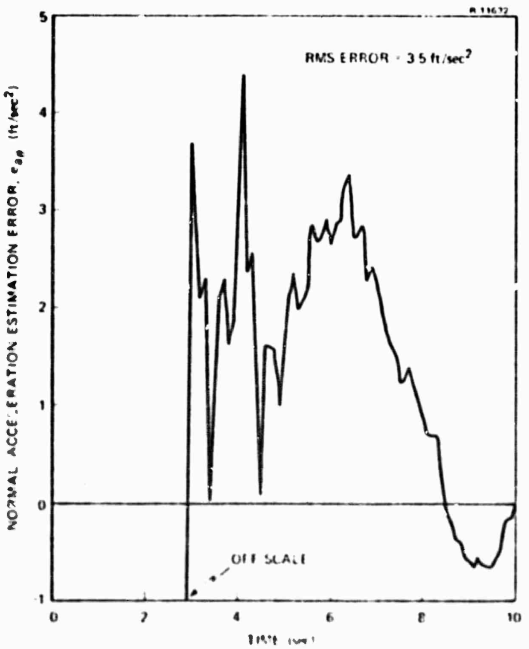

(c) Normal Acceleration Estimation Error

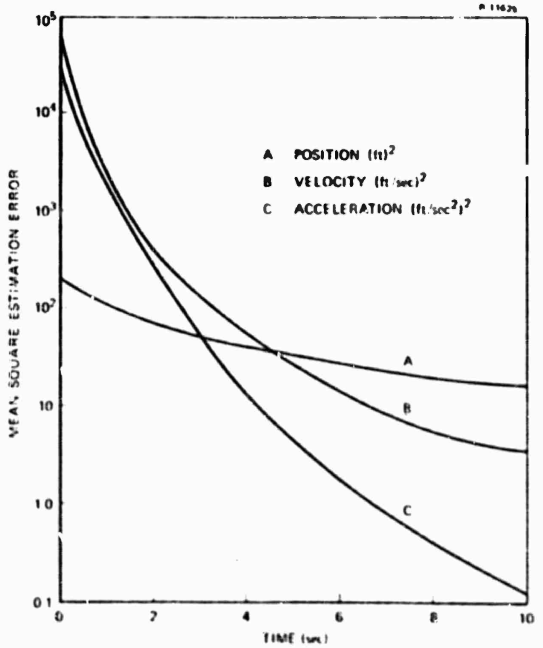

(d) Mean Square Values of Estimation Error

Figure 3.1-1 Estimation Errors and Their Mean Square Values versus Time for the Optimal Filter: Nominal Trajectory

curves are in qualitative agreement with the actual estimation errors shown in parts (a), (b), and (c) of the same figure.

Note that the estimation errors in Fig. 3.1-1 parts (b) and (c) become small relative to their initial values after approximately two seconds. The rms values given for the errors are calculated using only the last eight seconds of the simulation to remove the effect of this initial transient. For the purposes of target prediction discussed later, notice that the three estimation errors are highly correlated; that is, when the normal acceleration estimation error is large and positive, so are the position and velocity estimation errors. This tends to cause the components of the rms prediction error, contributed by the individual estimation errors, to combine additively. Section 4.3 develops this point in more detail.

Figure 3.1-2 gives a clearer illustration of the convergence of the normal acceleration estimate as a function of time relative to the actual value of normal acceleration. Note the rapid convergence to a small percentage error.

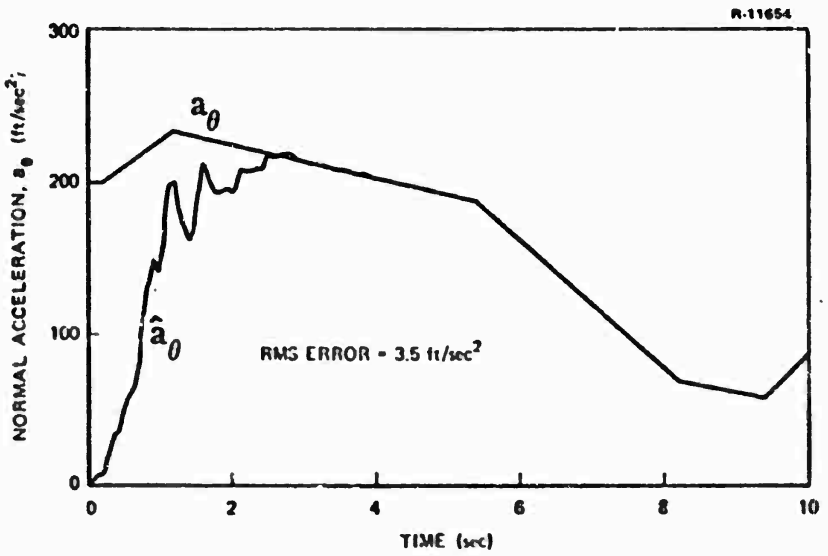

Figure 3.1-2 Normal Acceleration and its Estimate for Optimum Filter: Nominal Trajectory

The results in this section demonstrate the accuracy with which the optimum filter can track the target's states if sufficient knowledge is available to construct the filter. In the next section, practical designs will be discussed where this knowledge is not available.

3.2 PRACTICAL FILTER DESIGN AND PERFORMANCE

The last section demonstrated how an optimum filter would work if the target and measurement model were accurately known. The primary unknowns which make the optimum design impractical are $\dot{a}_\theta(t)$, the time history of acceleration rate, and σ_v, the true rms measurement noise level. This section assumes that σ_v is known and the major problem is dealing with the unknown target normal acceleration. The problem of σ_v being different than its assumed value is left until Section 4.2 where measurement noise sensitivity is discussed.

One common method of dealing with the unknown input $\dot{a}_\theta$ is to assume that it can be approximated by white noise and construct a Kalman-type tracking filter as described in Appendix A. Recall that the reference model equation is

$$\dot{\underline{x}} = F\underline{x} + \underline{b}(t) \tag{3.2-1}$$

A proposed filter design is based upon a model of the form

$$\dot{\underline{x}}_m = F\underline{x}_m + \underline{u}(t) \tag{3.2-2}$$

where the notation $\underline{x}_m(t)$ denotes the model representation for $\underline{x}(t)$ and

$$\underline{u}(t) = \begin{bmatrix} 0 \\ 0 \\ u_3(t) \end{bmatrix}$$

The quantity $u_3(t)$ is assumed to be a gaussian white noise process with

$$E[u_3(t)\, u_3(\tau)] = q\delta(t-\tau) \qquad (3.2\text{-}3)$$

That is, the unknown input $\dot{a}_\theta$ is modeled as gaussian white noise with a spectral density equal to q, (see Appendix A). Recalling Fig. 2.3-2, it is clear that the $\dot{a}_\theta$ signal shown does not look like white noise. However, the white noise model has two advantages. First it does not increase the order (number of states) of the filter beyond that required for the optimum filter discussed in the last section. Second, if the target has a constant acceleration, then $\underline{b}(t) = \underline{0}$ in Eq. (3.2-1) and can be modeled exactly in Eqs. (3.2-2) and (3.2-3) by setting $q = 0$. Furthermore, the white noise model is a good approximation to $\dot{a}_\theta$ if the effective bandwidth of the latter is large relative to other dynamic effects.

The filter design based on Eqs. (3.2-2) and (3.2-3) is the same as that discussed in Section 3.1 except that $\underline{b}(t)$ is unknown and not included in the filter equations and the matrix Q_n, which originally was zero, now becomes

$$Q_n = \int_{t_n-\Delta t}^{t_n} e^{F(t_n-\tau)} \begin{bmatrix} 0 & 0 & 0 \\ 0 & 0 & 0 \\ 0 & 0 & q \end{bmatrix} \left(e^{F(t_n-\tau)}\right)^T d\tau$$

The filter algorithm is

$$\underline{\hat{x}}_n = \Phi \underline{\hat{x}}_{n-1} + \underline{k}_n \left[z_n - H\Phi \underline{\hat{x}}_{n-1}\right] \qquad (3.2\text{-}4)$$

where $\underline{k}_n$ is the Kalman gain sequence defined by Eqs. (A.1-14), (A.1-15), and (A.1-16) when they are based upon the design model. Note that the Kalman gain sequence depends upon the choice of q. This algorithm will be called the suboptimal third-order fixed filter.

The value for the spectral density, q, chosen for the suboptimum filter in Eq. (3.2-4) can be any positive number; however the particular value chosen

effectively determines the filter bandwidth and is therefore very important to the performance of the filter. A low value of q results in a low-bandwidth tracking filter which can accurately track targets that manuver very little -- i.e., the rms value of $\dot{a}_\theta$ is small and target motion is low frequency in nature so a low-bandwidth filter can be used to eliminate the measurement noise from the data. On the other hand, if the target is highly evasive and its motion has high frequency components, then a large value of q is needed so that the filter has a high bandwidth and can respond rapidly to the target motion. In this case, for a fixed measurement rate and measurement noise level, even the best choice of q will give poorer tracking accuracy than the case where q is small and the target manuvers very little. Thus the proper choice of q, and consequently the filter bandwidth, is dependent upon how evasively the target maneuvers. Hereafter, q will be referred to as the design parameter for the third-order fixed filter.

To be more specific, Fig. 3.2-1 shows the results of a series of simulations for the same conditions given in Eq. (3.1-7), except that the sub-optimal filter derived above is employed. The trajectory for $\dot{a}_\theta(t)$ chosen here is that of Fig. 2.3-2(b), the nominal case. The figure shows the mean square estimation errors, again calculated by time-averaging over the last eight seconds of each run to eliminate the effect of the initial transient. The mean square estimation errors of angular position, angular velocity, and normal acceleration are plotted for a wide range of choices of q, the model spectral density which must be selected by the filter designer. All three curves are minimized at approximately the same value of q. Thus, there is a "best" choice for q for this trajectory; but it cannot be determined unless $\dot{a}_\theta(t)$ is known a priori.

Figure 3.2-2 shows how the mean square normal acceleration estimation error varies as a function of q, for the different target trajectories shown in Fig. 2.3-2. The bottom curve in Fig. 3.2-2 is the nonevasive case

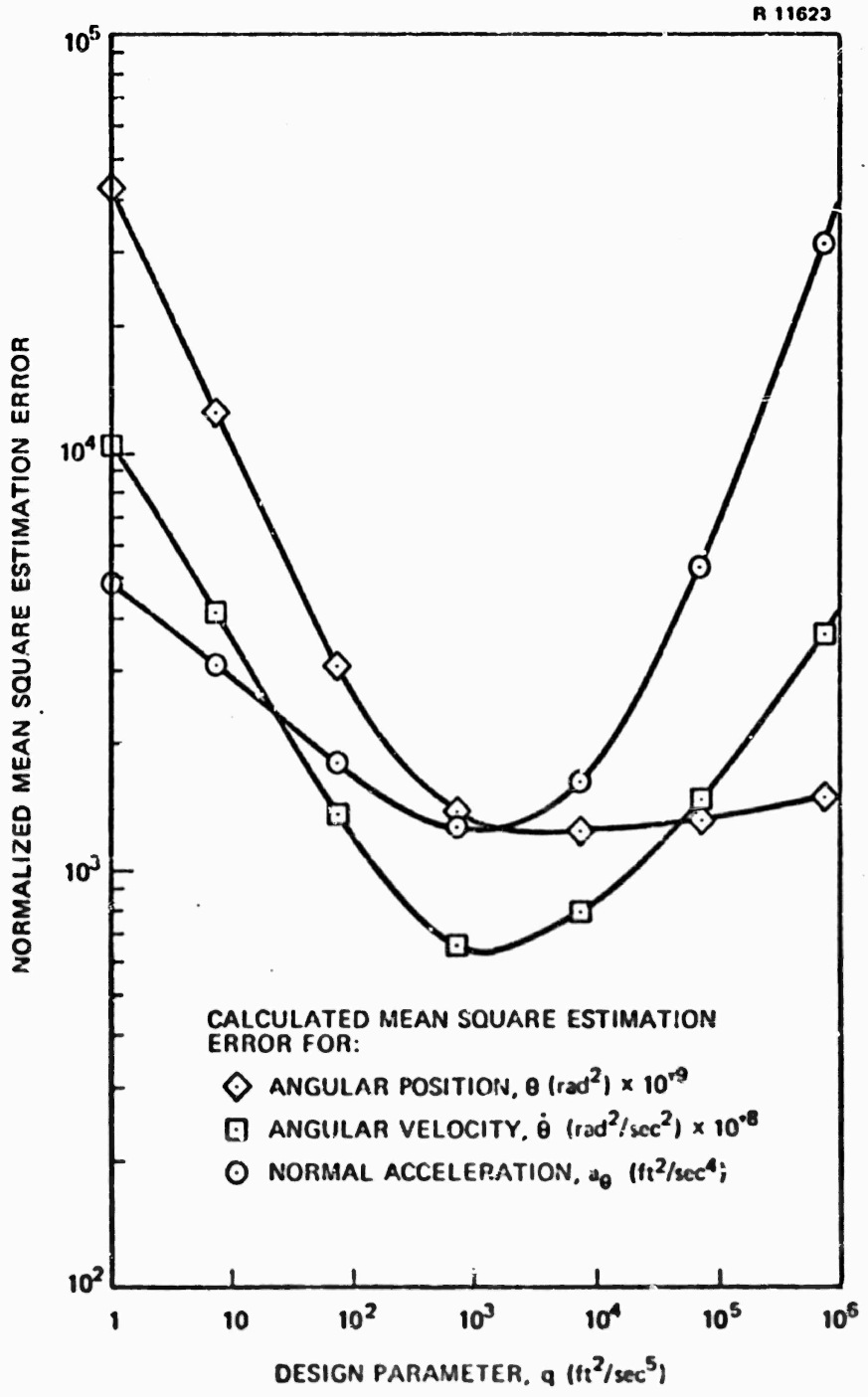

Figure 3.2-1 Third-Order Fixed Filter Performance versus the Filter Design Parameter: Nominal Trajectory

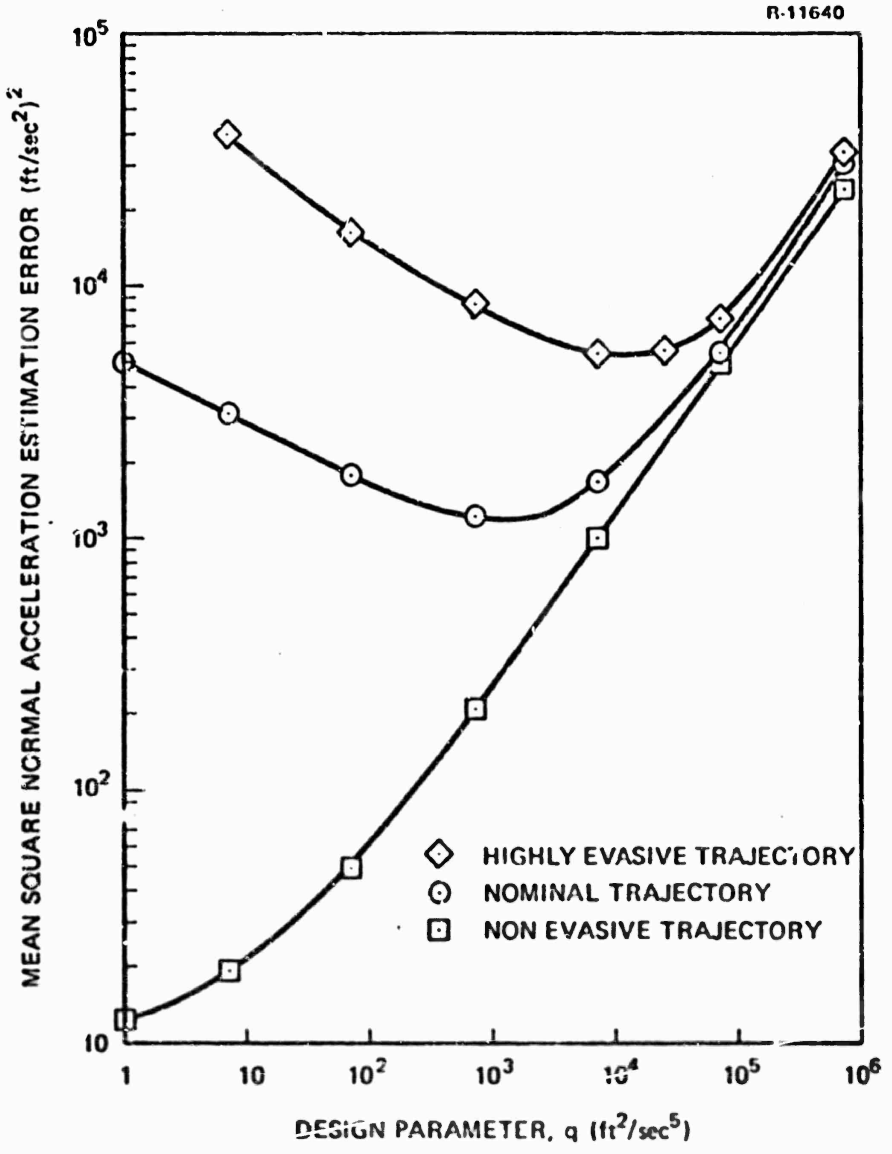

Figure 3.2-2 Trajectory Sensitivity of the Third-Order Fixed Filter

(Fig. 2.3-2(a) where the target acceleration is constant. This curve indicates, as stated earlier, that the optimum choice of q is zero for the nonevasive case. The middle curve corresponds to the nominal trajectory (Fig. 2.3-2(b)) and the best q is near 10^3. Finally, the top curve corresponds to the worst-case evasive trajectory (Fig. 2.3-2(c)) with the best value of $q \simeq 10^4$. Recall that

the optimum filter of Section 3.1 gives the same rms estimation errors regardless of the time-history of $\dot{a}_\theta(t)$ because $\dot{a}_\theta(t)$ is assumed known; this is evidently not the case for the suboptimal filter evaluated in Fig. 3.2-2. The filter's performance deviates farther from optimum as the rms value of $\dot{a}_\theta(t)$ increases, even if the best choice of q is known.

To further clarify the operation of the third-order fixed filter design, it is useful to plot the target normal acceleration and its estimate as a function of time for the nominal trajectory for three different values of q. This is done in Figure 3.2-3 for q equal to 7.5, 750, and 75,000 ft^2/sec^5. The rms estimation error differs significantly between these three plots. Part (a), which is the low q case, corresponds to a filter having a low bandwidth. Observe that the estimate $\hat{a}_\theta$ has difficulty tracking rapid changes in a_θ, however, the time history of $\hat{a}_\theta$ is very smooth indicating that most of the measurement noise is suppressed by the filter. By comparison, Fig. 3.2-3(c), corresponds to a relatively high bandwidth filter. Here $\hat{a}_\theta$ can track a_θ when it varies rapidly, but a lot of the measurement noise gets through the filter and degrades the estimate. Fig. 3.2-3(b) is a medium bandwidth filter and represents a nearly optimum tradeoff between tracking ability and the amount of measurement noise that corrupts $\hat{a}_\theta$; thus it has a lower rms estimation error than the other two cases.

The third-order fixed filter models $\dot{a}_\theta$ as white noise and consequently a_θ as the output of an integrator driven by white noise; in this model the target acceleration is called a random walk process. In an effort to improve the filter's performance, other models for a_θ can be investigated. For example, in another set of simulations, a_θ was modeled as the output of a low pass filter with time constant, τ, driven by white noise with spectral density, q; i.e.,

$$\dot{a}_\theta = -\frac{1}{\tau} a_\theta + \frac{1}{\sqrt{\tau}} u_3 \qquad (3.2\text{-}5)$$

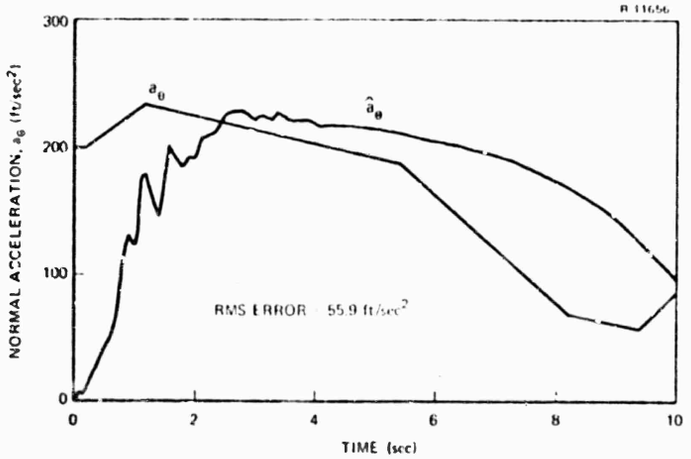

(a) Low Bandwidth Filter, $q = 7.5\ ft^2/sec^5$

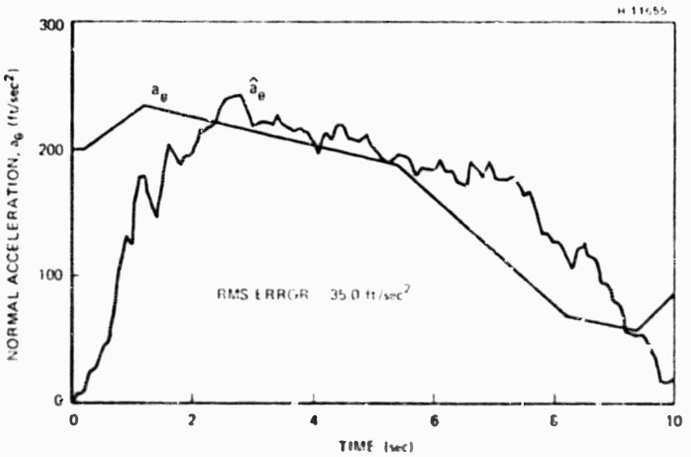

(b) Medium Bandwidth Filter, $q = 750\ ft^2/sec^5$
(Nearly optimum choice of q)

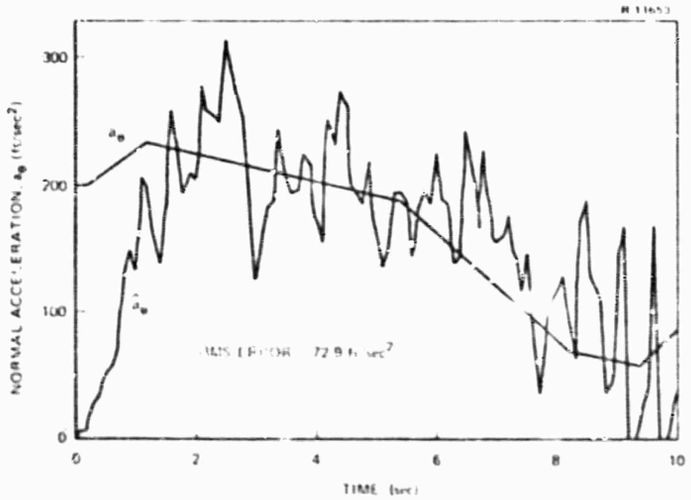

(c) High Bandwidth Filter, $q = 75{,}000\ ft^2/sec^5$

Figure 3.2-3 Third-Order Filter Normal Acceleration Estimates: Nominal Trajectory

In this case two parameters must be selected, τ and q. A filter based upon this model was simulated using the highly evasive trajectory in Fig. 2.3-2(c). The mean square normal acceleration estimation errors as functions of the parameters in Eq. (3.2-5) are shown in Fig. 3.2-4. For comparison, the results for the random walk acceleration model are also given. It is clear from this figure that the random walk model yields better performance than the more complex low-pass model just described. Note also that the various low-pass models are slightly more sensitive to the incorrect choice of q and approach the random walk model as τ is increased.

Another possibility is to try a higher-order acceleration model. For example, in Fig. 3.2-5, a_θ is represented as the output of a double integrator driven by gaussian white noise with spectral density, q. Using this model, the

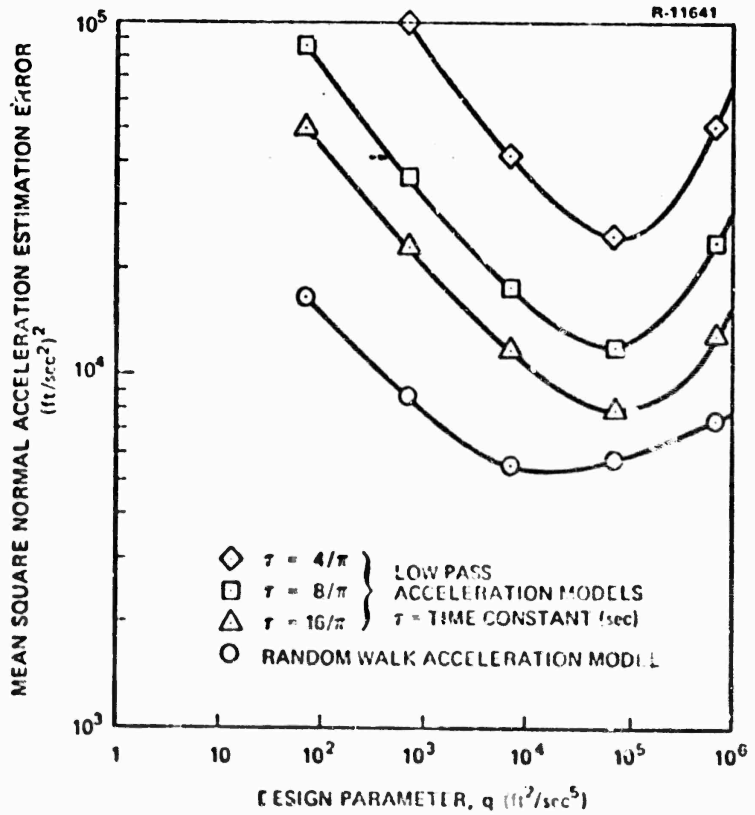

Figure 3.2-4 Performance of Low Pass Acceleration Models: Highly Evasive Trajectory

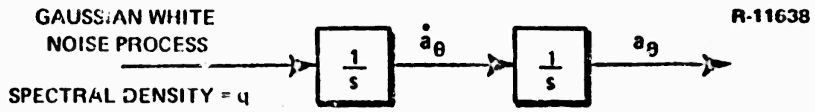

Figure 3.2-5 Doubly Integrated Gaussian White Noise Model for Target Acceleration

equations of Appendix A give a fourth-order fixed filter design. Figure 3.2-6 shows the rms normal acceleration estimation errors achieved with this model for the three test trajectories and compares these errors with those obtained using the third-order fixed filter that assumed a random walk acceleration model. Again it is clear that in each case, the simpler third-order filter works better than the fourth-order filter.

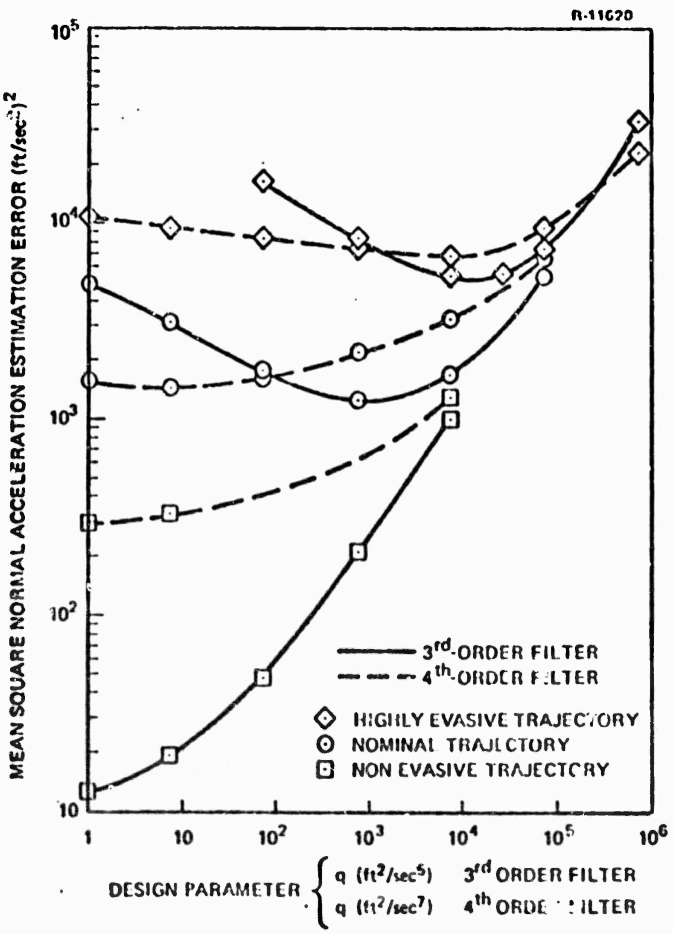

Figure 3.2-6 Comparitive Performance of Third-Order and Fourth-Order Fixed Filters for Three Trajectories

These studies indicate that the fixed filter design, based upon the random walk model for a_θ shown in Fig. 2.3-1 is preferable if the tracking situation is similar to that tested here; i.e., for the given data rate, measurement noise level, and target maneuver characteristics. The main value of these studies is that they show the type of procedure that must be followed to design a filter for a particular class of tracking situations. Clearly the third-order suboptimal filter cannot perform nearly as well as the ideal, but impractical optimum filter described in Section 3.1; however it appears to do about as well as possible if the target maneuver time-history is not known a priori. The primary design problem is the choice of q since its best value is related to the unknown rms value of $\dot{a}_\theta$ over the trajectory. In the next section adaptive designs are considered in an attempt to overcome this problem.

3.3 ADAPTIVE TRACKING FILTER DESIGN

Two steps are important in the design of a target tracking algorithm. First, a mathematical model for target acceleration must be chosen based upon theoretical considerations and experimental work, as described in previous sections. This model must be general enough to cover all anticipated target acceleration profiles. Second, a tracking filter must be designed based upon this model, the target's equations of motion, and the measurement error statistics. Its performance should be as good as possible despite changes in the target's acceleration profile, errors in the particular dynamic model selected for target acceleration, and variations in the measurement noise level. One approach is to experimentally determine the values of the filter design parameters that give the best average performance over all anticipated tracking situations; alternatively the parameters could be optimized for the worst case--i.e., for the most violent target maneuvers and highest measurement noise level. However, a fixed parameter design based on either of these

procedures is likely to perform significantly worse than a design matched to the actual target maneuver characteristics encountered.

A potentially better design than the fixed parameter filter is an adaptive filter which can identify each particular tracking situation as it arises and adjust itself for achieving the best performance. For example, if the type of target trajectory could be identified on-line, then the proper choice of the bandwidth parameter q for the third-order filter could be made. Many different adaptive filtering techniques have been investigated in the past ten years and an extensive literature review was conducted to determine which methods might be useful for the target tracking problem treated here. Three techniques which seem promising are described in this section and computer simulation results are presented in the next chapter. All of these methods start by assuming that the filter is to have the same basic structure as the optimal Kalman filter outlined in Appendix A. They differ in how they change or augment this structure to make the filter adjust for modeling errors and changing conditions. References 1 through 17 contain the adaptive filtering theory found to be pertinent to the tracking problem. The techniques described in this report were developed from this background and represent both applications and extensions of existing techniques.

3.3.1 Adaptive Bandwidth Filter

The general structure of the adaptive bandwidth filter is shown in Fig. 3.3-1, consisting of two connected filters. Filter 1 is a fixed configuration fourth-order Kalman filter which produces estimates of the target evasive maneuver level, that is, the rate of change of target angular acceleration, $\dot{a}_\theta$. Filter 2 is an adaptive bandwidth, third-order Kalman filter which estimates the target's angular position, angular velocity, and normal acceleration. The bandwidth of the latter is controlled by the estimate of target evasive

maneuver level obtained from Filter 1. Thus if the target is not evading and $\dot{a}_\theta$ is small, then the estimate $\hat{\dot{a}}_\theta$ will be small and Filter 2 is adjusted to have a low bandwidth to achieve good noise suppression. If the target begins to change its angular acceleration rapidly, Filter 1 will reflect this fact in its estimate of acceleration rate and will accordingly raise the bandwidth of Filter 2. Essentially this adaptive filter tries to detect how much the target is maneuvering and then adjusts itself to the proper bandwidth for that maneuver level.

The design of the fourth-order fixed filter is the same as that discussed in Section 3.2 where target acceleration is modeled as the output of a double integrator driven by white noise with a spectral density designated by the parameter q; see Fig. 3.2-5 for a block diagram of this model.

Recalling that the third-order filter, investigated in Section 3.2, develops appreciable acceleration estimation errors when the target maneuvers evasively, it is expected that the estimates of acceleration rate from

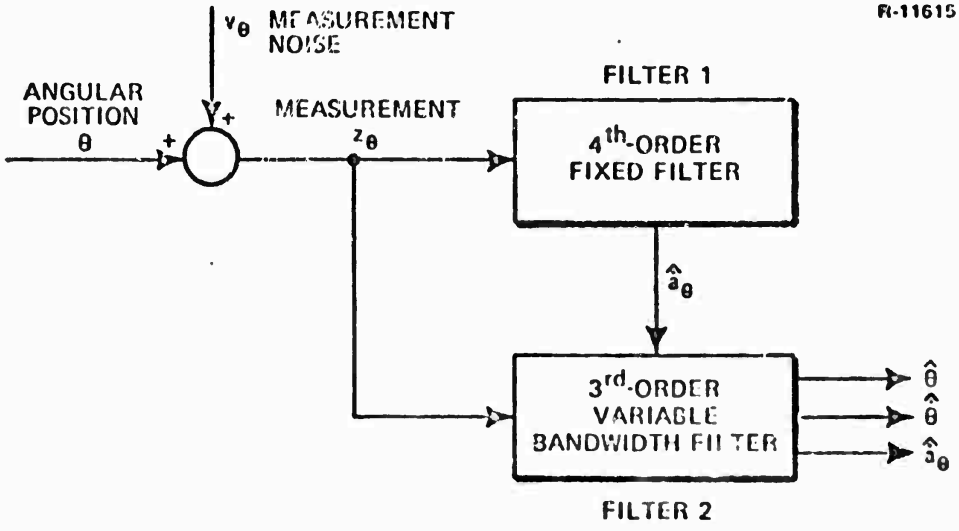

Figure 3.3-1 Adaptive Bandwidth Filter

the fourth-order filter will not be very accurate. However, the philosophy of this design does not require accurate estimates of $\dot{a}_\theta$. What is needed is a general idea of its magnitude so that the bandwidth of the third-order filter can be appropriately adjusted. Assuming that a rough estimate is available for $\dot{a}_\theta$, the design of the variable bandwidth filter in Fig. 3.3-1 is now discussed.

Filter 2 is a third-order Kalman filter which models target acceleration as the output of an integrator driven by gaussian white noise with a spectral density of q. For a constant q, this is the same third-order filter described in Section 3.2. In that section it was determined that the best choice of q was related to the rms value of the acceleration rate for a particular trajectory. For a highly evasive trajectory, the rms value of $\dot{a}_\theta$ is large and a large value of q is required to minimize the rms estimation error. This effectively provides a large filter bandwidth permitting the filter estimates to track the changing target acceleration. Likewise for a nonevasive trajectory where the acceleration rate is small, q should be small so that the filter has a low bandwidth to achieve good noise suppression. In the adaptive design of Fig. 3.3-1, q is calculated on-line using the estimates of $\dot{a}_\theta$ from the fourth-order filter, in the manner described below.

Figures 3.3-2 and 3.3-3 show the results of a series of simulations made to find the optimum choice of the design parameter assuming the target acceleration rate is known. Figure 3.3-2 is a plot of the steady state mean square normal acceleration estimation error produced by a third-order fixed filter which is tracking a target whose acceleration rate is held constant. Each curve is for one particular value of $\dot{a}_\theta$ and shows how the estimation error varies with the choice of q. Except for the fact that acceleration rate is constant, the simulation conditions here are the same as those specified in Section 3.1, Eq. (3.1-7). It is clear from Fig. 3.3-2 that for each value of $\dot{a}_\theta$

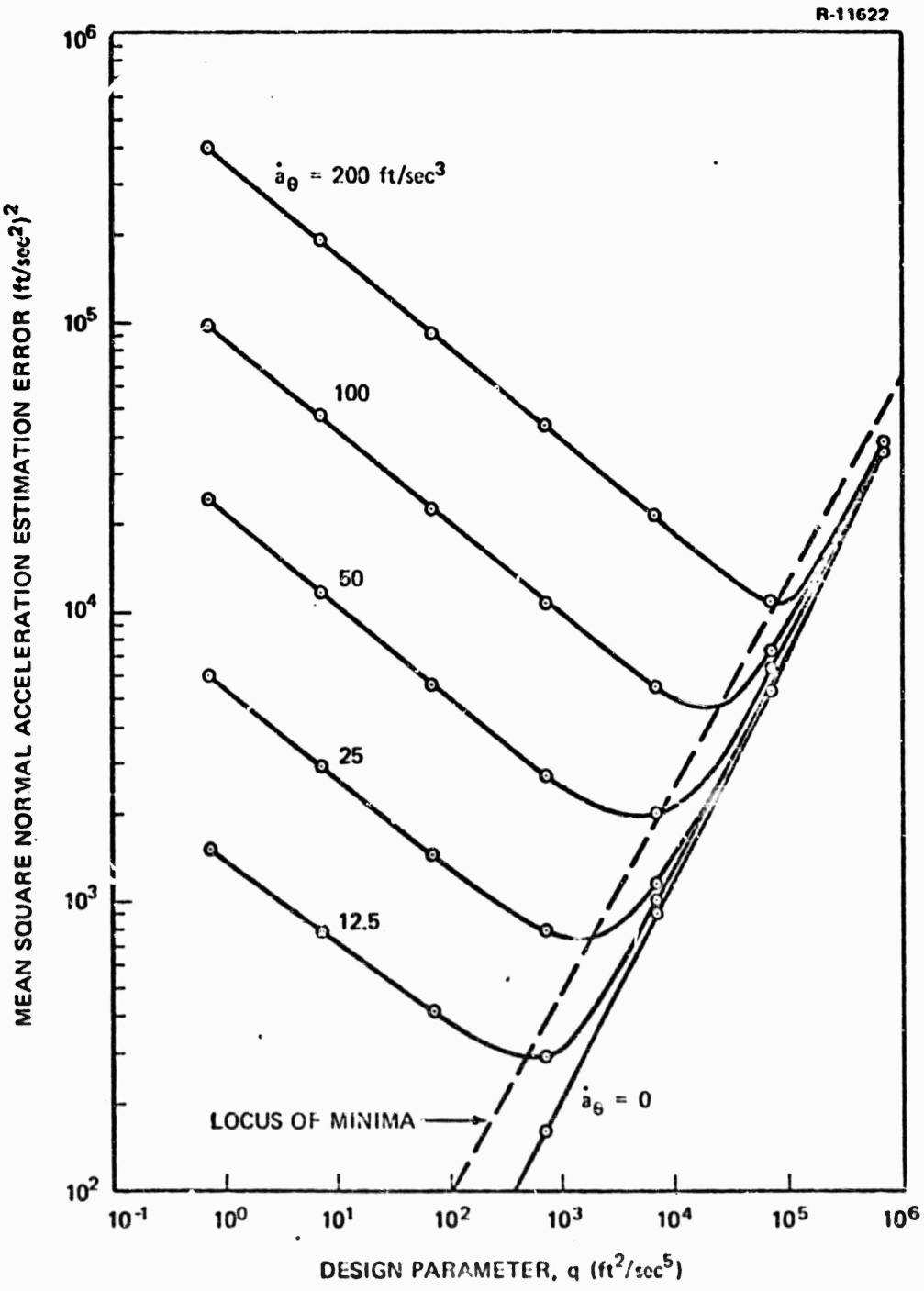

Figure 3.3-2 Mean Square Normal Acceleration Estimation Error versus q for Various Constant Values of Acceleration Rate

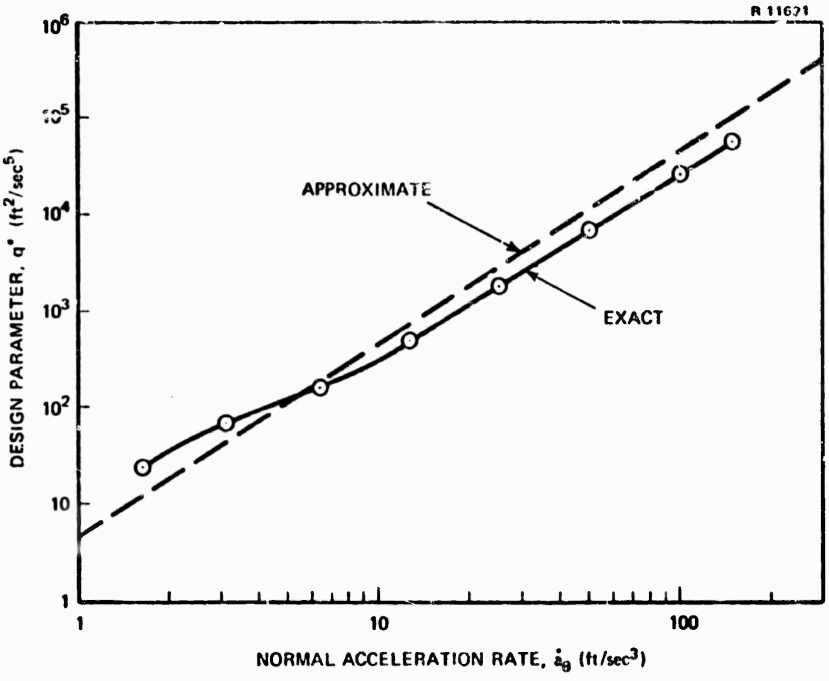

Figure 3.3-3 Optimum Design Parameter versus Target Acceleration Rate: Derived from Fig. 3.3-2

there is an optimum choice of q. The dashed line in the figure is the locus of the minima of the curves. The solid curve in Fig. 3.3-3 is a plot of the best value of the design parameter, designated q*, for each value of acceleration rate. This shows how to choose q for the variable bandwidth filter if the target acceleration rate is known. To simplify the implementation, the dashed curve approximation in Fig. 3.3-3 is used, which is described by the equation

$$q^* \cong 4.8\,(\dot{a}_\theta)^2 \qquad (3.3\text{-}1)$$

This approximation is justified because it results in only small errors in the choice of q*; much larger errors will be incurred in estimating the value of $\dot{a}_\theta$ to be used in Eq. (3.3-1). The fact that q* depends upon the square of the acceleration rate is in agreement with the general relationship between q and the rms value of $\dot{a}_\theta$ indicated in the experiments of Section 3.2.

Replacing $\dot{a}_\theta$ by $\hat{\dot{a}}_\theta$ in Eq. (3.3-1), the third-order filter bandwidth parameter is adjusted according to

$$q = 4.8\,(\hat{\dot{a}}_\theta)^2 \qquad (3.3\text{-}2)$$

and the filter gains $\underline{k}_n$, needed to mechanize Eq. (3.2-4), are computed on-line as shown in Fig. 3.3-4.

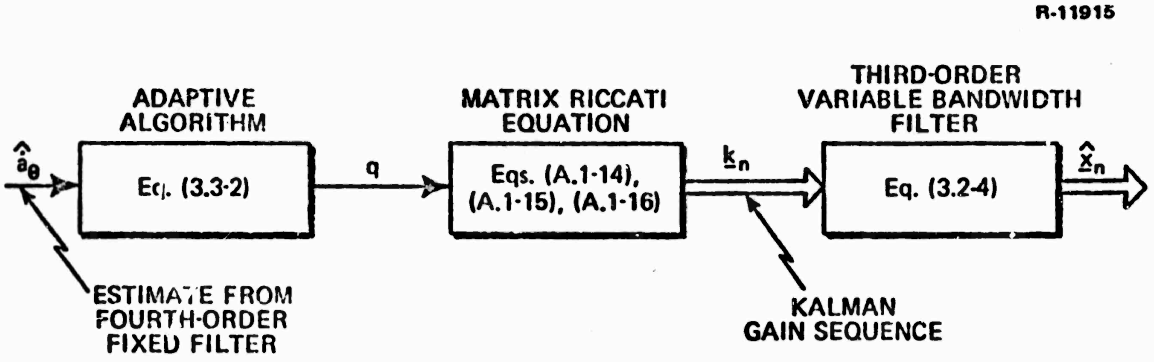

Figure 3.3-4 Functional Diagram of Adaptive Bandwidth Filter Design

The design in Fig. 3.3-4 is based upon the specific set of experimental conditions defined in Eq. (3.1-7). Perhaps the quantity that is least accurately known is the rms value of the measurement noise. If a different level of noise were used in the reference model then Eq. (3.3-2) would have to be rederived. Thus, this adaptive design will be sensitive to inaccurate knowledge of the measurement noise statistics.

Finally, the bandwidth parameter, q, for the fixed fourth-order filter must be selected. Since this quantity is to remain fixed and its optimum value depends on the rms acceleration rate, there is no a priori "best" choice. Here its value is arbitrarily picked to yield the best estimates of $\dot{a}_\theta$ for the nominal trajectory in Fig. 2.3-2(b). This value is determined from Fig. 3.2-6 to be approximately 7.5 ft^2/sec^7. This completes the choice of design parameters for the adaptive bandwidth filter to be used in the simulations described in the next chapter, where the various adaptive techniques are compared.

3.3.2 Hypothesis Testing Filter

This section presents an application of the general hypothesis testing theory discussed in Appendix B. The hypothesis testing filter partially circumvents the problems of fixed filter designs by optimizing the filter design parameters on-line. It assumes that over some time interval, T, the optimum filter is one member of a set of N possible known filters -- i.e., is one of N hypotheses. These filters are run in parallel and an algorithm operates on each set of estimates to calculate the probability that each hypothesis is correct. The final state estimate is the sum of the estimates from all N filters, each weighted by the probability that the corresponding filter is optimum.

Figure 3.3-5 shows the structure of the hypothesis testing filter for the target tracking problem. For the purpose of limiting the amount of computation required, only three parallel filters are considered, each based on the third-order model developed in Section 3.2. Different values of the design

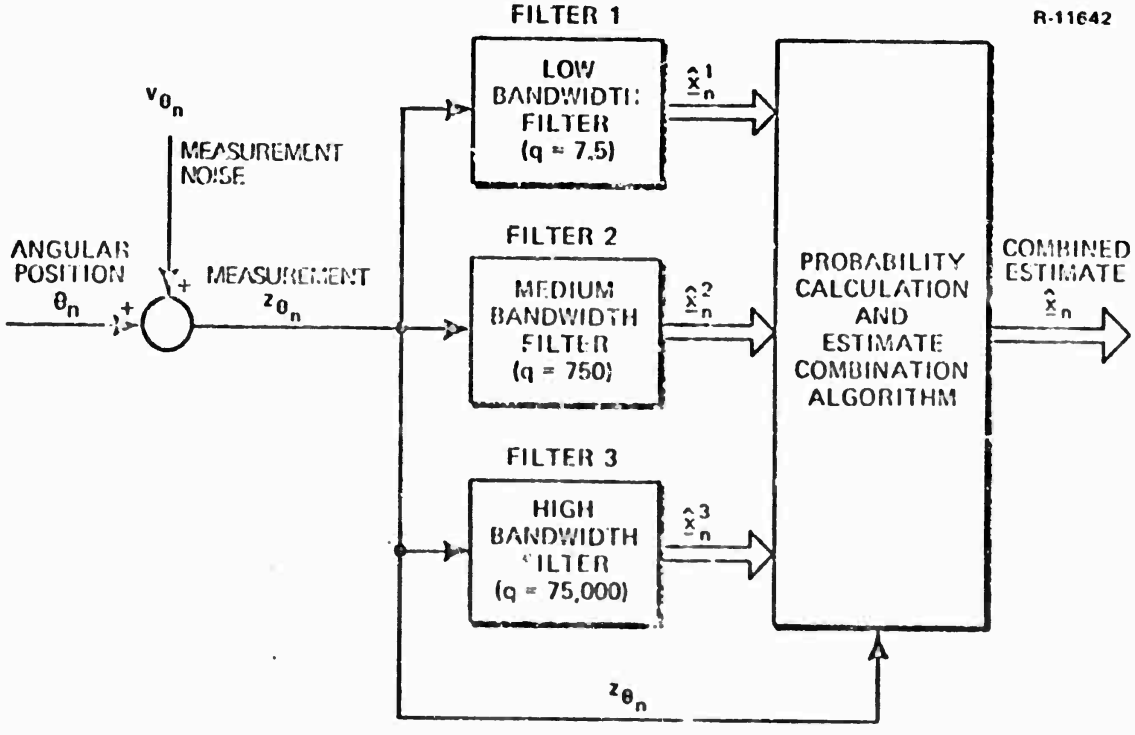

Figure 3.3-5 Hypothesis Testing Filter

parameter q are chosen to represent different hypotheses about the target behavior. The low, medium, and high values of q shown in the figure correspond to low, moderate, and high target evasive maneuver levels.

Following the notation of Appendix B, H^1 is the hypothesis that Filter 1 is optimum over the interval T. H^2 and H^3 are designated in a similar manner. The interval measurement history, Z_n, up to and including the most recent measurement z_{θ_n} is the set

$$Z_n = \left\{ z_{\theta_{n-m-1}}, \ldots, z_{\theta_{n-1}}, z_{\theta_n} \right\}$$

where m is the number of measurements taken in the interval.

Given the three estimates of the system state $\underline{x}_n$ during the interval, denoted by $\hat{\underline{x}}^1_n$, $\hat{\underline{x}}^2_n$, and $\hat{\underline{x}}^3_n$, and generated by Kalman filters designed according to the procedure described in Section 3.2, the probability of each hypothesis conditioned on the measurements, denoted by $p\{H^k | Z_n\}$, is given recursively by

$$p\{H^k | Z_n\} = \frac{f\left(z_{\theta_n} | H^k, Z_{n-1}\right) p\left\{H^k | Z_{n-1}\right\}}{\sum_{k=1}^{3} f\left(z_{\theta_n} | H^k, Z_{n-1}\right) p\left\{H^k | Z_{n-1}\right\}} \qquad (3.3\text{-}3)$$

where $f\left(z_{\theta_n} | H^k, Z_{n-1}\right)$ is a known normal probability density function defined in Appendix B. In this manner, the probability that each hypothesis is true is calculated at every sampling time in the interval.

The estimate produced by the hypothesis testing filter immediately after a measurement is

$$\underline{\hat{x}}_n(+) = \sum_{k=1}^{3} \underline{\hat{x}}_n^k(+)\, p\left\{H^k|Z_n\right\} \qquad (3.3\text{-}4)$$

with the corresponding covariance matrix given by

$$P_n(+) = \sum_{k=1}^{3} P_n^k(+)\, p\left\{H^k|Z_n\right\} \qquad (3.3\text{-}5)$$

To complete the filter design, it is necessary to select the reset interval, T, and the a priori probabilities needed to initialize Eq. (3.3-3) at the beginning of each interval. The interval T should reflect the approximate length of time over which the target's behavior is likely to remain constant. The a priori probabilities for each hypothesis should be chosen using any knowledge available which indicates the relative probabilities of the various types of target behavior. For example, if it is reasonably certain that the target will have a highly evasive trajectory, then the a priori probability of the third hypothesis should be set much higher than that of the others.

At the end of each interval the filters are reset to test for the possibility that a change has occured in the target manuver characteristics. This is done by resetting all three estimates and covariance matrices to the combined estimate and combined covariance matrix as calculated by Eqs. (3.3-4) and (3.3-5) at the end of the interval, and the probability of each hypothesis is reset to its a priori value. This procedure allows the tracking filter to periodically adapt to new target behavior.

This design has two disadvantages. First, it requires approximately three times as much computation as the third-order fixed filter discussed in Section 3.2 and about 30% more computation than the adaptive bandwidth design

which only requires that two filters be implemented. Second, it will be demonstrated in the results of Chapter 4 that this design is very sensitive to the proper choice of the design value for the rms measurement noise level; that is, if the noise level is not known accurately and the filter is designed assuming the wrong value, the estimation accuracy is seriously degraded. This limits the use of the hypothesis testing filter to tracking situations where the measurement noise level is fairly well known a priori. Otherwise, this design is theoretically sound and can be expected to work quite well as long as the assumptions upon which it is based are not seriously violated.

3.3.3 Residual Testing Filter

The residual testing filter is similar to the design discussed in the last section; its complete details are given in Appendix B. The motivation for this particular design is the noise sensitivity problem discovered when the hypothesis testing filter was tested for various rms measurement noise levels; it is an attempt to retain the advantages of the hypothesis testing scheme while reducing its noise sensitivity. Figure 3.3-6 shows the structure of the residual testing filter, where the individual filters 1, 2, and 3 are exactly the same design as those in Fig. 3.3-5. That is, Filters 1, 2, and 3 are designed for low, moderate, and high target maneuver levels, respectively. The difference between this approach and the hypothesis testing filter is the manner in which the final state estimate is calculated from the three individual state estimates.

This residual testing technique does not attempt to calculate the probability that one of the individual filters is optimum over an interval. Instead it observes each state estimate over the interval T, at the end of which a decision is made as to which estimate is best. Over the next interval, the residual testing filter's output is the output of that individual filter which worked best over the previous interval.

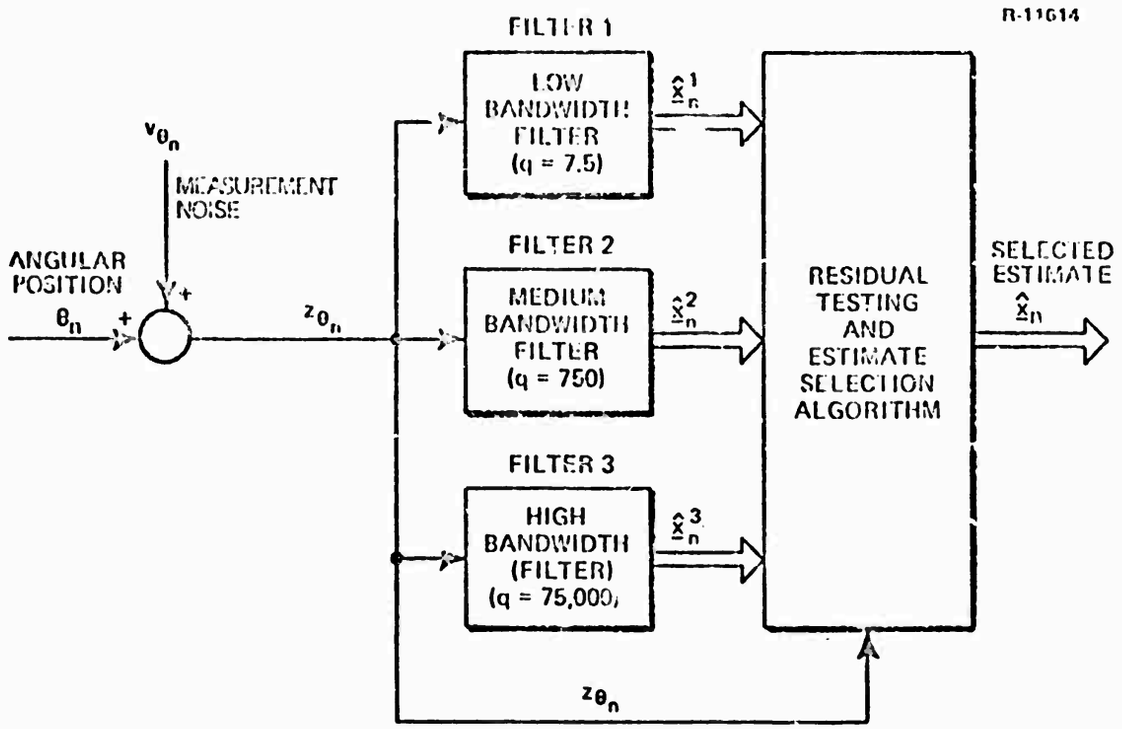

Figure 3.3-6 Residual Testing Filter

The best of the three parallel filters over an interval is defined to be that one whose residual sequence has the smallest mean square value. Elements of the residual sequence for the k^{th} filter are defined as

$$\gamma_n^k = z_{\theta_n} - H\hat{\underline{x}}_n^k(-) \qquad (3.3\text{-}6)$$

The mean square value is computed from the residual sequence using

$$\hat{\bar{g}}^k = \frac{1}{M}\sum_{n=n_o}^{n_o+M-1}(\gamma_n^k)^2 \qquad (3.3\text{-}7)$$

where n_o is the value of the time index n at the beginning of the interval, T, and M is the total number of samples in the interval. This calculation is performed for each filter, i.e., k = 1, 2, and 3, and at the end of the interval that filter which has the lowest value of $\hat{\bar{g}}^k$ is judged best. Its estimates are the

output of the residual testing filter over the next interval. The justification for this adaptive procedure is discussed in detail in Appendix B.

At the end of every interval, each filter is reset to the state estimate and covariance matrix of the filter which is judged to be best. This is done to permit adaptation to changes in target behavior. The design of the residual testing filter is completed by choosing the reset interval, T. This must be a practical compromise between the objective of achieving rapid adaptation, which requires a small T, and achieving an accurate estimate of the rms level of the residuals, which requires a reasonable averaging interval in Eq. (3.3-7).

The computational requirements of the residual testing scheme are essentially the same as those for the hypothesis testing filter. However, it has the advantage that it is less sensitive to differences between the actual and design values for the rms measurement noise level than the other adaptive filter design techniques as demonstrated by the simulation results presented in the next chapter.

In this chapter, practical-suboptimum target tracking filters were designed and discussed in relation to the optimum design. Both fixed and adaptive filter structures applicable to the target tracking problem were considered. In the next chapter, these designs are compared and evaluated in a variety of tracking situations to see which of them would make good target tracking filters in a practical application.

4. TRACKING FILTER PERFORMANCE EVALUATION

This chapter gives the results of simulations designed to compare the performance of the fixed and adaptive tracking filters discussed in the preceeding chapter. In the first half of this chapter the results are presented in terms of the accuracy with which the filter can estimate the target's position, velocity, and acceleration and in the second half these same results are presented in terms of the accuracy with which the filter can predict the future position of the target. The filters are evaluated for different levels of target evasive behavior, levels of measurement noise, data rates, amounts of correlation in the measurement noise, and target ranges. In Section 4.4, the sensitivity of prediction error to projectile velocity and target closing velocity is also discussed. The advantages and disadvantages of each filter are analyzed and related to the specific properties of each design.

4.1 TRACKING FILTER EVALUATION PROCEDURE

To give a fair and logical comparison between several filters, it is necessary to define a nominal tracking situation. Each algorithm is designed based upon this nominal situation; performance results are then compared for a variety of different operating conditions. The following set of conditions define the nominal tracking situation:

- The target's normal acceleration profile is given in Fig. 2.3-2(b), the nominal case with the rms value of acceleration rate ($\dot{a}_\theta$) equal to 30 ft/sec^3.
- The target's range (r) is 10,000 ft.

- The measurement noise sequence $v_\theta(t_n)$ is a white gaussian sequence with an rms level of $\sigma_v = 1.4$ mrad, i.e., the rms angular measurement error is 1.4 mrad, or equivalently, the rms position measurement error normal to the line-of-sight at 10,000 ft is 14 ft.

- The data rate is 10 measurements per second.

- The initial estimate at t = 0 for all filters is $\underline{\hat{x}}_0 = \underline{0}$.

- The initial covariance of the estimation error at t = 0 for all filters is

$$P_0(-) = \begin{bmatrix} 2.0 \times 10^{-6}\,(\text{rad})^2 & 0 & 0 \\ 0 & 7.1 \times 10^{-4}\,(\text{rad/sec})^2 & 0 \\ 0 & 0 & 2.7 \times 10^{4}\,(\text{ft/sec}^2)^2 \end{bmatrix}$$

- The initial condition on the target is

$$\underline{x}(0) = \begin{bmatrix} 2.0 \times 10^{-3} & (\text{rad}) \\ 4.0 \times 10^{-2} & (\text{rad/sec}) \\ 2.0 \times 10^{2} & (\text{ft/sec}^2) \end{bmatrix} = \begin{bmatrix} \theta(0) \\ \dot{\theta}(0) \\ a_\theta(0) \end{bmatrix}$$

This nominal tracking situation is selected to be generally representative of digital gun fire control system capabilities. The tracking filters are evaluated by holding all of the above conditions constant except one, which is varied to test the sensitivity of each design to a change in that condition only. Six different tracking filter designs were investigated. These are specified below.

Filter A -- Third-Order Fixed - Filter A is the third-order fixed design discussed in Section 3.2 which models the target's normal acceleration

as the output of a single integrator driven by white gaussian noise with a spectral density of q. For this design, q is chosen to be equal to 750 (ft^2/sec^5), which is approximately the best value for the nominal target acceleration profile, as indicated by Fig. 3.2-1.

Filter B -- Adaptive Bandwidth - The adaptive bandwidth filter is discussed in Section 3.3.1. Its structure is specified in Figs. 3.3-1 and 3.3-4.

Filters CE, CL, and CH -- Hypothesis Testing - The design of the hypothesis testing filter is discussed in Section 3.3.2 and its structure is shown in Fig. 3.3-5. In each case the reset interval chosen is T = 2 seconds. This choice is made because any shorter interval does not give the probability calculation algorithm, (Eq. (3.3-3)), sufficient time to converge to the correct hypothesis in the nominal tracking case, whereas a longer reset time reduces the filter's ability to adapt rapidly if the tracking situation changes. Filters CE, CL, and CH are exactly the same design except for the choice of the a priori probabilities, $p\{H^k\}$, at the beginning of each reset interval. Filter CE assumes that all three of the hypotheses are equally probable at the start of each interval. Filter CL assumes that there is a high probability that the low maneuver filter is optimum; specifically

$$\left.\begin{aligned} p\{H^1\} &= 0.90 \\ p\{H^2\} &= p\{H^3\} = 0.05 \end{aligned}\right\} \text{Filer CL}$$

Filter CH assumes that there is a high probability that the filter designed for the highly evasive manuver case is optimum. The a priori probabilities chosen are

$$\left.\begin{aligned} p(H^1) &= p(H^2) = 0.05 \\ p(H^3) &= 0.90 \end{aligned}\right\} \text{Filter CH}$$

Filter D -- Residual Testing - The design of the residual testing, filter is discussed in Section 3.3.3 and its structure is shown in Fig. 3.3-6. Here again the reset interval chosen is 2 seconds because this is the shortest interval found to permit a realistic choice between the three parallel filters based on the analysis of the residual sequence. For shorter intervals there is not enough data to make an accurate estimate as to which filter is operating best under the nominal tracking conditions.

The six filters and their letter designations are summarized as follows:

- A - Third-Order Fixed Filter
- B - Adaptive Bandwidth Filter
- CE - Hypothesis Testing Filter (Equal Probability)
- CL - Hypothesis Testing Filter (Low Evasion Probability)
- CH - Hypothesis Testing Filter (High Evasion Probability)
- D - Residual Testing Filter

4.2 FILTER PERFORMANCE AND SENSITIVITY COMPARISONS

In this section the six filters described above are compared in terms of rms errors in the estimates of the current (not predicted) target position, velocity, and acceleration under different tracking situations. The rms estimation error shown on the figures is calculated by taking the square root of the time average of the estimation error squared over the period from two seconds until ten seconds. This is done to omit the initial transient in the estimation error. The transient is due to the large initial errors in the estimates which are rapidly eliminated by all of the filter designs-- for example, see Fig. 3.2-3. In all of the results presented, except for the range sensitivity study, only the rms normal acceleration estimation error is shown because the

accuracies of the angular position and angular velocity estimates for the various filters usually compare in the same manner. As shown in Section 4.3, target acceleration estimation error is the primary contributor to prediction error.

4.2.1 Sensitivity to Target Maneuver Level

Figure 4.2-1 shows how each filter performs for the three target acceleration profiles defined in Fig. 2.3-2. The results for the six filters are presented in two parts for clarity; the results for Filters A and CE are shown in each part of the figure for comparison purposes. Note that the rms normal acceleration estimation error goes up almost linearly as a function of the target's rms normal acceleration rate for each design. Thus, as the target increases its level of evasive maneuvers, all designs have decreasing accuracy.

For the nominal trajectory--i.e., the mildly evasive case--the simple third-order fixed filter is best, as expected, since it is optimized for this case. The other filters give only a slightly higher rms error, except for the hypothesis testing filter (CH) which assumes that there is a high probability that the target will maneuver in an evasive manner; for the nominal trajectory this is a poor assumption, which is reflected in the filter's performance.

For the nonevasive trajectory, Filter CH again works poorly, as expected. However, Filters B and CL offer a signficant improvement over Filter A, the fixed third-order filter. Filter B (adaptive bandwidth) is clearly best able to recognize the fact that the target is not changing its normal acceleration and lowers its bandwidth accordingly by reducing q to achieve a lower rms estimation error. Filter CL also works well because it assumes that there is a high probability that the target is nonevasive and, for this

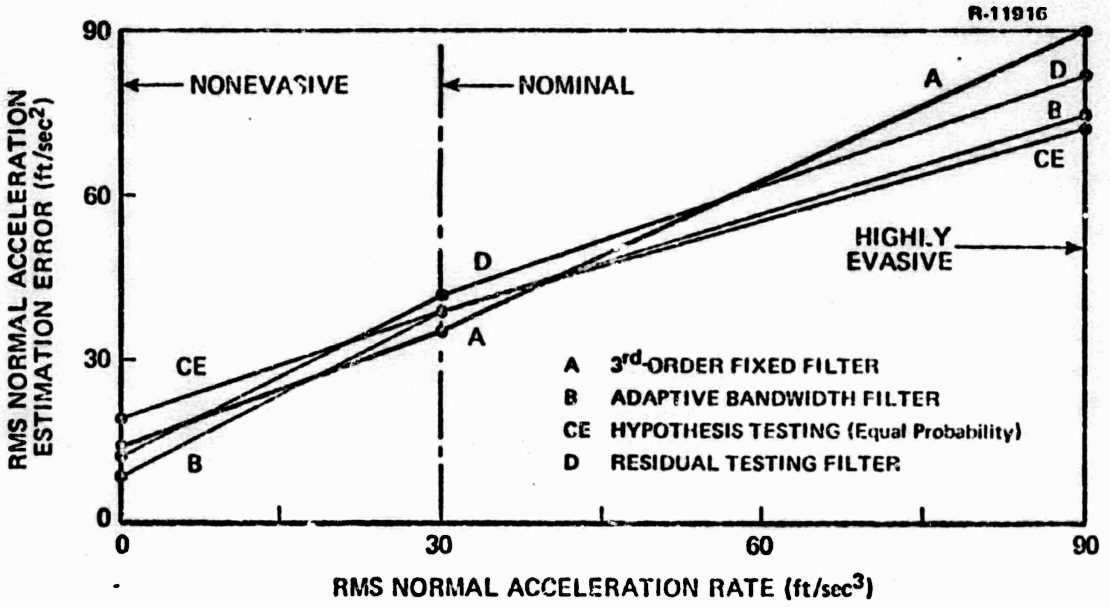

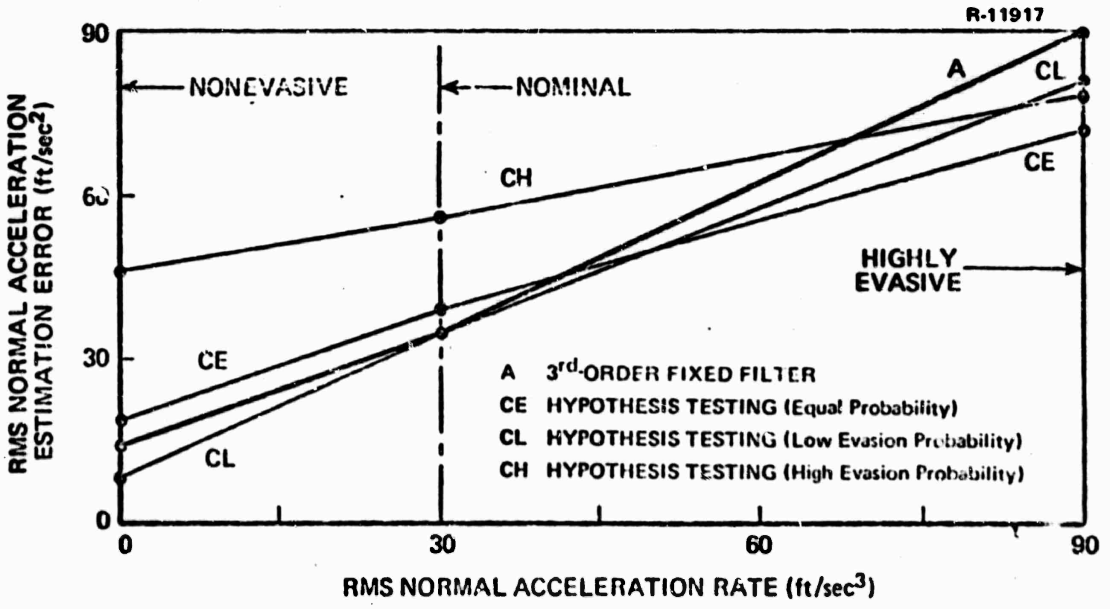

Figure 4.2-1 Tracking Filter Sensitivity to rms Acceleration Rate (Nonevasive, Nominal, and Highly Evasive Trajectories)

trajectory, this is an accurate assumption. Filter CE, the equiprobability hypothesis testing filter, works fairly well compared to the others considering the fact that it assumes that all types of trajectories are equally probable, when the actual trajectory is nonevasive. Filter D, the residual testing filter, has only a slightly lower rms estimation error than that of the much simpler Filter A. Figure 4.2-2 shows time-histories of the acceleration estimates of the CE and CL filters for the nonevasive case and demonstrates the importance of a priori probabilities in the hypothesis testing design, since the two filters are exactly the same except for the choice of their a priori probabilities.

For the evasive trajectory, all of the adaptive designs offer an improvement over the fixed design. In Fig. 4.2-1, notice that the CH filter gives the curve with the smallest slope. This indicates that for sufficiently violent target manuvers (more violent than those tested here), the CH filter would be the best. Figure 4.2-3 shows the acceleration estimate of the CE filter for this case.

In general, Fig. 4.2-1 shows that adaptive designs yield some improvement over the fixed design if the change in target behavior is radical. It also shows that even the best design has a high rms estimation error if the target behaves evasively. Filter B, using the adaptive bandwidth principle, gives the best overall performance. The biggest percentage improvement in estimation error achieved by the adaptive filters over the fixed design is at low rms acceleration rates. At high rates no design significantly reduces the tracking error below that of the third-order fixed filter which is optimized for the high rate case.

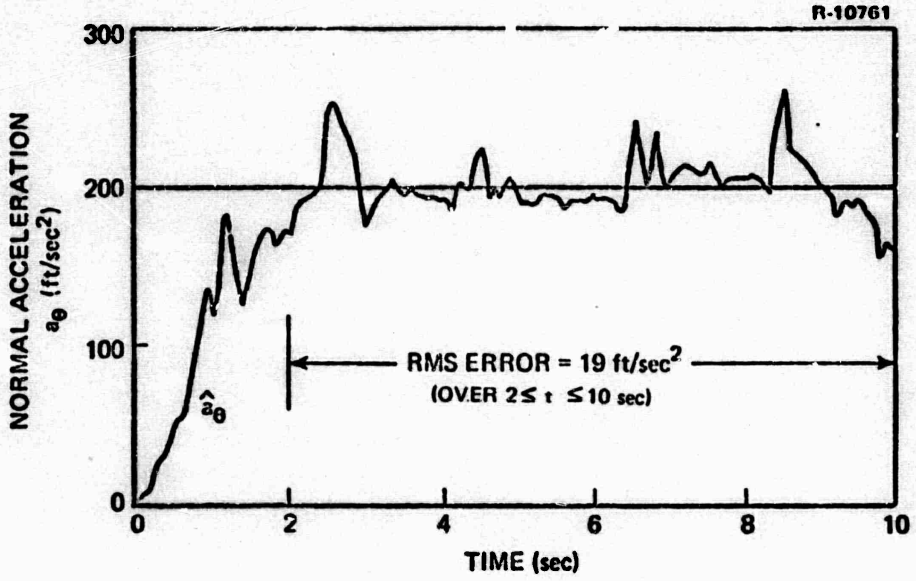

(a) Hypothesis Testing Filter (Equal Probability) – Filter CE

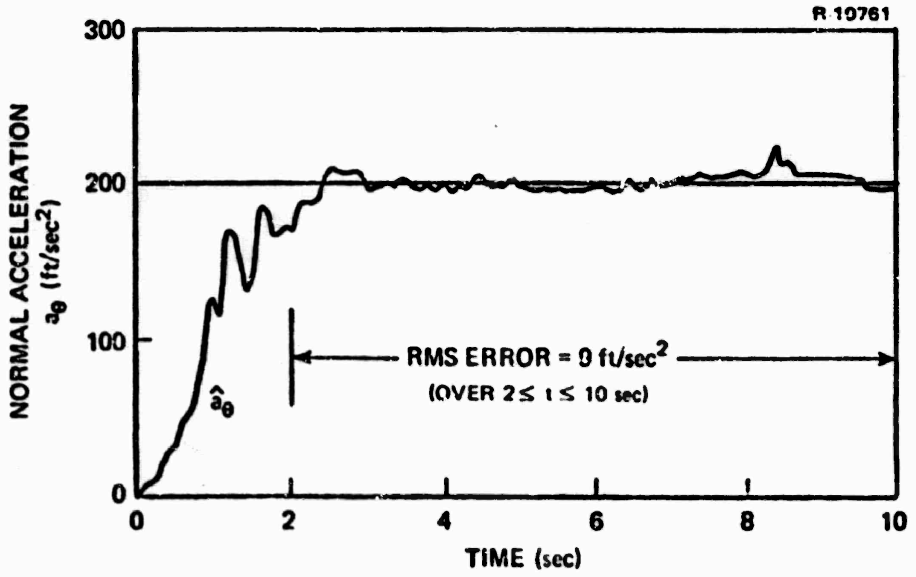

(b) Hypothesis Testing Filter (Low Evasion Probability) – Filter CL

Figure 4.2-2 Normal Acceleration and Its Estimate using Hypothesis Testing Filters CE and CL: Nonevasive Trajectory

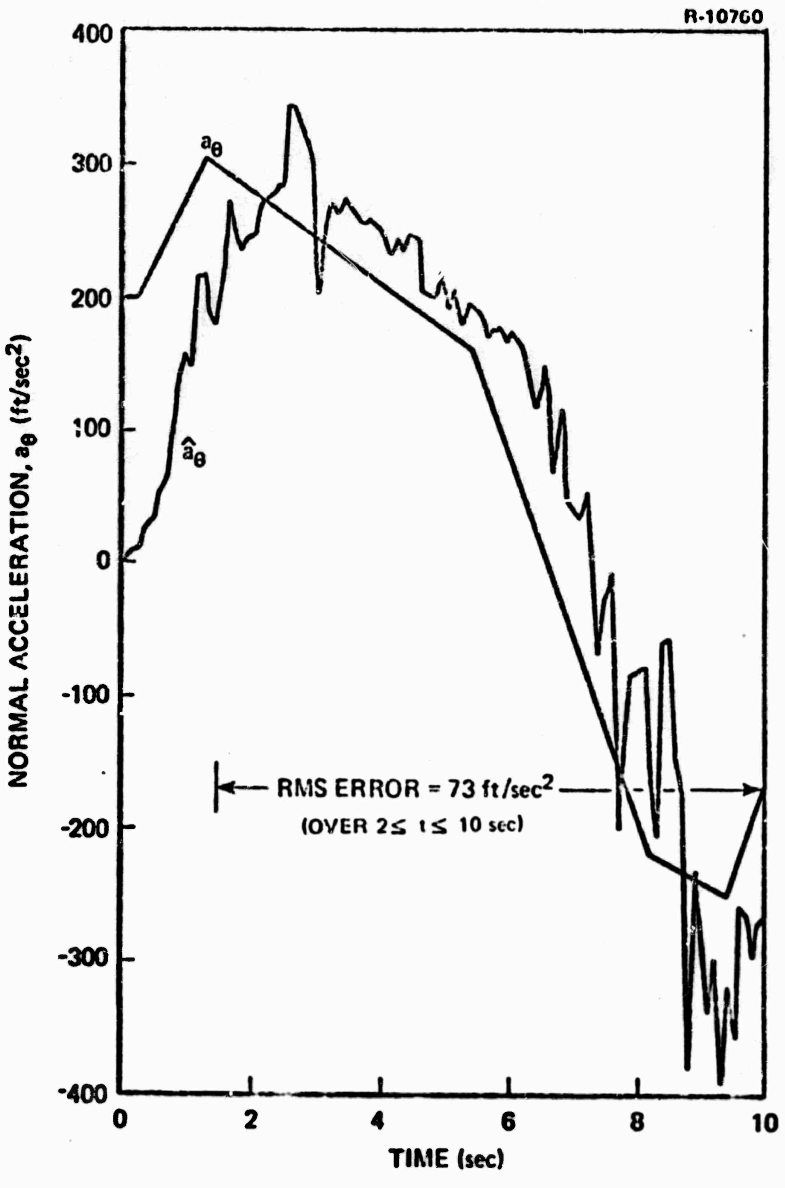

Figure 4.2-3 Normal Acceleration and Its Estimate Using Hypothesis Testing Filter CE: Highly Evasive Trajectory

A further demonstration of the adaptive designs at low maneuver levels is provided in Fig. 4.2-4 where Filters B and CL are compared with two versions of the third-order fixed filter designated A* and A**. The former is designed (q = 7.5 ft^2/sec^5) so that, for the nonevasive trajectory, its rms

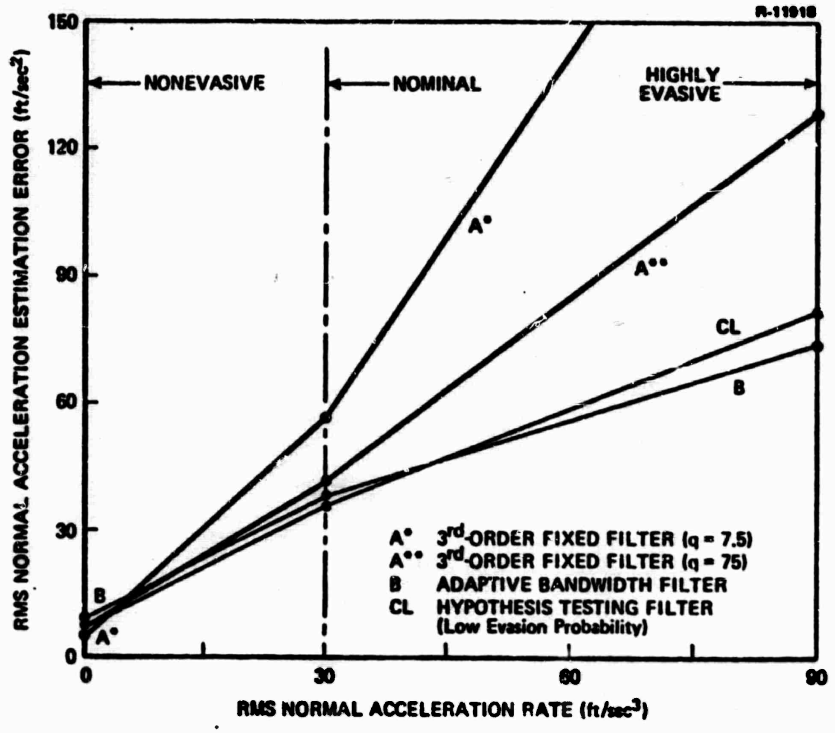

Figure 4.2-4 Comparison of Adaptive Filters versus Fixed Filters Optimized for the Nonevasive Trajectory

acceleration estimation error is one-half that achieved with Filter CL. Thus, the A* filter is very close to the optimum design (q = 0) for this trajectory, but its performance is degraded for the nominal and highly evasive trajectories. This demonstrates dramatically the price paid for a near optimum design if the target does not behave as assumed.

The filter designated A** is the same as A* except its value of q is selected to have the same rms error as filter CL for the nonevasive case. This fixed design does nearly as well as the adaptive designs (CL, B) for the nominal trajectory but its performance is poor for the highly evasive case. Thus, if the filters are "matched" to have the same rms error for a nonevasive target, the adaptive filters perform much better if the target acutally is evasive.

4.2.2 Sensitivity to Measurement Noise Level

All of the filters have been designed assuming a nominal rms measurement noise level of 1.4 mrad. This section describes what happens to the rms normal acceleration estimates if the actual measurement noise level is significantly higher or lower than the design value. This is an important sensitivity study because the measurement errors in an actual tracking situation are to some extent determined by variable factors such as weather and target cross-section; thus the rms error level may not be known accurately at any given time. Figure 4.2-5 shows the simulation results obtained for the nominal target trajectory.

For the nominal noise level, the results are the same as these given in Section 4.2-1 for the nominal trajectory case. When the noise level is decreased, all the filters yield approximately the same rms error except for Filter D which gives the best performance. The high noise case gives the most interesting and important sensitivity results. Compared with Filter A, all of the adaptive designs except Filter D are extremely sensitive to measurement noise which is higher than the assumed level. This sensitivity to measurement noise level is common to many adaptive techniques and motivates the residual testing scheme, Filter D. This behavior will be explained presently.

The adaptive bandwidth filter (B) is sensitive to measurement noise level because its bandwidth is controlled by estimates of acceleration rate. As the estimate $\hat{\dot{a}}_\theta$ increases, the bandwidth of the filter also increases through the mechanization of Eq. (3.3-2). This is the desired result if the actual rms acceleration rate also increases. However, if the measurement noise level increases, then the state estimates produced by the fourth-order fixed filter in Fig. 3.3-1 become more noisy; hence the rms level of $\hat{\dot{a}}_\theta$ will

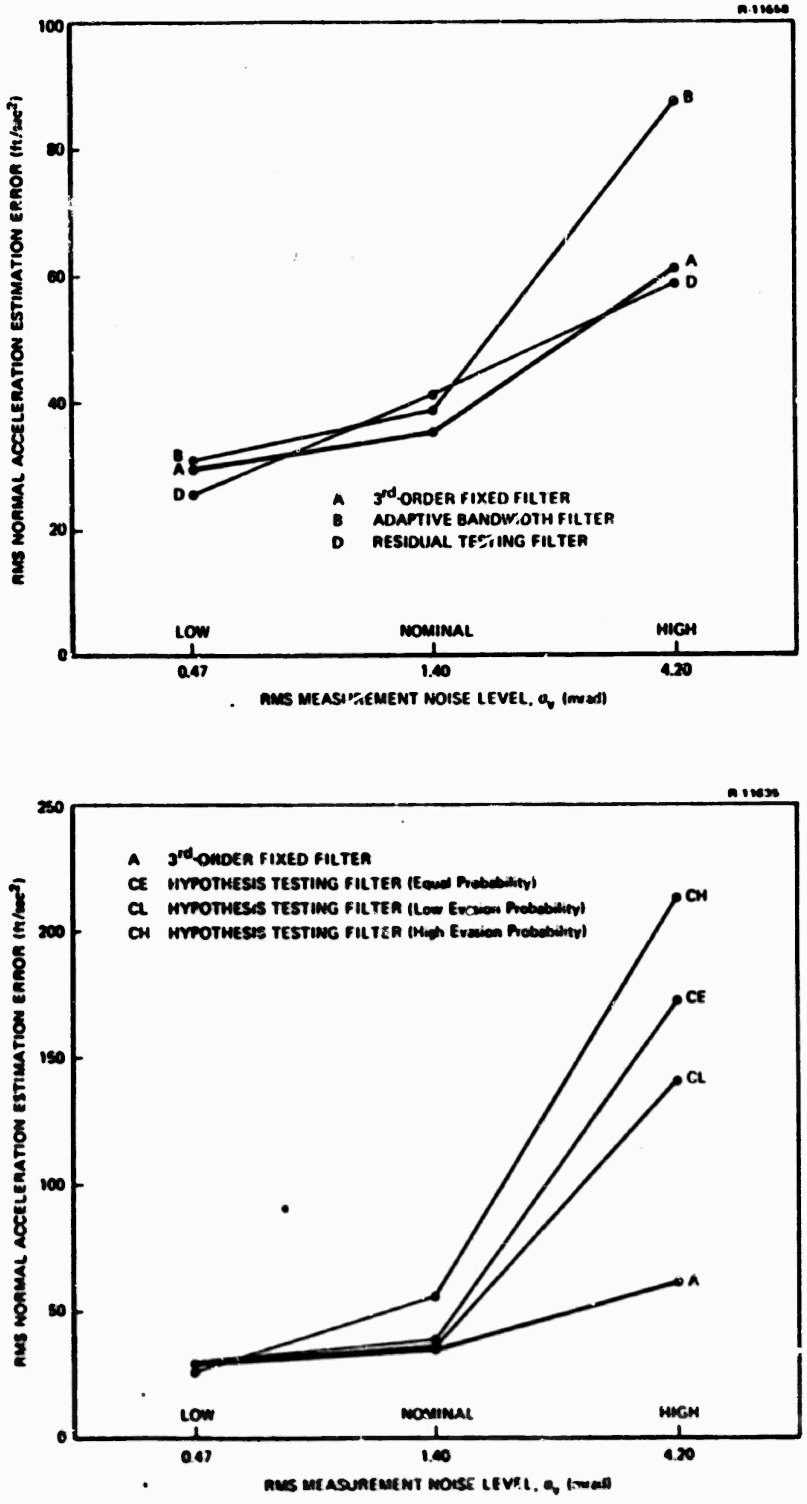

Figure 4.2-5 Tracking Filter Sensitivity to Measurement Noise Level

be higher due to its increased noise content. Consequently, the adaptive bandwidth filter cannot tell whether the estimated rms acceleration rate has increased due to an evasive maneuver or to higher measurement noise, but its bandwidth will be raised in both cases. In the former case its bandwidth should be raised; in the latter it should be lowered. Thus the filter adapts in the wrong direction when changes in rms measurement noise levels occur.

The hypothesis testing filter suffers from the same difficulty described above. The design based on the nominal noise level tells the filter how much noise to expect in the estimates. If the actual noise level is greater than its assumed value, the filter effectively interprets the increased fluctuations in the measurements as caused by increased target evasive action and erroneously determines the high bandwidth filter in Fig. 3.3-5 to be the most probable.

The residual testing filter (D) overcomes the noise sensitivity problem because its bandwidth is directly related to the rms value of the residual sequence of each parallel filter in Fig. 3.3-6. As discussed in Section 3.3-3 and Appendix B.2, this sequence is a direct reflection of the actual estimation error. Filter D determines which of the parallel filters has the lowest rms residuals and therefore provides the smallest estimation error. Another way of looking at this is to notice that the hypothesis testing and adaptive bandwidth filters have designs in which the adaptive algorithm depends upon the assumed level of noise. If this level is incorrect, they adapt in the wrong direction. On the other hand, the adaptive part of the residual testing filter is independent of the actual measurement noise level; therefore it adapts correctly.

One possible means of reducing the noise sensitivity of Filters B, CH, CL, and CE would be to design them assuming the highest level of measurement noise that might ever be encountered. This would work well in the high noise case, but the estimates would compare poorly with those of Filters A and D if

the actual noise level were much lower. In situations where the measurement noise level is poorly known or changing, a better approach is to use a filter which is designed for the most likely noise level but is insensitive to changes around this design value; for example, the residual testing filter designed for the nominal noise level.

4.2.3 Sensitivity to Correlated Measurement Noise

In the tracking problem, the sensor (e.g., radar) receiver noise is usually wide-band so that white gaussian noise is a good model. However the total measurement error can also contain low frequency, correlated noise components caused by a slowly varying target cross section, due to the target's own motion. The simulation described here is conducted to see how much correlated noise affects estimation accuracy. Except for the measurement noise, the tracking situation is the nominal case defined in Section 4.1. Only Filter A is tested, but similar results would be obtained for all of the filters.

The measurement noise sequence is generated by driving the difference equation for a low-pass filter with the output of a gaussian random number generator. The details of the measurement noise model used in this simulation are presented in Section 2.3, where the correlation time is denoted by the variable τ.

Figure 4.2-6 shows that increasing the correlation initially increases the error. As the correlation time becomes very large, (i.e., $\tau > 1$ sec.), the error begins to decrease because very low-frequency noise has little effect on the estimation of a time-derivative such as target acceleration.

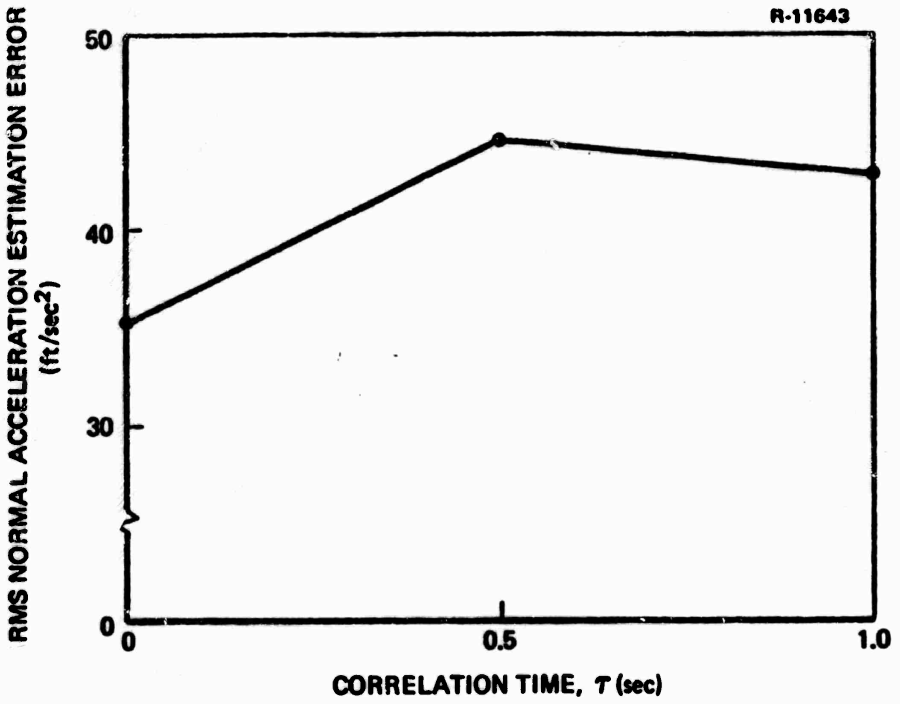

Figure 4.2-6 Sensitivity of Filter A to Measurement Noise Correlation

4.2.4 Sensitivity to Data Rate

One means of improving estimation accuracy is to increase the information available to the filter by increasing the frequency with which measurements are taken. Thus far ten measurements per second has been assumed to be a reasonable data rate for the tracking system. To see how much improvement is possible, Filter A was exercised at data rates of twenty and fourty measurements per second; the results are shown in Fig. 4.2-7. It is clear from this graph that a higher data rate will improve estimation accuracy; However, this improvement is achieved at the expense of increased computer time requirements--i.e., if the data rate is doubled, then it takes approximately twice as much computer time to calculate the estimates for a given computer design; thus; a faster computer might be required. Data compression (prefiltering) techniques could probably be useful for reducing the computation time required at high data rates (Ref. 20).

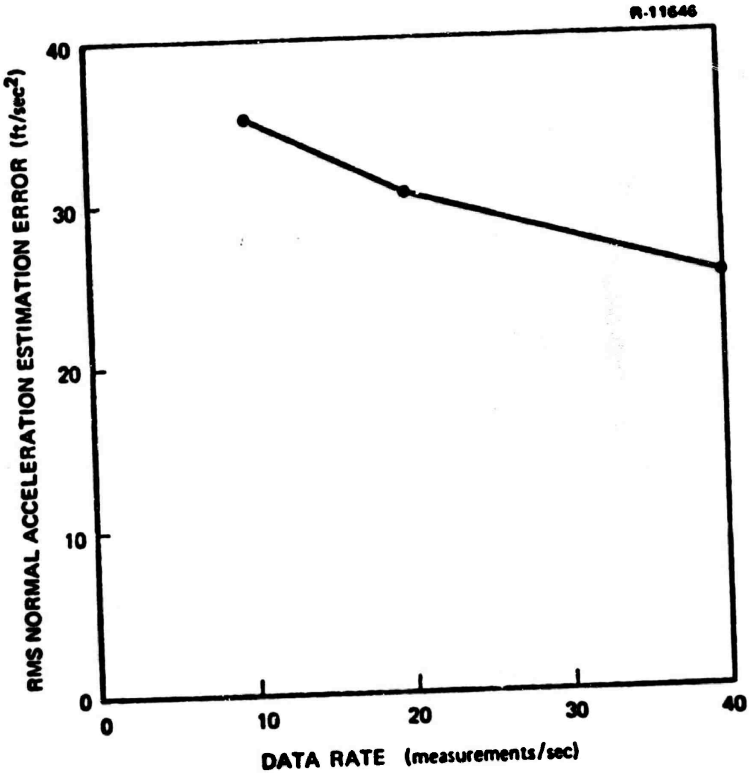

Figure 4.2-7 Sensitivity of Filter A to Data Rate

4.2.5 Sensitivity to Target Range

All of the results presented so far have assumed that the target is at a constant range of 10,000 ft. However, an attacking target will be at this range only once during its trajectory; thus it is important to know how the estimation errors of each filter vary with range.

To determine the estimation error sensitivity to range, a set of simulations was performed under the nominal tracking situation with the range parameter r changed for Filters A, B, CE, and D. Figure 4.2-8 shows results for ranges from 2,500 to 25,000 ft. In part (a) of this figure the rms position

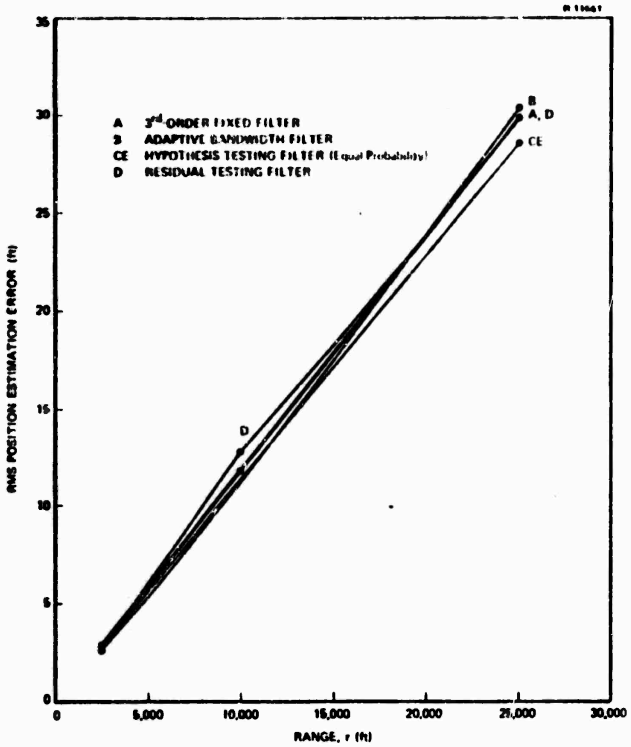

(a) Position rms Estimation Error versus Range

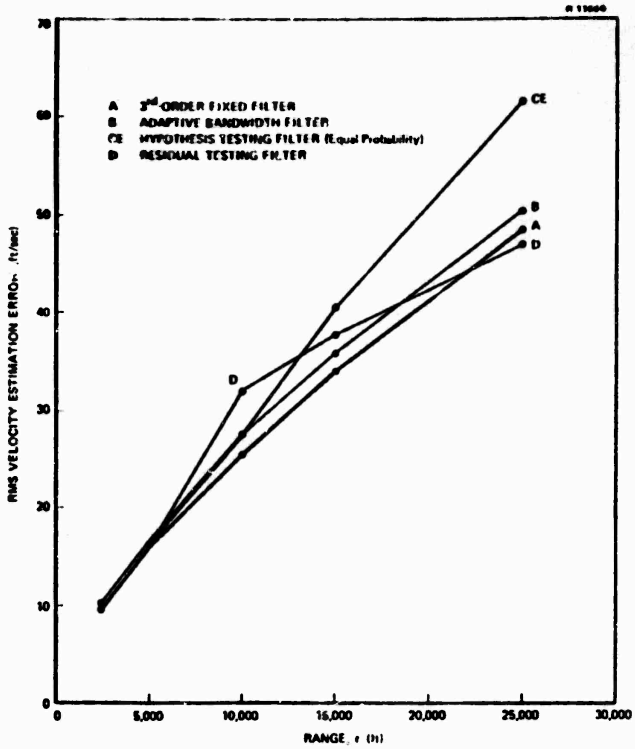

(b) Velocity rms Estimation Error versus Range

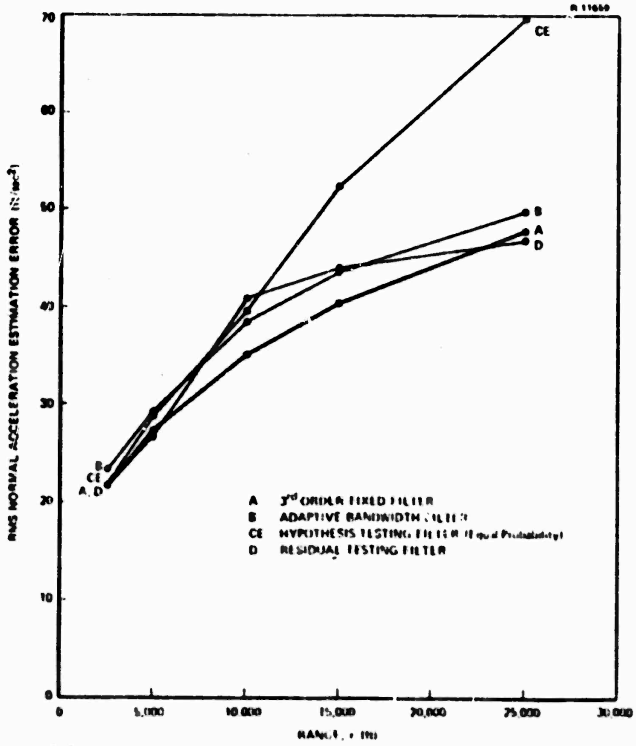

(c) Normal Acceleration Estimation Error versus Range

Figure 4.2-8 **Position, Velocity and Acceleration rms Estimation Errors versus Range for Filters A, B, CE, and D: Nominal Trajectory**

estimation error in feet is plotted against range for the four filters. This error is calculated using the small angle approximation for the angle estimation error. Thus the position estimation error e_p is given by

$$e_p = r \sin(e_\theta) \tilde{=} r e_\theta$$

where r is range in feet and e_θ is angular estimation error in radians. Likewise in part (b) of the figure, the velocity estimation error in feet per second is found by using

$$e_v \tilde{=} \dot{r} e_{\dot{\theta}}$$

where $e_{\dot{\theta}}$ is equal to $\dot{\theta} - \hat{\dot{\theta}}$, the angular velocity estimation error. In part (c) of Fig. 4.2-8, the rms normal acceleration estimation error is shown.

As expected, the estimates become more accurate as the range of the target decreases since this is an angle measuring system. For a constant rms angular measurement error, the measured position error decreases linearly with range, and consequently the estimated position, velocity, and acceleration become more accurate as the signal-to-noise ratio of the data improves. In practice, the rms angular measurement error may vary with range; this effect is not included in this study because it is dependent upon the particular target encountered and tracking sensor used.

All of the filters have approximately the same range sensitivity as shown in Fig. 4.2-8 except for the hypothesis testing filter which does poorly at the longer ranges. This seems to be due to the fact that the higher effective noise level at longer ranges (i.e., the measured position error is larger) makes it more difficult to calculate the probability of each hypothesis.

4.2.6 Summary of Filter Estimation Accuracy

The results described in this section show the merits of each adaptive design in terms of estimation accuracy. If the rms measurement noise level is well known, then all of the adaptive designs offer some advantage over the fixed filter (A) for targets with widely different maneuvering characteristics. For this case the adaptive bandwidth filter (B) appears to give the best tradeoff between complexity and estimation accuracy. The price paid for this design is the requirement that both a third-order and a fourth-order tracking filter be implemented, giving a more than two-fold increase in computational requirements over the third-order fixed filter. If accurate a priori knowledge is available about the probabilities of various target trajectories, then the hypothesis testing filter (CE, CL, or CH) is the best choice. However it is more complex than Filter B and it is especially sensitive to changes in measurement noise level and target range, so it must be used with caution.

For tracking situations where the measurement noise level is unknown or changing, the fixed third-order filter and the residual testing filter yield the best performance. The residual testing filter can offer better estimates than the fixed filter if the target changes its behavior over a wide range, or if the measurement noise varies sufficiently. The cost of this is a three-fold increase in computation over the fixed third-order design.

4.3 PREDICTION ERROR EVALUATION PROCEDURE

In this section, the procedure used to evaluate the tracking filter designs in terms of prediction error is specified. Prediction error is defined as the error made by the filter in predicting the future position of the target. A simple, but realistic, scenario for an attacking target provides the basis for plots of rms predicted position error versus time-to-go, t_{go}. The position

error is measured normal to the true line-of-sight and time-to-go is defined as the time remaining until the attacking target reaches the ship. This is a more practical basis for tracking filter evaluation than comparing target trajectory estimation errors because the ultimate effectiveness of a gun fire control system is determined by the projectile miss distance which depends upon the rms predicted target position error. Other sources of miss distance such as ballistic dispersion and gun pointing error are not considered here; however, these will tend to be much smaller than the target prediction errors for highly evasive targets.

The simplified scenario for an attacking target depicted in Fig. 4.3-1 is based upon several assumptions, which are not necessary in an actual situation, but make possible a clear comparison of the performance of different tracking filters. First, assume the target is approaching the ship at a constant radial or closing velocity denoted by v_T, and its evasive action consists of motion perpendicular to the line-of-sight. Thus, the target's range as a function of time is assumed known, but its angular position, θ, must be estimated and predicted. Second, it is assumed that the projectile fired from the ship travels with constant radial velocity, v_P. If the target is at range r when it is fired, then using the above assumptions the range at intercept, r_I, defined as the range at which the projectile and target are the same distance from the ship, is given by

$$r_I = \frac{v_P r}{v_P + v_T} \tag{4.3-1}$$

and the time-to-go, t_{go} is

$$t_{go} = \frac{r}{v_T} \tag{4.3-2}$$

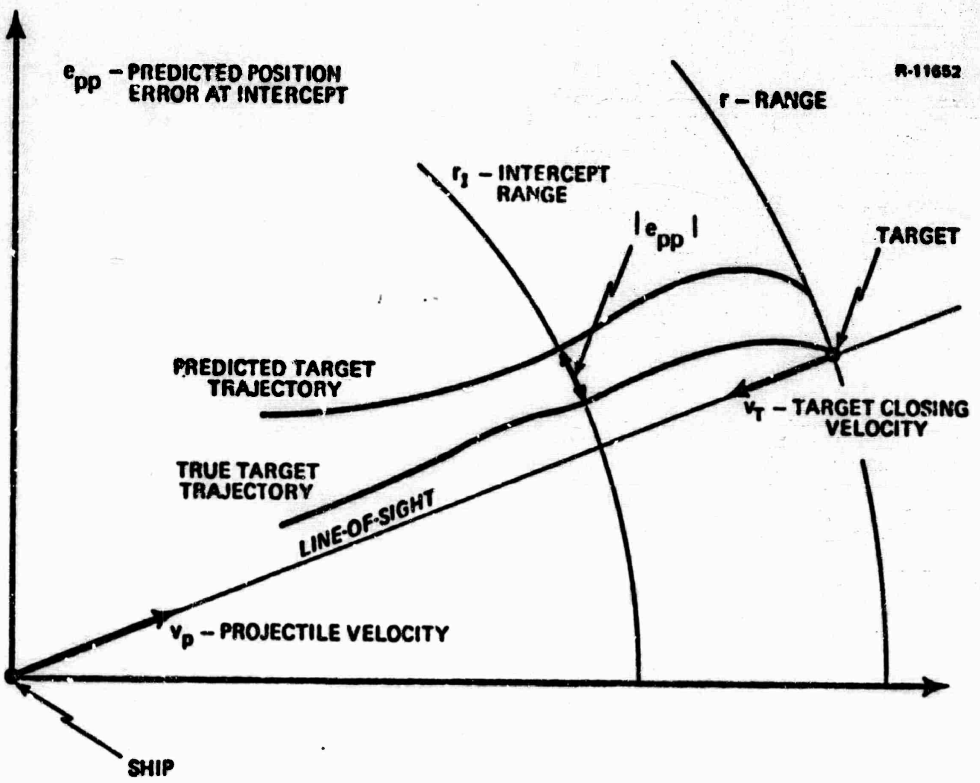

Figure 4.3-1 Target Prediction Scenario

The prediction time, t_p, is defined as the time required for the projectile and the target to reach the intercept range r_I measured from the time when the projectile is fired. Thus t_p is given by

$$t_p = \frac{r_I}{v_p} \tag{4.3-3}$$

or

$$t_p = \frac{r}{v_p + v_T} \tag{4.3-4}$$

Using Eqs. (4.3-1) through (4.3-4), range, intercept range and prediction time as functions of time-to-go are

$$r = v_T t_{go} \tag{4.3-5}$$

$$r_I = \frac{v_P v_T}{v_P + v_T} t_{go} \qquad (4.3\text{-}6)$$

$$t_p = \frac{v_T}{v_P + v_T} t_{go} \qquad (4.3\text{-}7)$$

These three equations along with choices for v_P, v_T, and a range of values for t_{go} define the variables needed for target prediction. The final step is to find the rms predicted position error as a function of time-to-go.

For a particular value of t_{go}, the target is at range r and the tracking filter provides estimates of its position, velocity and acceleration normal to the line-of-sight. These estimates are then used to predict the position of the target t_p seconds later when it reaches the intercept range. The difference between the predicted and actual target positions is the predicted position error given by

$$e_{pp} = e_p(t_0) + e_v(t_0) t_p + e_{a_\theta}(t_0) \frac{t_p^2}{2} + e_{\dot{a}_\theta}(t_0) \frac{t_p^3}{6} \qquad (4.3\text{-}8)$$

where e_{pp} is the predicted position error perpendicular to the line-of-sight at the intercept range, $e_p(t_0)$, $e_v(t_0)$, $e_{a_\theta}(t_0)$, and $e_{\dot{a}_\theta}(t_0)$ are the position, velocity, acceleration, and acceleration rate estimation errors at the start of prediction, and t_p is the prediction time. Equation (4.3-8) follows directly from the third-order target model assumed in designing the filters and the assumption that the acceleration rate is constant during the prediction interval. Figure 4.3-2 shows how the last three terms of Eq. (4.3-8) affect the error in predicted position as a function of t_p, for various values of the estimation errors. Evidently the predicted position error increases rapidly with prediction time if significant errors exist in the estimates of target acceleration and acceleration rate.

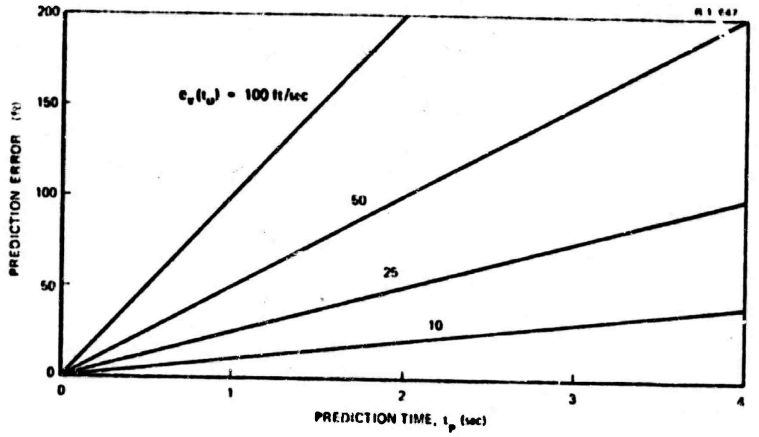

(a) Prediction Error Due to $e_v(t_0)$ versus Prediction Time

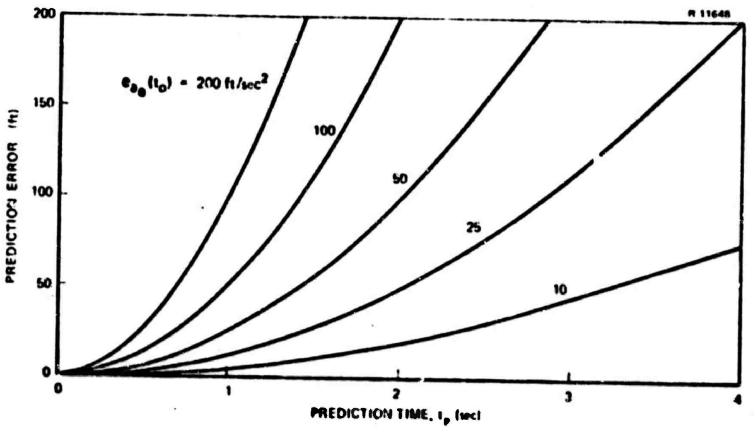

(b) Prediction Error Due to $e_{a_\theta}(t_0)$ versus Prediction Time

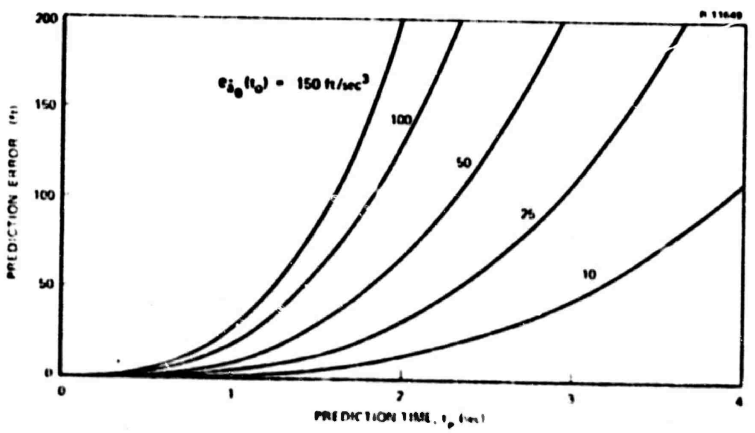

(c) Prediction Error Due to $e_{\dot{a}_\theta}(t_0)$ versus Prediction Time

Figure 4.3-2 **Effect of Estimation Error Components on Prediction Error versus Prediction Time**

Because the estimation errors in Eq. (4.3-8) are random, prediction accuracy can be described in terms of the rms value of the predicted position error as a function of prediction time, denoted by σ_{pp} and defined by

$$\sigma_{pp} = \left(E\left[e_{pp}^2 \right] \right)^{1/2} \tag{4.3-9}$$

where E [.] denotes expected value. The expansion of Eq. (4.3-9) with substitution from Eq. (4.3-8) leads to an expression for σ_{pp} which contains cross terms of the form $E[e_p e_v]$, $E[e_p e_{a_\theta}]$, etc. Recall that in Section 3.1, it is shown that the position, velocity, and acceleration estimation errors are highly correlated. In this case, a good approximation is

$$E\left[e_p e_{a_\theta} \right] = \left(E\left[e_p^2 \right] E\left[e_{a_\theta}^2 \right] \right)^{1/2} \tag{4.3-10}$$

Similar expressions apply for the other cross-product terms. Substituting the latter into Eq. (4.3-9) produces

$$\sigma_{pp} = \sigma_{e_p}(t_0) + \sigma_{e_v}(t_0)\, t_p + \sigma_{e_{a_\theta}}(t_0)\, \frac{t_p^2}{2} + \sigma_{e_{\dot{a}_\theta}}(t_0)\, \frac{t_p^3}{6} \tag{4.3-11}$$

where $\sigma_{e_p}(t_0)$ is the rms value of $e_p(t_0)$, etc. This approximation is worst case in the sense that less than perfect correlation between the estimation errors leads to an actual value of rms prediction error less than that given by Eq. (4.3-11).

To calculate the rms value of e_{pp} using Eq. (4.3-11) it is necessary to know the prediction time, t_p, and the various rms estimation errors at the start of the prediction interval, which are functions of the range r. The quantities t_p and r are given by Eqs. (4.3-5) and (4.3-7) respectively as functions of time-to-go, t_{go}. The range sensitivity studies in Section 4.2-5 indicate

how the rms position, velocity, and acceleration estimation errors vary with range. The rms acceleration rate estimation error, $\sigma_{\dot{a}_\theta}$, is equal to the actual rms target acceleration rate; i.e., the rms value of $\dot{a}_\theta$, because the filters do not estimate $\dot{a}_\theta$. It was found in Section 3.2 that attempts to estimate this variable using a fourth-order filter actually degrade the overall estimation accuracy; the rate estimates are so poor that they may as well be set equal to zero. The latter policy is followed here. In subsequent calculations of the rms predicted position error this term will be neglected, which is the same as assuming that the target has a constant acceleration over the prediction interval. The effect of a change in target acceleration during the interval can be determined from Fig. 4.3-2(c) and added to the prediction error.

With the above convention for handling $\sigma_{\dot{a}_\theta}$, the rms predicted position error is given by

$$\sigma_{pp} = \sigma_{e_p}(t_0) + \sigma_{e_v}(t_0)t_p + \sigma_{e_{a_\theta}}(t_0)\frac{t_p^2}{2} \qquad (4.3\text{-}12)$$

The three rms estimation errors needed by this equation are calculated as follows: For each filter, normalized range sensitivity curves are plotted and approximated by curves of the form $y = x^a$ shown in Fig. 4.3-3, which give a good fit to the normalized range sensitivity curve of each filter. Figure 4.2-8 shows the original range sensitivity of position, velocity, and acceleration estimation error for Filters A, B, CE, and D. These curves were plotted again with the horizontal scale normalized to 10,000 ft--i.e., 1 corresponds to 10,000 ft-- and the vertical scale normalized to the rms estimation error at 10,000 ft--i.e., 1 corresponds to a particular filter's rms position, velocity, or acceleration estimation error at 10,000 ft. Figure 4.3-4 is an example of

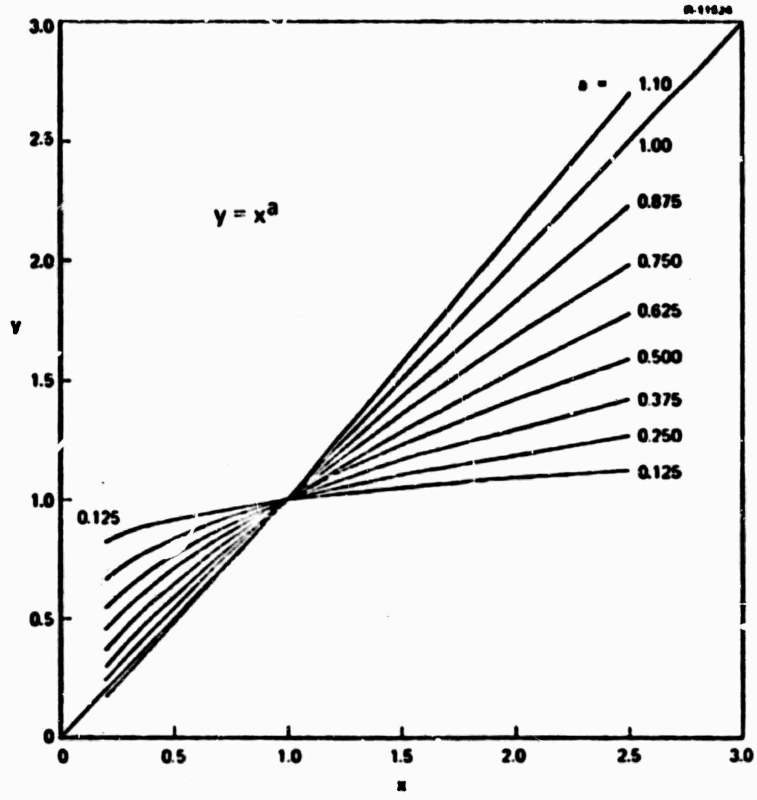

Figure 4.3-3 Range Sensitivity Approximating Functions

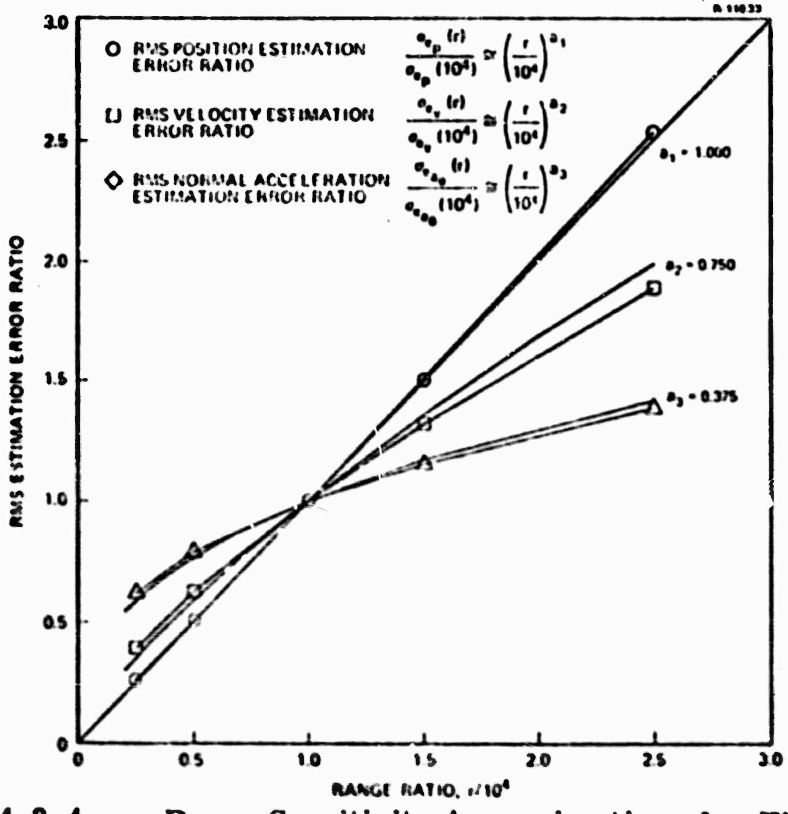

Figure 4.3-4 Range Sensitivity Approximations for Filter A: Nominal Trajectory

this for Filter A, showing both the approximating curves and the actual simulation results taken from Fig. 4.2-8.

This procedure has been carried out for each of the tracking filters for which range sensitivity studies were conducted--i.e., Filters A, B, CE, and D. The approximate range sensitivity curves obtained are based on the nominal target trajectory and nominal rms measurement noise level; but they can be used to obtain the approximate rms estimation errors as a function of range for a particular filter in any tracking situation if the rms estimation errors are known at 10,000 ft. Now, since time and range are directly related in this scenario by the constant target closing velocity, the rms errors at the start of the prediction time are defined by the range at that time.

This completes the detailed description of the prediction error evaluation procedure. In summary, for a particular target closing velocity v_T and a particular projectile velocity v_P, the prediction time t_p, the target range at firing r, and the intercept range r_I are calculated as functions of time-to-go, t_{go}. This assumes that the target closes at a constant velocity and evades only by moving perpendicular to the line-of-sight and that the projectile travels at a constant radial velocity. Using the rms estimation errors obtained for each filter in each tracking situation, and the results of the range sensitivity study provided in Section 4.2, the rms predicted position error normal to the line-of-sight is calculated as a function of time-to-go, assuming the target does not change its acceleration during the prediction interval. The results of the analysis--plots of rms predicted position error versus time-to-go for each filter operating in a particular tracking situation--are presented in Section 4.4.

4.4 PREDICTION ERROR PERFORMANCE AND SENSITIVITY

This section compares the performance of Filters A, B, CE, and D by showing how their rms predicted position errors vary with time-to-go. A detailed account of how these results are obtained is given in Section 4.3 together with an explanation of the approximations and assumptions involved. From the results presented in this section a general idea of the kill probability could be obtained by assuming a particular rate of fire, projectile lethal radius, and rms gun pointing error. The results not only show the comparitive performance of the filters but also indicate the overall accuracy that is likely to be achieved with any good tracking filter for the types of target maneuvers considered in this report.

To complete the specification of the target attack scenario described in the last section, the projectile velocity, v_P, and the target closing velocity, v_T, must be chosen. For most of the results presented in this section, these quantities are taken to be

$$v_P = 2600 \text{ ft/sec}$$

$$v_T = 1300 \text{ ft/sec}$$

At the end of this section, the sensitivity of the rms predicted position error to changes in these values is shown. With this choice of v_P and v_T, the range r, intercept range r_I, and the prediction time t_p are completely specified as functions of time-to-go (Eqs. (4.3-5), (4.3-6), and (4.3-7)) as shown in Fig. 4.4-1.

4.4.1 Sensitivity to Target Maneuver Level

The target rms predicted position errors corresponding to the estimation errors achieved for the three different target trajectories, in the otherwise

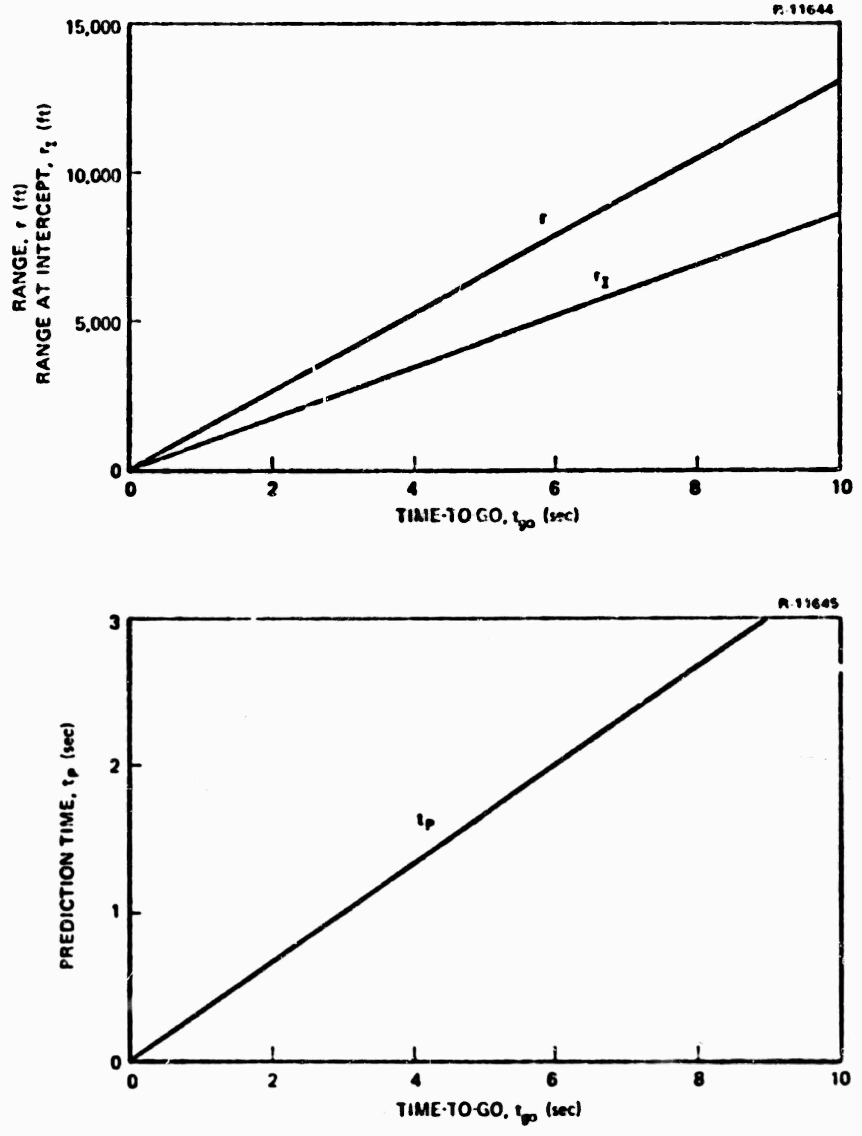

Figure 4.4-1 Target Range, Intercept Range, and Prediction Time versus Time-To-Go for v_P = 2600 ft/sec and v_T = 1300 ft/sec

nominal tracking situation defined in Section 4.1, are given in Fig. 4.4-2. The results are given for Filters A, B, CE, and D, and for each of the target trajectories defined in Fig. 2.3-2. To interpret these curves, assume that only rms predicted position errors less than 100 ft are of interest and anything larger is an almost sure "miss"; then the length of time a particular curve is below this 100 ft threshold is important. For example, in Fig. 4.4-2(a) Curve

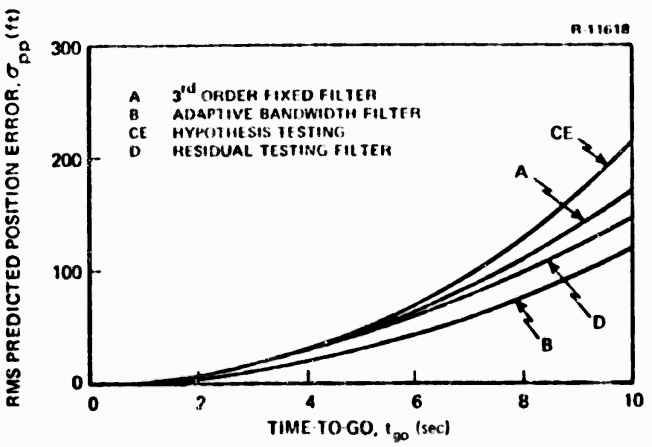

(a) Nonevasive Case - rms ($\dot{a}_\theta$) = 0

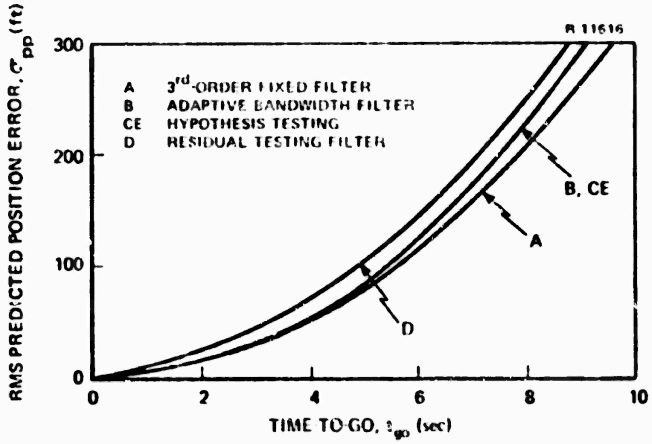

(b) Nominal Case - rms ($\dot{a}_\theta$) = 30 ft/sec^3

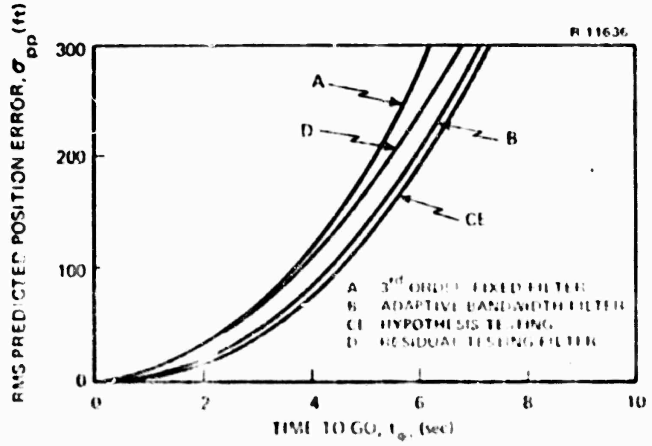

(c) Highly Evasive Case - rms ($\dot{a}_\theta$) = 90 ft/sec^3

Figure 4.4-2 RMS Predicted Position Error versus Time-To-Go: Sensitivity to Target rms Acceleration Rate, Filters A, B, CE, and D

B for the adaptive bandwidth filter is below 100 ft for approximately 9 seconds before the target reaches the ship. Thus there are 9 seconds of firing time during which there is some chance of hitting the target. If the gun fires one projectile per second, then there are nine firing opportunities before the target reaches the ship. Suppose that one projectile is fired at t_{go} = 9 seconds, one is fired at t_{go} = 8 seconds and so on until t_{go} = 1 second. The rms predicted position error associated with each of these projectiles can be found from the height of the curve at the respective time it is fired. Thus the rms error for the projectile fired at t_{go} = 4 seconds is about 20 ft and from Fig. 4.4-1 the range at intercept is about 3600 ft, the range to the target when the projectile is fired is 5200 ft, and the total prediction time is 1.3 sec. If the gun pointing error is small compared to the predicted position error and if the target does not change its acceleration drastically during the prediction time, the rms error of 20 ft found here is a good indication of the miss distance. Knowing the projectile lethal radius, the rms miss distance, and the number of firings, the kill probability can be estimated.

Comparing the three parts of Fig. 4.4-2, it is clear that the prediction error is very sensitive to the level of evasive maneuver. For the highly evasive case, the firing interval during which the error is less than 100 ft is around four seconds for Filters B and CE. There is very little time to fire, the associated errors are relatively large, and the kill probability would be much lower than for the nonevasive case.

The simulation results indicate that the best tracking filter for these conditions is the adaptive bandwidth filter (B). It is clearly best for the nonevasive case and works almost as well as any of the others at higher target maneuver levels, especially when rms errors under 100 ft are considered to be critical. The differences between the performance of the various designs are not great compared to their sensitivity to maneuver level. Depending upon

the lethal radius of the projectile and the pointing accuracy of the gun, these differences may or may not have a significant effect on overall kill probability. In addition, large prediction errors caused by the target changing its acceleration during the prediction interval (See Fig. 4.3-2(c)) could decrease the importance of the performance differences shown. It is important to note that much better accuracy would be achieved for the nonevasive trajectory if the filters were designed for this case rather than for the nominal trajectory; this point is discussed in detail in Section 4.2.1.

4.4.2 Sensitivity to Measurement Noise Level

The target rms predicted position errors achieved for three different noise levels, based on the rms estimation errors obtained in Section 4.2.2 are given in Fig. 4.4-3. The rms predicted position error increases significantly as the measurement noise increases, as would be expected. The choice of a "best" tracking filter for this set of conditions is not clear. Filters A and B are superior for the high noise case; however Filter CE is best in the low noise case, but worst in the high noise case. These results taken together with those presented in Fig. 4.2-2 indicate that filter B (adaptive bandwidth) would probably be the best choice over the conditions tested. However, in practice the best choice also depends upon the likelihood of the off-nominal tracking conditions occurring.

4.4.3 Sensitivity to Correlated Measurement Noise

Figure 4.4-4 shows the sensitivity of Filter A to correlated measurement noise for the nominal tracking situation, using the results obtained in Section 4.2.3. The figure shows the decrease in accuracy that occurs if the

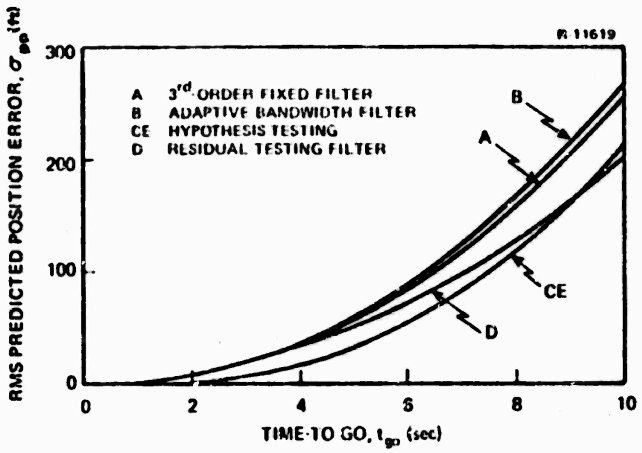

(a) rms Measurement Noise Level = 0.47 mrad (Low Noise Case)

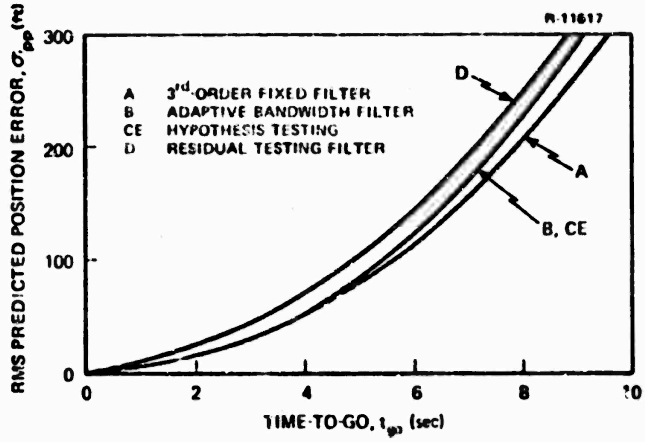

(b) rms Measurement Noise Level = 1.40 mrad (Nominal Noise Case)

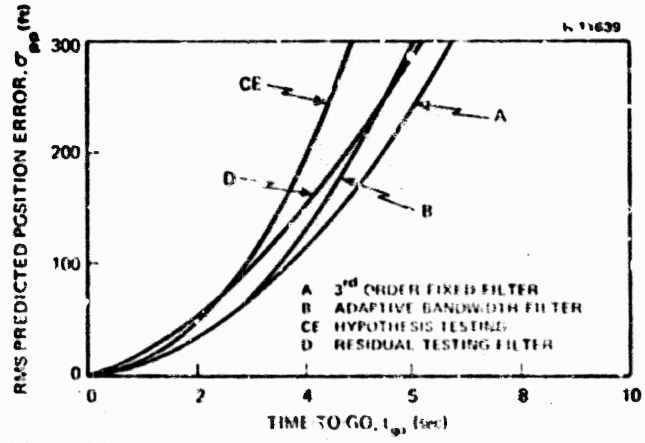

(c) rms Measurement Noise Level = 4.20 mrad (High Noise Case)

Figure 4.4-3 Prediction Error Sensitivity to rms Measurement Noise Level: Nominal Trajectory

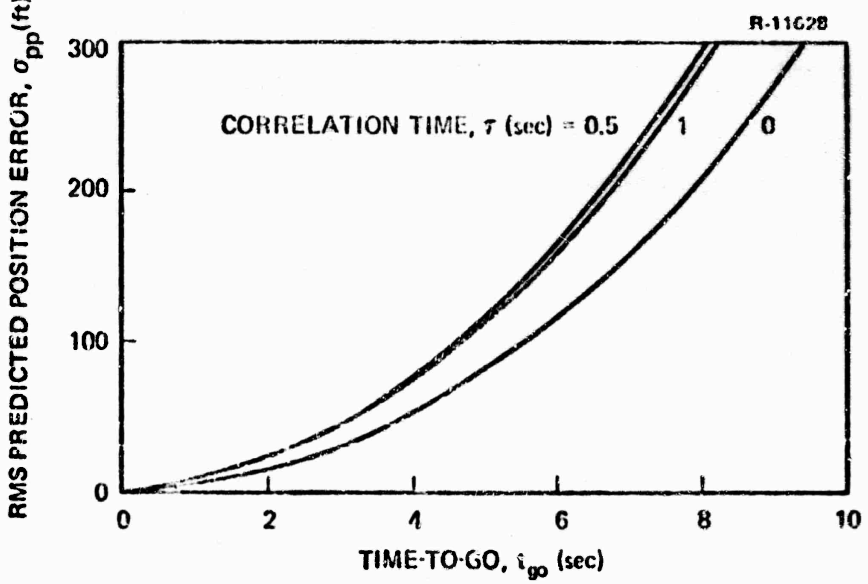

Figure 4.4-4 Prediction Error Sensitivity to Measurement Noise Correlation for Filter A: Nominal Trajectory

rms measurement noise level remains constant but its correlation time, τ, is changed from $\tau = 0$ to $\tau = 0.5$ and $\tau = 1$ sec. Note that the error increases by as much as 59% over the range of τ.

4.4.4 Sensitivity to Data Rate

Figure 4.4-5 shows the improvement in prediction accuracy that is obtained for Filter A in the nominal tracking situation if the measurement data rate is increased from 10 measurements per second to 20 and 40 measurements per second. Evidently significant improvement is possible at a higher rate, but whether this improvement justifies the additional computer time required depends upon the tradeoff between increased cost and improved kill probability.

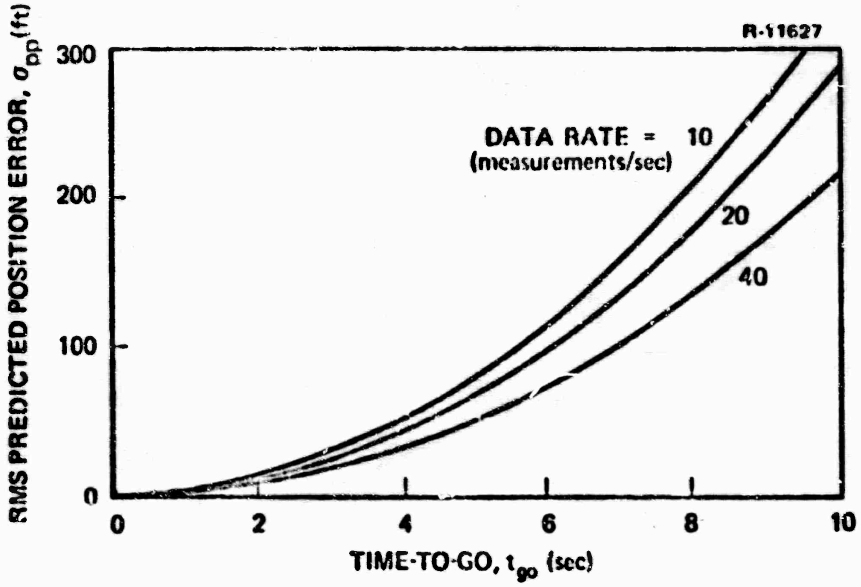

Figure 4.4-5 Prediction Error Sensitivity to Measurement Data Rate for Filter A: Nominal Trajectory

4.4.5 Sensitivity to Target and Projectile Velocity

It is instructive to see how the prediction results change if different values are chosen for the projectile velocity, v_P, and the target closing velocity, v_T. Figure 4.4-6 shows the results for Filter A operating in the nominal tracking situation where v_T = 1000 ft/sec and v_P is varied from 2000 to 3500 ft/sec. An increased projectile velocity helps by directly reducing the required prediction time for a given time-to-go and hence the prediction error. Figure 4.4-7 shows the effect of variations in target closing velocity. Increasing v_T increases the prediction error for a given value of time-to-go because the corresponding value of target range at the firing instant is increased (see Eq. (4.3-5)). There is a great advantage to targets which have a very high closing velocity, as well as the ability to maneuver at the level of the nominal trajectory used for this investigation.

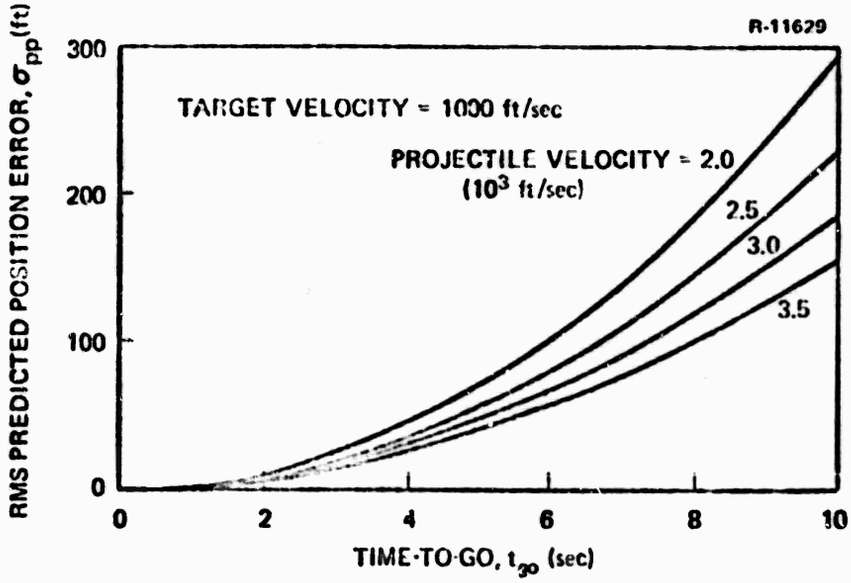

Figure 4.4-6 Prediction Error Sensitivity to Projectile Velocity for Filter A: Nominal Trajectory

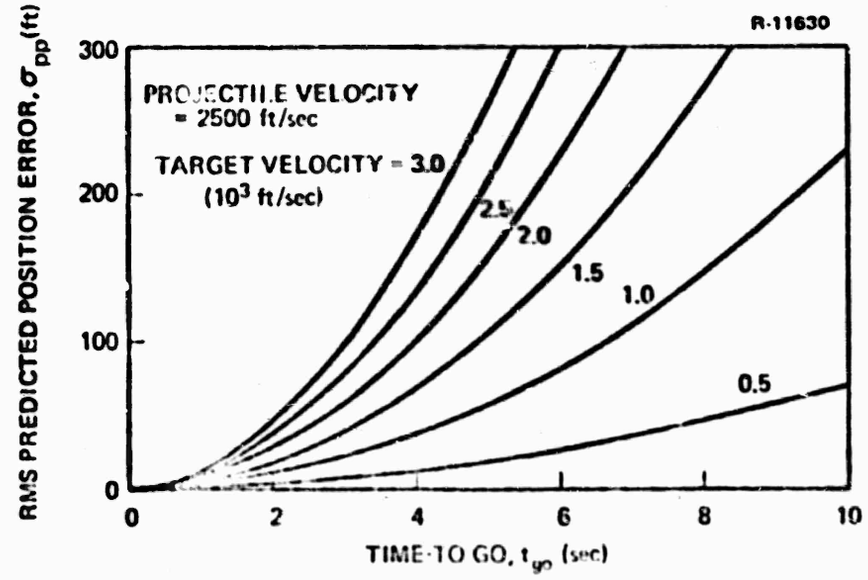

Figure 4.4-7 Prediction Error Sensitivity to Target Closing Velocity for Filter A: Nominal Trajectory

4.4.6 Summary of Prediction Error Results

Several general conclusions can be drawn from the results presented in the preceding sections. First, and most important, tracking filter design can be crucial to the ultimate effectiveness of the gun fire control system, so a careful and thorough design effort is needed for each specific application. No one filter design of either the fixed or adaptive type is necessarily best for all target engagement situations. The final selection of the tracking filter depends very much on the complete environmental range in which it must operate, the speed and size of the computer available, and the relative importance assigned to tracking accuracy for each situation. Even for a well specified set of tracking situations, a single filter will be the best for each member of the set and the final design must be selected on the basis of subjective judgements as to the relative importance or probability of each situation.

Tracking filter comparisons should be based upon prediction error rather than estimation error. Certainly these performance measures are closely related, but prediction is ultimately required to direct the gun pointing and prediction error depends upon prediction time and the target motion model, as well as the tracking filter's current estimates of position, velocity, and acceleration. What might appear to be a large difference in performance between two filters based upon estimation error may not be such a large difference in terms of prediction error, and vice versa, depending upon the attack scenario.

The choice between adaptive and fixed designs depends upon the specific application. Adaptive designs have the ability to offer large performance improvements in some situations but they should not be considered as the answer to all design problems. They require additional complexity and computation time and may be overly sensitive to unexpected changes in the

measurement noise level. Adaptive tracking filters must be applied cautiously and should always be judged against a good fixed (nonadaptive) design. The range of possible adaptive methods is virtually infinite and there can never be complete assurance that the best design for a particular application has been found.

The results in this chapter indicate that guided projectiles are needed in gun fire systems which are required to have a high kill probability against targets with a modest manuver capability. Figure 4.4-2(b) shows the size of the rms predicted position errors for the various tracking filters if the target's rms acceleration rate, normal to the line of sight, is approximately 1 g/sec. For time-to-go greater than six seconds all of the filters have a rms prediction error greater than 100 ft, which exceeds the lethal radius of a conventional projectile. The important concept here is the following: In this attack scenario, the target will be very close to the ship before the rms predicted position error is smaller than the lethal radius of the projectile. This means that the gun is effective against the target during only the last few seconds of the engagement. Thus, there is not enough time to fire more than a few times and even if the target is hit it still might continue on its trajectory to the ship and cause serious damage.

There is an ultimate limit on the prediction accuracy possible due to the flight time of the projectile. Even if the estimates from the tracking filter are perfect, it is not possible to determine the target's exact future position because the target can maneuver or change its acceleration during the prediction interval. As long as the target's future behavior is unknown or random and it has a large evasive capability, it is impossible to exactly predict its future position. In this case the magnitude of the minimum rms predicted position error is nearly independent of the tracking system and depends mostly upon the capabilities of the target.

Beyond these general conclusions, the results show that the specific adaptive designs tried in this report can be useful for gun fire control systems. For the case where the measurement noise is accurately known, the adaptive bandwidth and hypothesis testing filters give significant improvement in prediction error over the fixed design. The hypothesis testing design is especially useful if there is accurate knowledge of the relative probability of different target manuver levels. If the measurement noise is poorly know. and can vary as much as a factor of three above and below the nominal design level, the advantage of the adaptive designs is partially lost because they are more sensitive to measurement noise level than the fixed designs. However, the adaptive band width filter still performs adequately and might be a good design choice. The fixed filter design also has some good features. First it is less complex and requires much less computation than the adaptive designs. Second, it is not overly sensitive to the measurement noise level. The fixed filter might be adequate in many cases.

Finally, this report indicates the design and evaluation procedure which must be undertaken to select a tracking filter for a gun fire control system application. The results show quite clearly the large prediction errors that can result if the filter is not chosen carefully. Such errors can seriously degrade the gun system's kill probability and must be kept as small as possible through good tracking filter design.

5. SUMMARY AND CONCLUSIONS

5.1 SUMMARY

This report treats the subject of target tracking filter design for shipboard gun fire control systems. Particular emphasis is placed upon applications in which the target threat has the capability to maneuver evasively and the sensor measurement noise level may not be accurately known. To this end, a realistic but comparatively simple target tracking problem is defined to provide a basis upon which various filter designs are developed and evaluated. The optimum tracking filter for this problem is described in detail. The reason why it cannot be implemented becomes clear; i.e., in a practical tracking situation there is generally not enough known about the target and its behavior to design an optimum tracking filter. Suboptimum designs with both fixed and adaptive structures are proposed and developed as practical alternatives based upon the knowledge available about the target. Four designs were selected after a careful review of the technical literature for those methods well suited to this problem. They are:

- Fixed Filter -- This design is independent of the target's behavior and is selected to be insensitive to changes in that behavior; this is a good design "on the average" over the range of tracking situations anticipated.
- Adaptive Bandwidth Filter -- This design adjusts its own bandwidth based upon the observed target behavior; i.e., it tunes itself on-line to achieve improved tracking accuracy over a range of tracking situations.

- Hypothesis Testing Filter -- This design is a bank of fixed filters each designed for a different assumed level of target evasive behavior. The estimates of each filter are then weighted and combined to give an overall estimate. The weights are determined from the probabilities that each of the filters is optimum.

- Residual Testing Filter -- This design consists of the same bank of fixed filters used in the hypothesis testing filter above. The final estimate, however, is selected from that filter which appears to have been operating best in the recent past; i.e., that filter whose estimates have been in closest agreement with the measured data.

A comparative study was conducted of the four designs described above in which tracking error and prediction error were the performance measures. Tracking error was defined as the error the filter makes in estimating the target's position, velocity, and acceleration, while prediction error is the error the filter makes in predicting the target's future position. The advantages and disadvantages of each design were investigated over a wide range of potential tracking situations. The sensitivity of estimation and prediction accuracy to changes in the following was studied:

- Target evasive manuver level
- Measurement noise level
- Measurement noise correlation time
- Measurement data rate
- Target range
- Target closing velocity
- Projectile velocity

5.2 CONCLUSIONS

Table 5.2-1 gives a qualitative comparison of the four tracking filter designs studied in this report. This comparison is based upon the rms predicted position errors shown in Figures 4.4-2 and 4.4-3 and indicates that the adaptive bandwidth filter gives the best overall trade-off between accuracy and complexity for the cases investigated. Parts (a) and (b) of Figure 4.4-2 are also repeated below to show the rms predicted position error normal to the line-of-sight achieved for each filter for both a nonevasive (constant target acceleration) and mildly evasive target trajectory. These figures give their results as a function of time-to-go, -- i.e., the time remaining before the target reaches the ship during a representative engagement. If the projectiles fired at the target have a maximum lethal radius of 50 ft it is clear that the

TABLE 5.2-1

TRACKING FILTER PERFORMANCE COMPARISON*

	Type of Tracking Filter	Tracking Situation					Filter Complexity
		Nominal Trajectory	Nonevasive Trajectory	Highly Evasive Trajectory	High rms Measurement Noise	Low rms Measurement Noise	
A	3rd-order Fixed	1	3	4	1	3	1
B	Adaptive Bandwidth	2	1	2	2	4	2
CE	Hypothesis Testing (Equal Probability)	3	4	1	4	1	4
D	Residual Testing	4	2	3	3	2	3

*Scale: 1 = Best, 4 = Worst

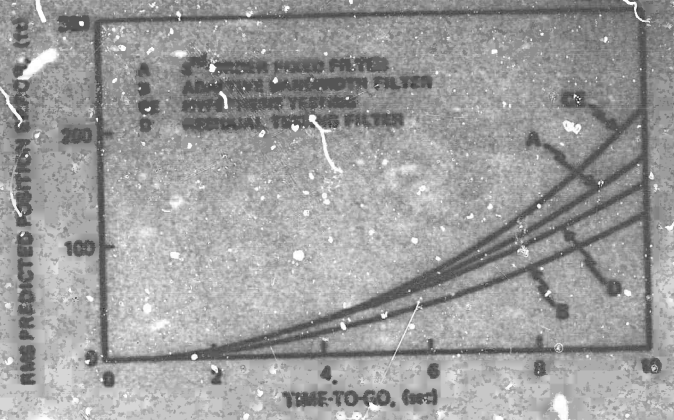

(a) Nonevasive Target

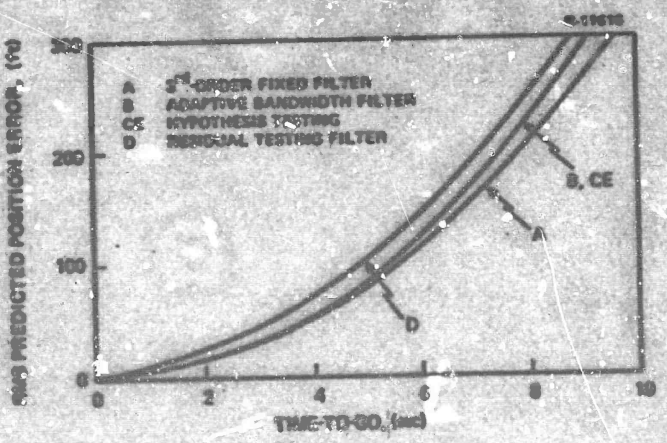

(b) Evasive Target

Figure 5.2-1 **RMS Predicted Position Error versus Time-To-Go for Several Different Tracking Filters**

gun system is an effective weapon against the evasive target for only a short time interval before the target reaches the ship.

The principal conclusions of this report are:

- Adaptive filter designs, based upon the nominal level of target acceleration rate considered in this report, potentially offer significant performance improvement over fixed designs in some tracking

applications. The greatest advantage of adaptive versus fixed designs occurs when the target acceleration rate is actually zero, as seen by comparing Figs. 5.2-1(a) and (b). For highly evasive targets, all designs give poor prediction accuracy and a fixed filter design is nearly as accurate as an adaptive design.

- A limited study of the case where the nominal target acceleration is assumed to be constant (see Fig. 4.2-4) indicates that adaptive filter designs perform significantly better than fixed filter designs when the target rms acceleration rate is actually quite large. This observation is consistent with the more traditional application of adaptive filtering techniques to track targets that are generally well-behaved, but occasionally perform unexpected maneuvers.

- The selection of a tracking filter requires a trade-off between accuracy and complexity. The adaptive designs require two to three times more computation than the fixed design while they achieve a 50% reduction (at low maneuver levels) in the prediction error for some of the cases investigated here.

- Adaptive filter designs are usually more sensitive to the measurement noise level than fixed designs. This can be very important if the actual level is changing in an unknown manner.

- For almost all cases tested, the prediction error results indicate that a guided projectile would be required to obtain acceptable lethality against targets that maneuver evasively, unless the target is to be allowed to get within a few thousand feet of the ship before it is engaged.

- Increased measurement rates improve prediction accuracy up to a point, but require increased computation speed in the tracking computer. The ultimate limit in prediction accuracy is determined, not by the tracking system, but by the ability of the target to manuver during the flight time of the projectile.

TECHNOLOGICAL FORECAST

PROBLEM DEFINITION

The problem addressed in this report is that of designing digital tracking algorithms for shipboard gun fire control systems which can track missile targets that are capable of unexpected, large evasive maneuvers. Targets having the capability of achieving acceleration and acceleration rate levels as high as 300 ft/sec^2 and 150 ft/sec^3, respectively, are considered. The objective of the study is to develop tracking algorithms having an adaptive structure, permitting automatic tracking of a wide variety of target maneuver characteristics. The solutions to this problem described in the report indicate the limitations in tracking performance and target prediction accuracy achievable with modern data processing technology. This information will be valuable to the Navy for determining those situations in which hardware improvements -- such as more accurate tracking sensors, higher measurement data rates, and faster projectiles -- are necessary in order to achieve acceptable projected miss distance.

STATE OF TECHNOLOGY

Modern data processing technology has previously been applied to the designing target tracking algorithms for the Navy's MK 86 Gun Fire Control System. Kalman filtering techniques are used to process radar tracking data to obtain estimates of target position, velocity, and acceleration for use in predicting the target's future position. However, the target

maneuvers investigated in these applications have typically been at levels on the order of one g or less. The emphasis of this study is on targets capable of much higher acceleration levels, and capable of changing their acceleration quite rapidly in an evasive fashion. During the study, adaptive filtering techniques were developed specifically for tracking these types of targets and their performance was evaluated under a wide range of tracking conditions.

6.3 SUGGESTIONS AND IMPLICATIONS

Several conclusions obtained from this study are summarized in Section 5.2. An important quantitative result is that all of the tracking techniques yield a predicted root mean square target position error in excess of 50 feet for evasive targets at ranges in excess of 5,000 feet, in all of the tracking situations investigated. This is near the lethal radius limit for conventional projectiles. Some improvement in prediction accuracy can be achieved by employing more accurate sensors at higher data rates; the former may require the use of infrared or optical tracking devices, and higher data rates will require increased computer capability to cycle the tracking algorithm computations at a faster rate. Alternatively, higher prediction errors can be tolerated if guided projectiles with the capability for homing on the target are developed. The output of this study includes specification of algorithm design techniques needed for tracking maneuvering targets, and indicates the target prediction accuracy limitations, thus providing a basis for judging whether hardware, as well as software, improvements are required to achieve an acceptable probability of kill against evading, maneuvering targets.

As stated previously, the work undertaken here was motivated by the increasing threat of the use of missiles against Navy shipping, with

their attendant high velocities and acceleration capabilities. Our effort was directed toward answering the question: How should target tracking algorithms be designed to cope with maneuverable targets which employ unpredictable evasive actions limited only by their maximum acceleration capability, and what are the target prediction accuracy limitations? However, in the near term, we expect that the guidance laws for most missiles will be designed to intercept a ship, without having a built-in evasive capability. The structure of these guidance laws may be known sufficiently well so that the tracking performance achieved with the optimal design described in Chapter 3 can be closely approximated by including a mathematical model of the missile guidance law within the design model of the tracking filter. An investigation of the target prediction accuracy achievable under these circumstances merits future study.

APPENDIX A

OPTIMAL FILTERING AND PREDICTION THEORY

The equations of the optimal (Kalman) filter for processing noisy measurement data are reviewed briefly in this appendix to provide the appropriate background and notational conventions necessary for the development of the adaptive tracking filters investigated in this report. Prediction theory is also reviewed and its relation to the Kalman filter is discussed. The development assumes a basic familiarity with random variables and state space notation, for linear systems; additional detail can be found in Ref. 18 and Chapters 1 through 4 of Ref. 19.

A.1 KALMAN FILTER EQUATIONS

To apply Kalman filtering to any estimation problem, it is necessary to derive a linear stochastic first-order vector matrix differential equation which models the manner in which the system states interact and propagate as a function of time. This equation has the general form

$$\dot{\underline{x}}(t) = F(t)\underline{x}(t) + G(t)\underline{u}(t) + \underline{b}(t) \qquad \text{(A.1-1)}$$

where $\underline{x}(t)$ is an $m \times 1$ column vector representing the system state, $F(t)$ is an $m \times m$ dynamics matrix which defines the interaction of the state vector components, and $\underline{u}(t)$ is a $p \times 1$ column vector of white gaussian noise inputs such that[1]

$$E[\underline{u}(t)] = 0; \quad \text{Cov}[\underline{u}] = E[\underline{u}(t)\,\underline{u}(\tau)^T] = Q(t)\delta(t-\tau)$$

[1] The symbol $E[\ ]$ denotes mathematical expectation; $\text{Cov}[\underline{u}]$ denotes the covariance matrix of $\underline{u}$.

The matrix G(t) is an m × p distribution matrix which indicates how each component of $\underline{u}(t)$ affects each component of the system state derivative, $\dot{\underline{x}}(t)$, and $\underline{b}(t)$ is a n × 1 column vector of known system inputs.

In the target tracking problem the components of the state vector $\underline{x}$ will typically include position and velocity variables plus additional components representing target acceleration and perhaps correlated measurement noise. Note that the F, G and Q matrices may be time-varying. In the target tracking problem the system state equation is nonlinear, unlike Eq. (A.1-1); however, the nonlinearities can usually be linearized about a nominal trajectory so that the linear estimation techniques described here can be applied.

The solution to Eq. (A.1-1) can be written for $t \geq t_0$ in the form

$$\underline{x}(t) = \Phi(t, t_0)\underline{x}(t_0) + \int_{t_0}^{t} \Phi(t, \tau)[G(\tau)\underline{u}(\tau) + \underline{b}(\tau)]d\tau \qquad \text{(A.1-2)}$$

where $\underline{x}(t_0)$ is the initial value of the system state vector at time t_0 and $\Phi(t, t_0)$, the state transition matrix, satisfies the matrix differential equation

$$\dot{\Phi}(t, t_0) = F(t)\Phi(t, t_0); \quad \Phi(t_0, t_0) = I \qquad \text{(A.1-3)}$$

When F is constant, Φ becomes the matrix exponential,

$$\Phi(t, t_0) = e^{F(t-t_0)} \qquad \text{(A.1-4)}$$

In a digital tracking system one is generally interested in the state vector at discrete instants of time. Equation (A.1-2) may be used to relate the states at two instants of time, t_{n-1} and t_n. The resulting difference equation can be written in the form

$$\underline{x}_n = \Phi_{n-1}\underline{x}_{n-1} + \underline{w}_{n-1} + \underline{b}_{n-1} \qquad \text{(A.1-5)}$$

where

$$\underline{x}_n = \underline{x}(t_n)$$

$$\Phi_{n-1} = \Phi(t_n, t_{n-1})$$

$$\underline{w}_{n-1} = \int_{t_{n-1}}^{t_n} \Phi(t_n, \tau)\, G(\tau)\, \underline{u}(\tau)\, d\tau$$

$$\underline{b}_{n-1} = \int_{t_{n-1}}^{t_n} \Phi(t_n, \tau)\, \underline{b}(\tau)\, d\tau \qquad \text{(A.1-6)}$$

Observe that $\underline{w}_n$ is a gaussian white sequence. That is

$$E[\underline{w}_n] = \underline{0}$$

$$E\left[\underline{w}_n\, \underline{w}_{n+j}^T\right] = [0]; \quad j \neq 0$$

$$E\left[\underline{w}_{n-1}\, \underline{w}_{n-1}^T\right] = Q_{n-1} = \int_{t_{n-1}}^{t_n} \Phi(t_n, \tau) G(\tau) Q(t) G(\tau)\, \Phi^T(t_n, \tau)\, d\tau \qquad \text{(A.1-7)}$$

At discrete instants of time, measurements of linear combinations of the state variables are made. The equation describing this measurement process has the general form

$$\underline{z}_n = H_n \underline{x}_n + \underline{v}_n \qquad \text{(A.1-8)}$$

where $\underline{z}_n$ is a vector of r measured quantities at time t_n, H_n is an $r \times m$ observation matrix describing the linear combinations of state variables which comprise $\underline{z}_n$ in the absence of noise, and $\underline{v}_n$ is an r vector of zero mean gaussian measurement errors with a covariance matrix, R_n at time t_n, defined

$$E\left[\underline{v}_n \underline{v}_m^T\right] = \begin{cases} 0 : & n \neq m \\ R_n : & n = m \end{cases}$$

At any time t_n, the objective of optimal estimation theory is to process all measurements taken up to that time to produce an estimate $\hat{\underline{x}}_n$ of the system state $\underline{x}_n$ having minimum error, in a statistical sense. The optimization criterion most often chosen is that of minimizing the mean square estimation error. This estimate is calculated with the Kalman filtering algorithm.

As new measurements become available there is essentially an instantaneous change in our knowledge of the state $\underline{x}_n$. Denoting the optimum estimate of $\underline{x}_n$ just prior to the availability of $\underline{z}_n$ as $\hat{\underline{x}}_n(-)$ and the optimum estimate of the state vector immediately after processing $\underline{z}_n$ is $\hat{\underline{x}}_n(+)$, the Kalman filter generates the updated optimum estimate of the system state according to the following algorithm:†

$$\hat{\underline{x}}_n(-) = \Phi_{n-1}\, \hat{\underline{x}}_{n-1}(+) + \underline{b}_{n-1}; \quad \hat{\underline{x}}_0(-) = E[\underline{x}_0] \qquad \text{(A.1-9)}$$

$$\hat{\underline{x}}_n(+) = \hat{\underline{x}}_n(-) + K_n\left[\underline{z}_n - H_n\, \hat{\underline{x}}_n(-)\right] \qquad \text{(A.1-10)}$$

† Only the discrete or sampled measurement form of the Kalman filter is considered here.

where

$\hat{\underline{x}}_{n-1}(+)$ = the optimal estimate of $\underline{x}_{n-1}$ given measurements $\underline{z}_1, \underline{z}_2, \cdots \underline{z}_{n-1}$

$\hat{\underline{x}}_n(-)$ = the optimal estimate of $\underline{x}_n$ given measurements $\underline{z}_1, \underline{z}_2, \cdots \underline{z}_{n-1}$

K_n = an m x r gain matrix further described below

Observe that Eq. (A.1-9) is merely the discrete form of the continuous time equation

$$\dot{\hat{\underline{x}}}(t) = F(t)\,\hat{\underline{x}}(t) + \underline{b}(t) \qquad \text{(A.1-11)}$$

The quantity K_n is the Kalman gain matrix. Let $\tilde{\underline{x}}_n$ denote the error made in estimating $\underline{x}_n$, i.e.,

$$\tilde{\underline{x}}_n = \underline{x}_n - \hat{\underline{x}}_n \qquad \text{(A.1-12)}$$

and let

$$P_n = \text{Cov}\,\tilde{\underline{x}}_n = E\left[\tilde{\underline{x}}_n \tilde{\underline{x}}_n^T\right] \qquad \text{(A.1-13)}$$

Then K_n is computed with the following recursion relations:

$$K_n = P_n(+) H_n^T R_n^{-1} = P_n(-) H_n^T \left[H_n P_n(-) H_n^T + R_n\right]^{-1} \qquad \text{(A.1-14)}$$

$$P_n(-) = \Phi_{n-1} P_{n-1}(+) \Phi_{n-1}^T + Q_{n-1}; \qquad \text{(A.1-15)}$$

$$P_n(+) = P_n(-) - P_n(-) H_n^T \left[H_n P_n(-) H_n^T + R_n \right]^{-1} H_n P_n(-)$$

$$= (I - K_n H_n) P_n(-) (I - K_n H_n)^T + K_n R_n K_n^T \qquad \text{(A.1-16)}$$

where the (+) and (-) notation again refers to the quantities before and after measurement.

The Kalman algorithm has two distinct phases. Equations (A.1-9) and (A.1-15) describe the time evolution of the state estimate and its error statistics between measurements under the influence of system dynamics and noise. This process is commonly referred to as extrapolation. Equations (A.1-10) and (A.1-16) indicate how the estimate and its error covariance are updated at the measurement time to reflect the new information available. The extrapolation and update phases of the Kalman filter are summarized in Fig. A.1-1. Information flow in a typical Kalman filter application is shown in Fig. A.1-2.

Perhaps the most unique feature of the Kalman filter is that the performance analysis of the filter is inherent in the algorithm for K_n. The matrix P_n is a complete description of the second-order error statistics. In particular, the diagonal terms of P_n represent the minimum mean-square error obtained in estimating each component of $\underline{x}_n$. Note that P_n is specified for all times by Eqs. (A.1-15) and (A.1-16). Knowledge of neither $\underline{x}_n$, $\hat{\underline{x}}_n$, nor $\underline{z}_n$ is required to obtain a performance analysis for the optimal filter.

In summary the following conditions must be met to implement an optimum Kalman filter:

R-1025

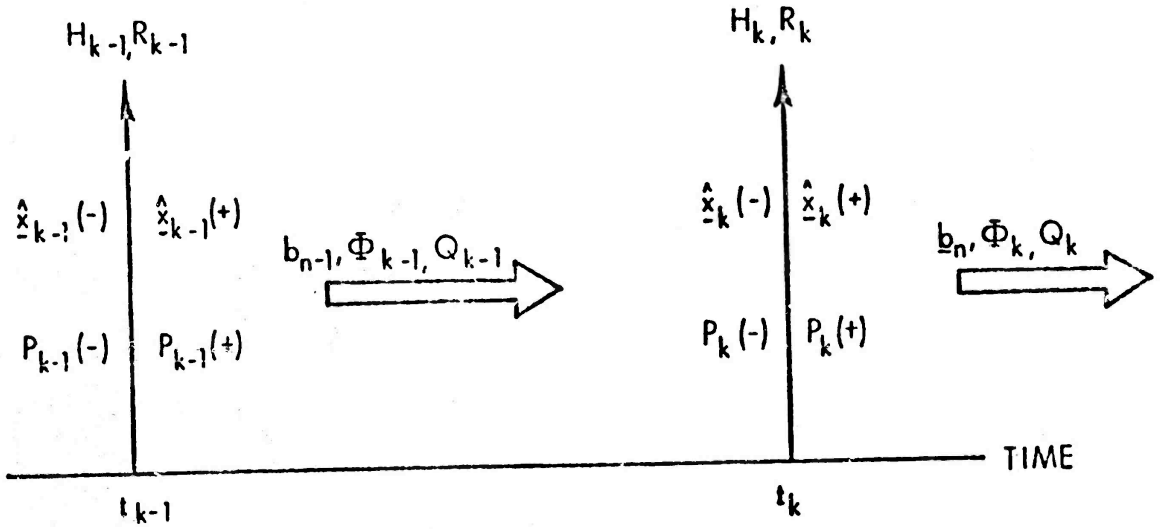

EXTRAPOLATION

$$\hat{x}_n(-) = \Phi_{n-1}\ \hat{x}_{n-1}(+) + b_{n-1}$$

$$P_n(-) = \Phi_{n-1}\ P_{n-1}(+)\ \Phi_{n-1}^T + Q_{n-1}$$

UPDATE

$$\hat{x}_n(+) = \hat{x}_n(-) + K_n \left[z_n - H_n \hat{x}_n(-) \right]$$

$$K_n = P_n(-)\ H_n^T \left[H_n P_n(-) H_n^T + R_n \right]^{-1}$$

$$P_n(+) = \left[I - K_n H_n \right] P_n(-)$$

Figure A.1-1 Equations for Each Phase of the Kalman Filter Algorithm

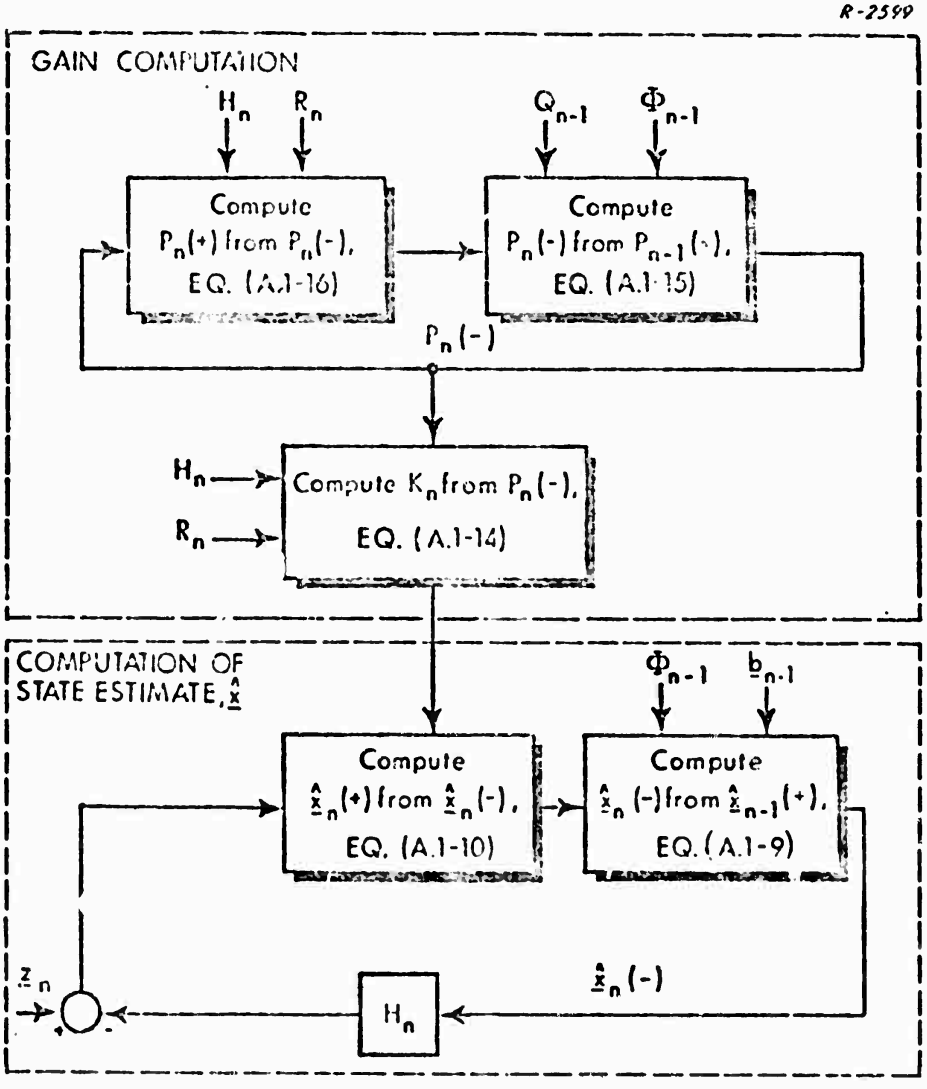

Figure A.1-2 Information Flow Diagram for Discrete Kalman Filter

- The system must be sufficiently described as being linear and obeying Eq. (A.1-1).
- F(t), G(t), and $\underline{b}(t)$ must be known functions of time.
- $\underline{u}(t)$ must be a vector of zero mean gaussian white noise inputs with known covariance matrix, Q (t).
- The measurements must obey Eq. (A.1-8) and H_n must be known for all n.
- $\underline{v}_n$ must be a vector of gaussian white noise measurement errors with its covariance matrix, R_n, and its mean known.
- To initialize the filter equations, Eqs. (A.1-9) and (A.1-15), $\hat{\underline{x}}_0(-) = E[\underline{x}_0]$ and $P_0(-) = E[\underline{x}_0 \underline{x}_0^T]$ must be provided.

If the tracking problem met all of the conditions above, then the design of an optimum tracking filter would just be the direct implementation of the Kalman filter equations. However, in practical situations one or more of these conditions are usually violated and the design problem is more difficult. The goal is then to design a suboptimal filter, based upon optimal filter theory, which gives nearly optimal performance. Suboptimal filter design and evaluation for the target tracking problem are the major topics of this report.

A.2 OPTIMAL PREDICTION THEORY

Given estimates of the current system state it is often required that a prediction be made of its future state. In the gun fire control problem the future position of the target is required so that the projectile will intersect the target at some future time. To aim the gun properly the future position of the target must be known. Kalman filter theory applies directly to this problem.

One way to think of the prediction problem is to look at how the Kalman filter operates when no measurements are being made. This is done by setting the H_n matrix in the measurement equation, Eq. (A.1-8), equal to zero; then Eq. (A.1-14) indicates that the Kalman gain matrix, K_n, is zero and the filter equations become

$$\hat{\underline{x}}_n(-) = \Phi_{n-1}\, \hat{x}_{n-1}(-) + \underline{b}_{n-1} \qquad \text{(A.2-1)}$$

$$P_n(-) = \Phi_{n-1}\, P_{n-1}(-)\, \Phi_{n-1}^T + Q_{n-1} \qquad \text{(A.2-2)}$$

Eq. (A.2-1) is the optimum prediction algorithm and Eq. (A.2-2) indicates the propagation of the prediction error covariance. To predict the future system state for any time t_n beyond the present time these equations are solved iteratively starting with the current state estimate and its covariance matrix. Note that these equations are independent and the predicted future state may be found without using Eq. (A.2-2).

APPENDIX B

ADAPTIVE FILTERING THEORY

The design of an optimal Kalman filter to estimate the states of a dynamic system requires an accurate statistical model of the system as outlined in Appendix A.1. This model completely determines the filter's structure which is independent of the measurement data. In practice, such a model is rarely available because the physical system is not well known in advance and may be changing unpredictably.

One approach to suboptimal filter design is to specify a fixed filter design and experimentally determine how well it works on the system in question. This technique is satisfactory in many situations where the assumed system model is a good approximation to the true system if the filter is designed to be insensitive to errors in the model. However, in many situations where an accurate system model is not known or the system is changing in an unknown manner no one fixed design gives adequate performance. It is this problem which motivates the search for adaptive filter structures to give improved performance.

Since the measurement data contains information about the system's structure as well as the system's state, it seems reasonable to try to design a filter which uses the data to identify the correct system model. Essentially, an adaptive filter is a suboptimal filter with a time-varying structure dependent upon the measurement data. If it is designed properly, it should be able to adjust itself to a previously unknown or changing system so that it gives near optimal estimates. The degree with which the performance of an adaptive filter approaches that of an optimal filter depends upon how fast the adaptation

occurs and how well the structure of the adaptive filter can model the structure of the optimal filter. Unfortunately, there is often no unique way to select a particular adaptive structure for a particular application. The literature describes many different types of adaptive schemes and the only way to judge their performance is by experimentally applying each to the design problem at hand. This appendix gives the details of two of the three adaptive filtering techniques tested in this report. The third, the adaptive bandwidth filter, is discussed in Section 3.3.1.

B.1 HYPOTHESIS TESTING FILTER

The design philosophy of the hypothesis testing filter is to operate a number of different filters in parallel and compare their estimates. This comparison is used to calculate a final estimate which is a weighted average of the individual estimates; those which appear to be the most accurate are given the largest weights. Specifically, assume that over some time interval, T, the optimum Kalman filter for a particular linear system is one of N known filters. If this assumption is correct, then it is possible to calculate the probability that each of the filters is optimum over that interval. The state estimate produced by the hypothesis testing filter is the sum of the estimates from each of the N individual filters weighted by the probability that each is optimum. This design is theoretically sound and can be expected to work very well as long as the assumptions upon which it is based are met. The primary disadvantage of the method is the requirement that N Kalman filters be implemented in parallel. If N is large and/or the order of each filter is large, this requirement means that the amount of computation required can easily become excessive. For the purposes of this report a simplified form of the general hypothesis testing filter is developed in this section. A much more general discussion can be found in Ref. 4.

Assume that the system to which this method is applied can be modeled by Eq. (A.1-5) with the deterministic input vector $\underline{b}_n = 0$, that is, only a vector of "white" gaussian noise sequences, $\underline{w}_n$, drives the system. This assumption represents some loss of generality, but many systems with unknown inputs can be modeled in this way. If $\underline{b}_n$ is known, however, it can easily be included in the equations which follow. The system equation then becomes

$$\underline{x}_n = \Phi_{n-1}\,\underline{x}_{n-1} + \underline{w}_{n-1} \qquad \text{(B.1-1)}$$

where

$$E\left[\underline{w}_{n-1}\,\underline{w}_{n-1}^T\right] = Q_{n-1} \qquad \text{(B.2-2)}$$

Further assume that for the time interval under consideration, the matrix Q_{n-1} is constant and designated by Q^*, which represents its true value over the interval, T. Assume that Q^* is not specifically known, but it is known to be one of the members of a set of N possibilities; i.e.,

$$Q^* \in [Q^1, Q^2, \ldots Q^N]$$

For each of these possibilities there is a distinct Kalman filter design defined by the equations

$$\hat{\underline{x}}_n^k(-) = \Phi_{n-1}\,\hat{\underline{x}}_{n-1}^k(+) \qquad \text{(B.1-3)}$$

$$\hat{\underline{x}}_n^k(+) = \underline{x}_n^k(-) + K_n^k\left[\underline{z}_n - H_n\,\hat{\underline{x}}_n^k(-)\right] \qquad k = 1, 2, \ldots, N \qquad \text{(B.1-4)}$$

$$P_n^k(-) = \Phi_{n-1}\,P_{n-1}^k(+)\,\Phi_{n-1}^T + Q^k \qquad \text{(B.1-5)}$$

$$K_n^k = P_n^k(-)\, H_n^T \left[H_n\, P_n^k(-)\, H_n^T + R_n \right]^{-1} \qquad \text{(B.1-6)}$$

$$P_n^k(+) = \left[I - K_n^k H_n \right] P_n^k(-) \qquad \text{(B.1-7)}$$

where the superscript k indicates the k^{th} filter in the set of N filters, each with covariance calculated assuming $Q^* = Q^k$. These equations also assume that Φ, H, and R_n are known and the same for each filter. For simplicity, the filter initial conditions, $P_0^k(-)$ and $\hat{\underline{x}}_0^k(-)$, are the same for each k. This completely defines the structure of the N Kalman filters.

The adaptive part of the design is based upon calculating the probabilities of N hypotheses conditioned on the measurements taken during the interval. The first hypothesis, designated H^1, is that Q^* equals Q^1. The second hypothesis, H^2, is that $Q^* = Q^2$, and so on. In other words, H^k is the hypothesis that the k^{th} filter in the set is optimum for the given measurement data. Once the probability of each hypothesis is known, the optimum state estimate is a linear combination of the estimates from all N individual filters, calculated by multiplying the estimate from each filter by the probability that the hypothesis corresponding to that filter is true and then adding all of these weighted estimates. A diagram of this structure is shown in Fig. B.1-1.

To discuss how the various probabilities are calculated it is necessary first to define the interval measurement history, Z_n. Let Z_n be the set of all measurements taken during the interval in question up to and including the m^{th} measurement, taken at time t_n,

$$Z_n = \left\{ \underline{z}_{n-m-1}, \cdots, \underline{z}_{n-1}, \underline{z}_n \right\}$$

where $\underline{z}_{n-m-1}$ is the first measurement taken in the interval at time t_{n-m-1}. The probability that hypothesis H^k is true, conditioned on the measurement history Z_n, is designated by $p\left\{ H^k \mid Z_n \right\}$.

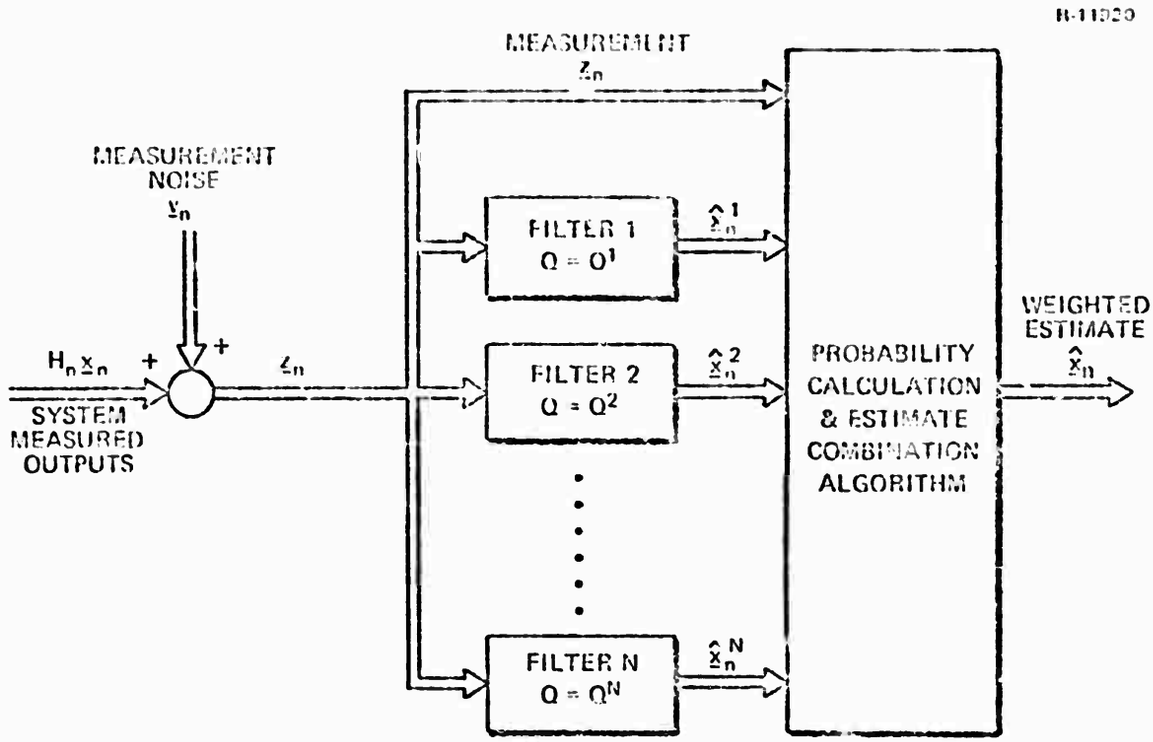

Figure B.1-1 Structure of Hypothesis Testing Filter

Given the estimates from each of the filters, the measurement data, and the a priori probability of each hypothesis at the beginning of the interval, it is possible to recursively calculate $p\left\{H^k \mid Z_n\right\}$. Using Bayes' rule (Ref. 4.) the formula for the k^{th} probability is

$$p\left\{H^k \mid Z_n\right\} = \frac{f\left(\underline{z}_n \mid H^k, Z_{n-1}\right) p\left\{H^k \mid Z_{n-1}\right\}}{\sum_{k=1}^{N} f\left(\underline{z}_n \mid H^k, Z_{n-1}\right) p\left\{H^k \mid Z_{n-1}\right\}} \qquad \text{(B.1-8)}$$

where $f(\underline{z}_n \mid H^k, Z_{n-1})$ is an r-dimensional normal probability density function, r being the dimension of the measurement vector $\underline{z}_n$. The value of this function is given by

$$f\left(\underline{z}_n | H^k, Z_{n-1}\right) = \frac{1}{(2\pi)^{r/2}|S_n^k|} \exp\left\{-\frac{1}{2}\left[\underline{z}_n - H_n \hat{\underline{x}}_n^k(-)\right]^T \left[S_n^k\right]^{-1} \left[\underline{z}_n - H_n \hat{\underline{x}}_n^k(-)\right]\right\} \tag{B.1-9}$$

where

$$S_n^k = H_n P_n^k(-) H_n^T + R_n \tag{B.1-10}$$

and $|S_n^k|$ indicates the determinant of the matrix S_n^k. Note that H^k is the k^{th} hypothesis while H_n is the state observation matrix. In this manner, $p\left\{H^k | Z_n\right\}$ is calculated for each k at each sampling time in the interval, T.

The overall estimate for the adaptive filter immediately after a measurement is given by

$$\hat{\underline{x}}_n(+) = \sum_{k=1}^{N} \hat{\underline{x}}_n^k(+)\, p\left\{H^k | Z_n\right\} \tag{B.1-11}$$

with its corresponding covariance given by

$$P_n(+) = \sum_{k=1}^{N} P_n^k(+)\, p\left\{H^k | Z_n\right\} \tag{B.1-12}$$

Up to this point, all of the development has been with respect to a single interval of length T. Theoretically, if only one of the N filters is optimum for all time, T should be set equal to infinity and the design is complete. The probability of the correct hypothesis will converge to one and the final estimate will be equal to the estimate from the optimum individual filter. If, however, the correct hypothesis changes with time because the correct model for the system changes, then a provision must be made for the adaptive

filter to restart the probability calculation to test for a new hypothesis being true. This is done by initializing the filters and the probability calculation every T seconds.

At the beginning of the first interval, the N filters must be initialized by setting each $\hat{\underline{x}}_0^k(-)$ and $P_0^k(-)$ to the a priori mean and covariance of the estimate. That is

$$\hat{\underline{x}}_0^k(-) = E[\underline{x}_0] \qquad \text{for all k} \tag{B.1-13}$$

$$P_0^k(-) = E\left[\tilde{\underline{x}}_0^k \tilde{\underline{x}}_0^{kT}\right] \qquad \text{for all k} \tag{B.1-14}$$

where

$$\tilde{\underline{x}}_0^k = \underline{x}_0 - \hat{\underline{x}}_0^k(-) \tag{B.1-15}$$

defines the initial estimation error vector. It is also necessary to choose a set of initial values for the probabilities calculated recursively using Eq. (B.1-8). This choice should reflect any knowledge available about the system. For example, if very little is known about which of the filters might be optimum it is natural to choose these a priori probabilities equal. After the first interval and at the end of each interval thereafter, the filters and the probability calculations are reset since a new hypothesis might hold over the next interval. Each probability, $p\{H^k, |Z_n\}$ is reset to its a priori probability and each of the N filters is re-initialized by setting its estimate equal to the combined estimate given by Eq. (B.1-11) and by setting its covariance matrix to that given by Eq. (B.1-12). The entire adaptive filter is then ready to calculate the probability of each hypothesis over the next interval and to continue calculating the weighted estimate.

The design of this filter requires a number of choices, the most important of which is the set of hypotheses or Q^k matrices. The reset interval,

the a priori probabilities of each hypothesis, and the filter initial conditions must also be selected to completely specify the design. These choices must reflect what is known in advance about the system and are all very important to the performance of the filter.

The hypothesis testing filter has some primary limitations in practice. First, the optimum Kalman filter for the system may not be one of the N possibilities over a particular interval. This could be due to system modeling errors, improper choice of the noise covariance matrix, R_n, or a choice for the Q^k set that does not cover all possibilities. Second, the choice of the reset interval and a priori probabilities is often somewhat arbitrary because of ignorance of the system dynamic behavior. Unfortunately the filter's performance is often very sensitive to these effects. In particular, as discussed in Chapter 4, if the noise covariance matrix R_n is incorrect, the adaptive algorithm can adapt in the wrong direction and give the highest weight to the estimates from that individual filter which is producing the poorest estimates. The final difficulty with this design is the requirement that N filters be built in parallel. This computational burden may be unacceptable in many applications.

B.2 RESIDUAL TESTING FILTER

The motivation for the adaptive design described in this section is the sensitivity of the hypothesis testing filter to the incorrect choice of R_n, the measurement noise covariance matrix. This problem is mentioned above and demonstrated dramatically in the results presented in Section 4.2 and 4.4. Basically, the adaptive algorithm of the hypothesis testing filter depends directly upon, R_n, (see Eq. (B.1-10)) and it can adapt in the wrong "direction" if R_n is not equal to the true noise covariance matrix. The residual testing filter has the same structure as hypothesis testing filter, (see Fig. B.2-1) but the adaptive algorithm is chosen differently. In this approach, the adaptive

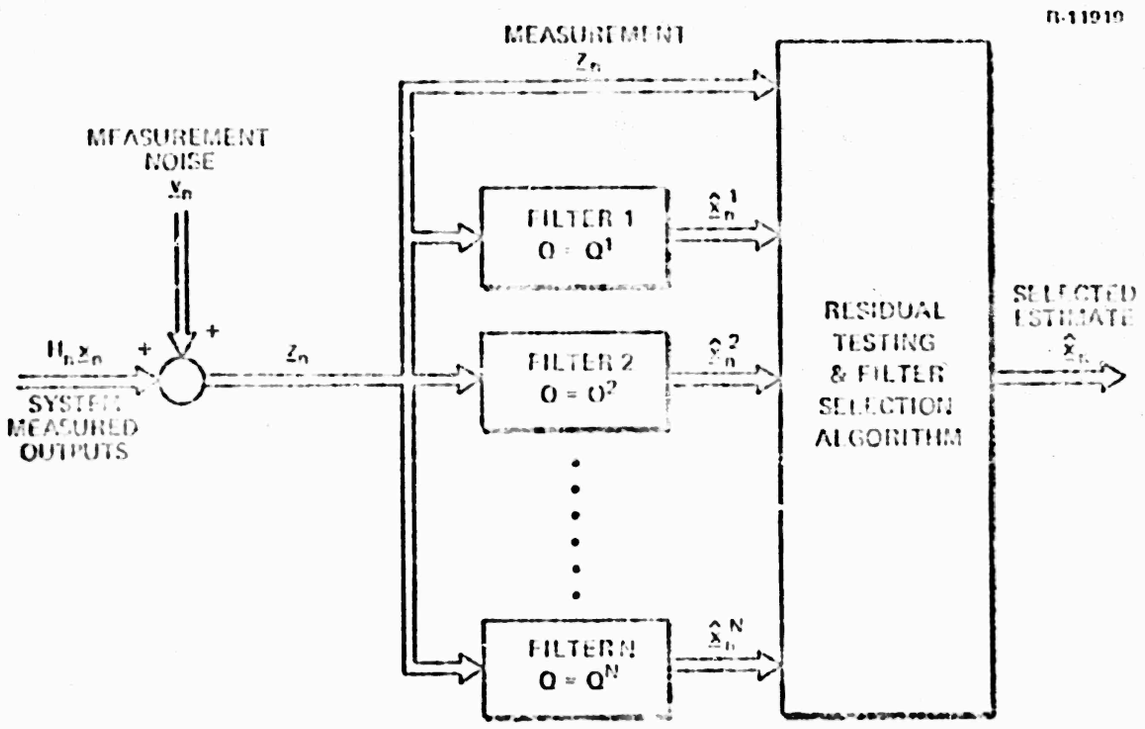

Figure B.2-1 Structure of Residual Testing Filter

part is designed so that it is independent of the choice of R_n for the individual filters. The adaptive algorithm observes all of the estimates over an interval T and at the end of the interval it makes a decision as to which filter is operating best. Over the next interval, the output of the adaptive algorithm is the output of that individual filter selected as best over the previous interval. Meanwhile the observation of all estimates continues so that a new choice can be made for the next interval.

The method by which the choice of a best filter is made at the end of each interval involves the use of the residual sequence of each filter, the elements of which are defined by

$$\gamma_n^k = \underline{z}_n - H_n \hat{\underline{x}}_n^k(-) \qquad \text{(B.2-1)}$$

This vector is premultiplied by the Kalman gain matrix, K_n^k, and used to update the state estimate after the measurement $\underline{z}_n$ is made (see Eq. (A.1-10)). Using the measurement equation, Eq. (A.1-8), and Eq. (A.1-12), the equation for $\underline{\gamma}_n^k$ becomes

$$\underline{\gamma}_n^k = H_n \underline{\tilde{x}}_n^k(-) + \underline{v}_n \tag{B.2-2}$$

where $\underline{\tilde{x}}_n^k(-)$ is the estimation error of the k^{th} filter just prior to the arrival of the measurement $\underline{z}_n$. A measure of each filter's performance is provided by the scalar quantity, g_n^k, defined as

$$g_n^k = \underline{\gamma}_n^{kT} A \underline{\gamma}_n^k \tag{B.2-3}$$

where A is any symmetric positive definite matrix. The expected value of g_n^k, denoted by $\bar{g}_n^k$, is given by

$$\bar{g}_n^k = E\left[\underline{\tilde{x}}_n^k(-)^T H^T A H \underline{\tilde{x}}_n^k(-)\right] + 2E\left[\underline{\tilde{x}}_n^k(-)^T H_n^T A \underline{v}_m\right] + E\left[\underline{v}_n^T A \underline{v}_n\right]$$

Since $\underline{\tilde{x}}_n^k(-)$ and $\underline{v}_n$ are independent random variables and $E[\underline{v}_n] = \underline{0}$, it follows that

$$\bar{g}_n^k = E\left[\underline{\tilde{x}}_n^k(-)^T H_n^T A H_n \underline{\tilde{x}}_n^k(-)\right] + E\left[\underline{v}_n^T A \underline{v}_n\right] \tag{B.2-4}$$

Kalman filter theory states that an optimal filter minimizes $E\left[\underline{x}_n^T B \underline{\hat{x}}_n\right]$ for any positive semidefinite matrix B. Noting that the matrix $H_n^T A H_n$ in Eq. (B.2-4) is positive semidefinite because A is positive definite, one logical means of selecting the best filter from a set of N is to select that which

minimizes $\bar{g}_n^k$. In other words, since an optimal filter is known to minimize $E[\tilde{\underline{x}}^T B \tilde{\underline{x}}]$ and the first term on the right side of Eq. (B.2-4) is of this form, then if one filter out of a group of filters is found to have a lower $\bar{g}_n^k$ than all the others, it is a likely choice for the optimum filter. If none of the filters is optimum, then that filter with the lowest value of $\bar{g}_n^k$ can be called "best". This is not a rigorous argument for choosing the best filter, but it is a logical method of doing so. In practice $\bar{g}_n^k$ is not known for each of the residual sequences, but an estimate of it can be made over some interval by calculating the time average of g_n^k. Setting A equal to the identity matrix, the estimate of $\bar{g}_n^k$ is

$$\hat{\bar{g}}^k = \frac{1}{M} \sum_{n=n_o}^{n_o+M-1} g_n^k ; \quad g_n^k = \underline{\gamma}_n^T \underline{\gamma}_n \qquad \text{(B.2-5)}$$

where n_o is the value of the time index n at the beginning of an interval and M is the total number of samples in the interval. This calculation is performed for each of the N filters and the filter that gives the minimum $\hat{\bar{g}}^k$ is selected as "best" over the next interval.

At the end of the interval, each filter is re-initialized to the estimate and covariance matrix of the filter which was judged best. Thus, at the start of each interval all of the N filters have the same initial conditions. This is done to reset any filter which may be working very poorly to the estimate and covariance which are probably most accurate.

The design of the residual testing filter consists of choosing a set of reasonable filters for the system, initial conditions for the filters, and a reset interval. These choices must be made based upon the particular system to which the filter is applied and should reflect any knowledge available about the

system. The filter has essentially the same computational requirements as the design developed in the last section. It is less sensitive to an incorrect choice for the measurement noise covariance; i.e., it does not adapt in the wrong direction. However, it tends to be less accurate than the hypothesis testing filter in cases where the design parameters for the latter are accurately known.

REFERENCES

1 Jazwinski, A.H. and Bailie, A.E., "Adaptive Filtering," Report No. 67-6, Analytical Mechanics Associates, Inc., Lanham, Maryland, March 1967.

2. Jazwinski, A.H., "Adaptive Filtering," Automatica, Vol. 5, pp. 475-485, 1969.

3. Fitzgerald, R.J., "Divergence of the Kalman Filter," IEEE Transactions on Automatic Control, Vol. AC-16, No. 6, December 1971.

4. Magill, D.T., "Optimal Adaptive Estimation of Sampled Stochastic Processes," Technical Report No. 6302-3, Stanford Electronics Laboratories, Stanford, California, December 1963.

5. Demetry, J.S. and Titus, H.A., "Adaptive Tracking of Maneuvering Targets," Naval Postgraduate School, Monterey, California, 15 April 1968.

6. Aldrich, G.T. and Krabill, W.B., "A Versatile Kalman Technique for Aircraft or Missile State Estimation and Error Analysis Using Radar Tracking Data," AIAA Guidance and Control Conference, August 1972.

7. Hampton, R.L.T. and Cooke, J.R., "Unsupervised Tracking of Maneuvering Vehicles," IEEE Transactions on Aerospace and Electronic Systems, Vol. AES-9, No. 2, March 1973.

8. Thorp, J.S., "Optimal Tracking of Maneuvering Targets." IEEE Transactions on Aerospace and Electronic Systems, Vol. AES-9, No. 4, July 1973.

9. Nahi, N.E. and Schaefer, B.M., "Decision-Directed Adaptive Recursive Estimators: Divergence Prevention," IEEE Transactions on Automatic Control,Vol. AC-17, No. 1 February 1972.

10. Sorenson, H.W. and Sacks, J.E., "Recursive Fading Memory Filtering." Journal of Information and Science. Vol. 3. April 1971.

11. Sorenson, H.W. and Sacks, J.E., "Nonlinear Extensions of the Fading Memory Filter," IEEE Transactions on Automatic Control, Vol. AC-16, No. 5, October 1971.

12. Gruber, M., "An Approach to Target Tracking," Technical Note 1967-8, Lincoln Laboratory, Massachusetts Institute of Technology, Lexington, Massachusetts, 10 February 1967.

13. Haddad, A.H. and Cruz, J.B., "Nonlinear Filtering for Systems with Random Models," Symposium on Nonlinear Estimation Theory San Diego, California, 1971.

14. Tarn, T.J. and Zaborsky, J., "A Practical, Nondiverging Filter," AIAA Journal, Vol. 8, No. 6, June 1970.

15. Will, T.J., "A FORTRAN Simulation of the Target Data Filtering Section of the AA Tracking Loop in the MK-86 GFCS," Thesis, Naval Postgraduate School, Monterey, California, June 1973.

16. Duiven, E.M. and Crawford, B.S., "MPMS/AIRS Calibration and Alignment Study," The Analytic Sciences Corp., Report No. TR-340-2-1, September 1973.

17. Price, C.F., "A Pointing and Tracking Algorithm for an Airborne Telescope Pointing System", The Analytic Sciences Corp., Contract No. F29601-73-C-0005, to be published.

18. Jazwinski, A. H., Stochastic Processes and Filtering Theory, Academic Press, New York, 1970.

19. Gelb, A., Ed., Applied Optimal Estimation, MIT Press, Cambridge, Massachusetts, 1974.

20. Curry, R.E., Mirchandani, P., and Price, C.F., "State Estimation with Coarsely Quantized, High-Data-Rate Measurements", submitted to IEEE Transactions on Aerospace and Electronic Systems.